



**Calhoun: The NPS Institutional Archive**  
**DSpace Repository**

---

Theses and Dissertations

1. Thesis and Dissertation Collection, all items

---

1970-06

The application of holographic interferometry  
to the determination of asymmetric  
three-dimensional density fields in free jet flow.

Matulka, Robert Dale

Monterey, California ; Naval Postgraduate School

---

<http://hdl.handle.net/10945/14890>

---

This publication is a work of the U.S. Government as defined in Title 17, United States Code, Section 101. Copyright protection is not available for this work in the United States.

*Downloaded from NPS Archive: Calhoun*



Calhoun is the Naval Postgraduate School's public access digital repository for research materials and institutional publications created by the NPS community. Calhoun is named for Professor of Mathematics Guy K. Calhoun, NPS's first appointed -- and published -- scholarly author.

**Dudley Knox Library / Naval Postgraduate School**  
**411 Dyer Road / 1 University Circle**  
**Monterey, California USA 93943**

<http://www.nps.edu/library>

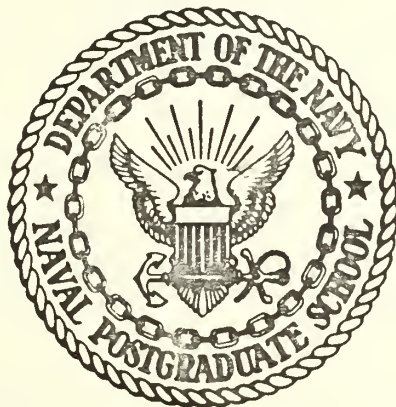
THE APPLICATION OF HOLOGRAPHIC INTERFEROMETRY  
TO THE DETERMINATION OF ASYMMETRIC  
THREE-DIMENSIONAL DENSITY FIELDS  
IN FREE JET FLOW

by

Robert Dale Matulka



# United States Naval Postgraduate School



## THESIS

THE APPLICATION OF HOLOGRAPHIC INTERFEROMETRY  
TO THE DETERMINATION OF ASYMMETRIC  
THREE-DIMENSIONAL DENSITY FIELDS  
IN FREE JET FLOW

by

Robert Dale Matulka

June 1970

*This document has been approved for public re-  
lease and sale; its distribution is unlimited.*

T136456





The Application of Holographic Interferometry  
to the Determination of Asymmetric  
Three-Dimensional Density Fields  
in Free Jet Flow

by

Robert Dale Matulka  
Lieutenant Commander, United States Navy  
B.S. , United States Naval Academy, 1960

Submitted in partial fulfillment of the  
requirements of the degree of

DOCTOR OF PHILOSOPHY

from the

NAVAL POSTGRADUATE SCHOOL

June 1970



## ABSTRACT

The successful application of holographic interferometry, and an associated mathematical reduction process, to the determination of an asymmetric three-dimensional density field of an aerodynamic phenomenon is reported.

An integral inversion method from the field of plasma physics has been computerized, extensively evaluated and applied to the determination of functions, both axisymmetric and asymmetric, which simulate aerodynamic density fields.

The application of holographic interferometry has been extended to provide multiple holograms about a test region, with sufficient coverage to provide interferometric data for the successful solution of the density field.

The analytical and experimental methods developed were applied to an experimental axisymmetric test field, the supersonic flow from a free jet, and shown to be comparable to a previous solution obtained by the Abel inversion method. Further, the free jet was tilted to provide a test field which was asymmetric in the plane of solution. Comparison of the resulting asymmetric solution was shown to be self-consistent with the previously obtained axisymmetric solution.



## TABLE OF CONTENTS

ABSTRACT - - - - -	2
I. INTRODUCTION - - - - -	7
II. THEORETICAL ANALYSIS - - - - -	8
A. THE INTERFEROMETRY OF AERODYNAMIC FIELDS - - - - -	8
1. The Mach-Zehnder Interferometer - - - - -	10
2. Holography - - - - -	11
3. Holographic Interferometry - - - - -	13
a. Dark Field - - - - -	14
b. Light Field - - - - -	15
B. THEORETICAL APPROACH - THE INTEGRAL INVERSION - - -	16
1. The Basic Equation to Invert - - - - -	16
2. Maldonado's Inversion - - - - -	16
a. The Analytical Procedure - - - - -	17
b. The Numerical Procedure - - - - -	20
c. The Computer Program - HOLOFER - - - - -	22
(1) The Basic Program - - - - -	22
(2) Add-on Functions, Field Modification - - - - -	23
(3) Shock Waves - - - - -	24
d. Symmetry - - - - -	24
(1) Axisymmetric Fields - - - - -	25
(2) With Planes of Symmetry - - - - -	25



3. Theoretical Results - - - - -	26
a. Artificial Data Generation - - - - -	26
b. Test Inversions - - - - -	27
(1) Axisymmetric - - - - -	27
(2) Non-Axisymmetric - - - - -	28
III. EXPERIMENTAL APPROACH - - - - -	29
A. DESCRIPTION OF THE APPARATUS - - - - -	29
1. The Holographic Table - - - - -	29
2. The Test Section - - - - -	30
3. Laboratory Techniques - - - - -	31
B. HOLOGRAPHIC EXPERIMENTAL RESULTS - - - - -	32
1. Non-Flow Holographic Experiments - - - - -	32
2. Free Jet Experimentation - - - - -	33
3. Experimental Techniques and Considerations - - - - -	34
a. Photographic Technique - - - - -	36
b. Data Reduction - - - - -	37
IV. THE APPLICATION OF THE INTEGRAL INVERSION TECHNIQUE TO THE EXPERIMENTAL RESULTS - - - - -	39
A. Axisymmetric Solution - - - - -	39
B. Non-Axisymmetric Solution - - - - -	40
C. Discussion of the Errors - - - - -	41
1. Numerical Inversion Errors - - - - -	41
2. Errors in the Data - - - - -	43





V. SUMMARY - - - - -	45
A. CONCLUSIONS - - - - -	45
B. RECOMMENDATIONS - - - - -	46
C. ACKNOWLEDGEMENTS - - - - -	46
APPENDIX A - OTHER INVERSION METHODS - - - - -	79
APPENDIX B - MATHEMATICAL FOUNDATIONS - - - - -	81
APPENDIX C - HOLOFER - - - - -	86
1. The Description of Input Parameters - - - - -	87
2. A Sample Terminal Dialogue - - - - -	93
3. The Terminal Executive Files - - - - -	95
4. The Program - - - - -	98
5. The Input Data Files Used in the Experiment - - - - -	145
BIBLIOGRAPHY - - - - -	150
INITIAL DISTRIBUTION LIST - - - - -	154
FORM DD 1473 - - - - -	157



## I. INTRODUCTION

Holography has enabled the aerodynamicist to "freeze" the interferometric view of a transient phenomenon and subsequently to view the field in three dimensions, as through a "window." This new capability has indicated the possibility of quantitatively determining the density in such a field, with no symmetric restrictions on its form.

To make quantitative determinations of asymmetric density fields, it was necessary to:

1) Invert the fringe number functions that describe the interferometric data,

$$g(\gamma', \xi) = \int_{x_1'}^{x_2'} f(x, \gamma) dx'$$

to obtain the asymmetric density function  $f$  from within the integral.

In the search for such an inversion process the possibility of using an asymmetric line integral inversion scheme which had been developed in the field of plasma emissivity [Maldonado, 1966], became evident. The method was evaluated by extensive computerized testing on density functions found in aerodynamics, including shock waves. The inversion method was found to be quite accurate, giving results which were generally within one percent of the test function.

2) Obtain holographic interferograms of sufficient angular coverage about a test region to provide the interferometric data required by the inversion process. To obtain the necessary experimental data, a holographic



work table was constructed and used to design the necessary optical arrangement. The capability of achieving multiple Q-switched holographic interferograms about a test region, with no opaque objects present, was demonstrated.

3) Apply real holographic interferometric data to an inversion process in order to demonstrate the practicality of the technique. A stepwise evaluation of the system included an axisymmetric evaluation of a free jet for comparison with the previously available solution of Winckler [1948]. Having attained a solution for the three-dimensional axisymmetric field, the asymmetric capability of the technique was tested by tilting the free jet, which destroyed the axisymmetry in the plane of inversion. The resulting data were inverted asymmetrically and compared with the axisymmetrically measured density. The result is shown to be a self-consistent comparison of the asymmetric inversion.

## II. THEORETICAL ANALYSIS

### A. THE INTERFEROMETRY OF AERODYNAMIC FIELDS

Holography has opened a new branch of interferometry for aerodynamic research. Ordinary Mach-Zehnder type interferograms have been restricted to the analysis of two-dimensional or axisymmetric flow fields. Such interferograms are able to examine only the light beam which has passed through the test region from a single direction. Holograms are able to reproduce a light wave in both amplitude and phase, and further to



simultaneously reproduce two such light waves which have occurred at different times. The resulting comparison of two reproduced light waves yields an interferogram which allows the analysis of the light which has passed through a test region from many different directions.

By interfering two coherent light waves with each other, interferometry compares their phases, and thus provides a measured comparison of their integrated index of refraction over their respective distances of travel from a common source to the film. This relative phase, expressed in multiples of wavelengths and commonly called fringe number, is described by the equation:

$$g = \frac{1}{\lambda} \int_{L_1}^{L_2} [n(x,y,z) - n_0(x,y,z)] dl \quad (1)$$

where:  $\lambda$  = the wavelength of the light at the film,

$n$  = the index of refraction seen by the traveling light wave,

$n_0$  = the index of refraction seen by the wave of the comparison scene,

$L_2 - L_1$  = the total distance of travel for each of the waves.

The index of refraction of a gas is well represented as a function of the gas density [Liepmann and Roshko, 1957] by the first two terms of a Taylor expansion:

$$n = 1 + \beta \frac{\rho}{\rho_s} + \dots \quad (2)$$

where:  $\rho_s$  = the gas density at which  $\beta$  is measured,

$\beta$  = the measured coefficient.





For air at 0°C. and 760 mm. Hg. ,  $\rho_s = .0012929$  gm/cc. , and for deep red light,  $\theta = .000291$ . Thus one can rewrite equation (1) :

$$g = \frac{\theta}{\rho_s \lambda} \int_{L_1}^{L_2} [\rho(x, y, z) - \rho_0(x, y, z)] dl \quad (3)$$

Equation (3) is a line integral equation for the unknown density. With sufficient evaluation of the function  $g$  (a function of three spatial variables which one obtains from the interferograms), one can invert the equation to obtain the density function.

### 1. The Mach-Zehnder Interferometer

Figure (1) is the schematic arrangement of a typical Mach-Zehnder interferometer [Ladenberg, ed. 1954]. The two light waves which are compared travel paths A and B respectively. Alignment of the instrument is critical to within the order of a wavelength of light, and the mirrors and lenses must be distortion free to one-tenth of that value. The chief practical disadvantage, however, is that one can evaluate the light beam from only one direction at a time through the test section.

By properly aligning the components with a uniform density field in the test section, one can exactly recombine the two light beams A and B at the film plane of the camera. Then with a flow in the test section, any phase differences recorded are those due to variations in the test section density. Such an interferogram is called "infinite fringe"

If one purposely misaligns one beam with the other (by rotating a mirror slightly) a deliberate fringe pattern is recorded. Variation in test section density is then recorded as a variation in the regularity of the



fringe pattern. This second variety of interferogram is called "finite fringe."

## 2. Holography

First reported by Denis Gabor [ 1948, 1949, 1951 ], holography is itself an interferometric process. By combining two coherent beams directly on a photographic film (Figures 2, 2a), one records a microscopically small interference pattern. Positions on the film where the two waves are in phase will record darkly. Positions where they are out of phase will remain light. When the developed photographic plate is reilluminated by the reference beam (Figures 3, 3a), the interference pattern acts as a very complex diffraction grating and diffracts three beams; these are the zero order, or transmitted illumination beam, and the positive and negative first orders, which are re-creations of the original object beam.

Mathematically, one can represent the phenomenon as the combination of any two general waves which obey the scalar wave equation [Brandt, 1968]. Let a wave be described as follows:

$$\tilde{E}(\vec{r}, t) = \tilde{A}(\vec{r}) e^{i\omega t} \text{ is the complex wave, where} \quad (4)$$

$$\tilde{A}(\vec{r}) = A(\vec{r}) e^{-i\psi(\vec{r})} \text{ is the spatial portion,} \quad (5)$$

$$A(\vec{r}) = a f(\vec{r}) \text{ is the spatial amplitude,} \quad (6)$$

$\psi(\vec{r})$  is the spatial phase function,

$a$  is the reference amplitude,

$f(\vec{r})$  is the spatial variation of amplitude, and



$\vec{r}$  is a position vector.

Since photographic film measures only the time averaged intensity over relatively many periods of the wave, one need not be concerned with the temporal portion  $e^{i\omega t}$  of the wave. Denoting the object and reference light beams by the subscripts o and r, one can represent the combination of both beams at the photographic plate as:

$$\tilde{A} = \tilde{A}_r + \tilde{A}_o = A_r e^{-i\psi_r} + A_o e^{-i\psi_o} \quad (7)$$

The intensity recorded will be:

$$I = \tilde{A}\tilde{A}^* = (\tilde{A}_r + \tilde{A}_o)(\tilde{A}_r + \tilde{A}_o)^* = |A_r|^2 + |A_o|^2 + \tilde{A}_r^*\tilde{A}_o + \tilde{A}_r\tilde{A}_o^* \quad (8)$$

where \* denotes complex conjugate. Assuming a linear ratio of intensity to transmittance of the developed hologram, the transmittance is:

$$T = 1 - T_1 I = 1 - T_1 (|A_r|^2 + |A_o|^2) - T_1 (\tilde{A}_r^* \tilde{A}_o) - T_1 (\tilde{A}_r \tilde{A}_o^*) \quad (9)$$

where  $T_1$  is the transmittance corresponding to unit intensity. Upon reillumination by the reference beam, the transmitted wave is:

$$\tilde{A}_r T = \left[ 1 - T_1 (|A_r|^2 + |A_o|^2) \right] \tilde{A}_r - \left[ T_1 |A_r|^2 \right] \tilde{A}_o - (T \tilde{A}_r \tilde{A}_o^*) \tilde{A}_o^* \quad (10)$$

where the quantities in square brackets represent attenuation. The first term represents the transmission of the reilluminating reference beam, the second term represents the production of an attenuated object beam, and the third term represents a modified reconstruction of the complex conjugate of the object beam (Figure 3). The modification of the conjugate object wave depends upon the nature and direction of the reference beam, but for simple reference waveforms there is usually only a magnification



and angular displacement to the opposite side of the reference wave. The negative sign on the reconstructed wave amplitude is immaterial, since a negative amplitude on a continuous wave simply represents a  $180^\circ$  phase change.

If the reillumination beam is different from the original reference beam, the reconstructed diffraction beams are distorted accordingly. For the most part, this distortion is due to different source location or different wavelength of light, which create magnification and angular displacement of the object waves.

For laboratory use, the reconstructed holographic image can be considered an almost exact duplication of the original.

### 3. Holographic Interferometry

The application of holography to interferometry [Heflinger, et. al., 1966] derives from the fact that the holographic film records the diffraction pattern almost linearly. When double exposed, the hologram records two diffraction patterns superimposed upon one another. Therefore, when a double exposed hologram is reilluminated, each recorded diffraction pattern will diffract its own first order beams. An observer will see both recorded scenes simultaneously. One may simply replace  $A_o$  by  $A_{o1} + A_{o2}$  in equations (8-10). To produce a holographic interferogram of a test section as in Figure 2, one exposes the hologram for one-half the exposure time with no flow in the test section (the uniform field provides the





comparison beam); then completes the exposure with the subject flow field present. The two reconstructed waves will interfere with each other in much the same manner as do the two waves of the Mach-Zehnder in the infinite fringe configuration.

If, instead of making a second exposure of the hologram, one replaces it exactly in position and reilluminates both the hologram and the object, one can again compare the two waves, except that in this case one of the object scenes is real and the other is a reconstructed virtual image. Such real-time holographic interferometry is called the "live" fringe technique.

The chief advantage of either method is that, except for differences in the test section, both the test and the comparison beams have traveled through exactly the same optical regions. Optical components are then automatically matched. In practice rather crude optical components can be used with excellent results.

By a slight rotation of the hologram or of one of the mirrors between exposures, one can achieve the same finite fringe presentation as with the Mach-Zehnder.

#### a. Dark Field Interferograms

Dark field interferograms are produced when the test section does not contain any light scattering properties. The observer looking at the reconstructed image is unable to focus on anything other than the



source; objects in the test section, as well as regions of interference, can only be observed as shadows. Such interferograms correspond to those taken by ordinary methods with only one direction of light beam passage through the test field, corresponding to only one light source.

#### b. Light Field Interferograms

True three-dimensional interferograms are obtained when a diffuser plate is placed between the source and the test section. The object beam then becomes diffused through the test section and appears to the observer as a continuous background of source points against which the test section, and its interference pattern, become a silhouette. Because each point of the diffuse plate acts as an individual source for any line of sight passing through it, equation (3) may be evaluated for any line which passes through both the diffuser plate and the hologram. A continuous evaluation of the function  $g$  can thus be provided as a function of position and angle. This function  $g$ , the fringe pattern, changes as the observer changes viewing aspect, but generally the fringe patterns cannot be localized by their parallax.

By arranging several holographic plates about a test section, as in Figure 4, one can obtain the fringe number function for a rather continuous segment of angular variation about the  $z$  axis of the field. The resulting array of integral values can be applied to the inversion of equation (3) to provide a solution for the density field in the test section.



## B. THE INTEGRAL INVERSION

### 1. The Basic Equation to Invert

Equation (3), rewritten for a plane of constant  $z$  is:

$$g(y', \xi, z_c) = Q \int_{x'_1}^{x'_2} f(x, y, z_c) dx' \quad (11)$$

where:  $f(x, y, z_c) = \frac{\rho(x, y, z_c)}{\rho_\infty} - 1 \quad (12)$

and:  $Q = \frac{\rho_\infty \beta}{\rho_s \lambda} \quad (13)$

$x'$  and  $y'$  are measured in a coordinate system which is rotated by an angle  $\xi$  about the  $z$  axis (Figure 5).

### 2. Maldonado's Inversion

The integral inversion method utilized in this investigation was first reported by C. D. Maldonado et. al. in 1965 [1966; Olsen, 1968]. It was used for obtaining plasma emissivity within a particular region from the measured values of emission intensity measured from outside the region. The form of the equation resulting from such emissivity studies is identical to that of equation (11). The procedure involves the representation of the function  $f$  of equation (11) in a complete set of orthogonal functions, with the expansion coefficients evaluated by use of the orthogonality condition.

An earlier method involving series expansion of the function  $f$  had been reported in 1962 by S. I. Herlitz. The method applied to cases of asymmetric function of finite domain. Maldonado's method follows similar logic, but it is applicable to asymmetric functions of infinite domain.



The function  $f$  is assumed to be squared integrable over the infinite plane so that it may be expanded in a complete set of orthogonal functions. The selection of a suitable set of orthogonal functions is discussed in Appendix B.

#### a. The Analytical Procedure

The unknown function may be expanded in a special set of functions  $U_{m+2k}^{\pm m}$  which are orthogonal with respect to the weighting function  $e^{-(\alpha^2 x^2 + \alpha^2 y^2)}$ :

$$f(x, y) = \sum_{m=0}^{\infty} \sum_{k=0}^{\infty} \epsilon_m \left[ C_{m+2k}^m(\alpha) U_{m+2k}^m(\alpha x, \alpha y) + C_{m+2k}^{-m}(\alpha) U_{m+2k}^{-m}(\alpha x, \alpha y) \right] \cdot e^{-(\alpha^2 x^2 + \alpha^2 y^2)} \quad (14)$$

where  $\epsilon_m = \frac{1}{2}$  for  $m = 0$ ,  $\epsilon_m = 1$  for  $m = 1, 2, 3, \dots$  and  $C_{m+2k}^{\pm m}$  are the unknown complex coefficients of expansion.  $\alpha$  is an arbitrary scale factor which may be considered the reciprocal of a non-dimensionalizing coefficient.

The functions  $U_{m+2k}^{\pm m}$  are defined:

$$U_{m+2k}^{\pm m}(\alpha x, \alpha y) = (-1)^k \alpha \left[ \frac{k! (\alpha^2 x^2 + \alpha^2 y^2)^m}{m! (m+k)!} \right]^{\frac{1}{2}} e^{\pm i m \phi} L_k^m(\alpha^2 x^2 + \alpha^2 y^2) \quad (15)$$

where:  $\phi = \tan^{-1}\left(\frac{y}{x}\right) - \frac{\pi}{2}$ , and  $L_k^m$  is the associated

Laguerre polynomial:

$$L_k^m(\alpha^2 x^2 + \alpha^2 y^2) = \sum_{s=0}^k \left[ \frac{(m+k)!}{(k-s)! (m+s)! s!} \right] \cdot \left[ (-1)^s (\alpha^2 x^2 + \alpha^2 y^2)^s \right] \quad (16)$$

The function  $U_{m+2k}^{\pm m}$  has a gauss transform:

$$I_{m+2k}^{\pm m}(\alpha y', \xi) = \int_{-\infty}^{\infty} U_{m+2k}^{\pm m}(\alpha x, \alpha y) e^{-\alpha^2 x'^2} dx' = \frac{e^{\pm i m \xi} H_{m+2k} \alpha y'}{[k! (m+k)!]^{\frac{1}{2}} 2^{m+2k}} \quad (16a)$$





where  $H_{m+2k}(\alpha y')$  are Hermite polynomials of order  $m+2k$ .

The particular advantage of the set of functions  $U_{m+2k}^{\pm m}$  is that they are "invariant in form" to a rotation of coordinate system [Maldonado, 1965]. That is, they remain an orthogonal set under a rotation of the coordinate system. Observe that in the equation for the polynomial (15), the angle  $\phi$  occurs only in the complex exponential term.

In terms of the expanded function  $f$ , and utilizing the transform relation of equation (16), equation (11) becomes:

$$g(y', \xi) = \sum_{m=0}^{\infty} \sum_{k=0}^{\infty} \epsilon_m \left[ k! (m+k)! 2^{m+2k} \right]^{-\frac{1}{2}} \left[ C_{m+2k}^m(\alpha) e^{im\xi} + C_{m+2k}^{-m}(\alpha) e^{-im\xi} \right] H_{m+2k}(\alpha) e^{-\alpha^2 y'^2} \quad (17)$$

Equation (17) is subject to the following orthogonality condition:

$$\int_{-\pi}^{\pi} e^{\pm im\xi} e^{\mp in\xi} d\xi \int_{-\infty}^{\infty} H_{m+2k}(\alpha y') H_{n+2l}(\alpha y') e^{-\alpha^2 y'^2} dy' = \frac{2\pi^{\frac{3}{2}}}{\alpha} \left[ (m+2k)! (n+2l)! 2^{m+2k} 2^{n+2l} \delta_{mn} \delta_{(m+2k)(n+2l)} \right] \quad (18)$$

Where  $\delta$  is the kroneker delta function. The solution of equation (18)

applied to equation (17) leads to the expansion coefficients:

$$C_{m+2k}^{\pm m} \alpha = \frac{\alpha}{2\pi^{\frac{3}{2}}} \left[ \frac{k! (m+k)!}{(m+2k)!} \right] \cdot \int_{-\pi}^{\pi} \int_{-\infty}^{\infty} g(y', \xi) e^{\mp im\xi} H_{m+2k}(\alpha y') dy' d\xi \quad (19)$$



Equation (17), with the coefficients of equation (19), represents the function  $g$  by a Gram-Charlier series in the radial direction, and by a Fourier series in the azimuthal direction.

Equation (14), with the coefficients of equation (19), becomes:

$$f(x, y) = \frac{\alpha}{\pi^{3/2}} \sum_{m=0}^{\infty} \sum_{k=0}^{\infty} \epsilon_m \frac{(k!(m+k)!)^{\frac{1}{2}}}{(m+2k)!} e^{-(\alpha^2 x^2 + \alpha^2 y^2)} \cdot \text{Real} \left[ \int_{-\pi}^{\pi} \int_{-\infty}^{\infty} g(y', \xi) e^{-im\xi} H_{m+2k}(\alpha y') dy' d\xi \cdot U_{m+2k}^m(\alpha x, \alpha y) \right] \quad (20)$$

or, inserting equation (15):

$$f(x, y) = \left(\frac{\alpha}{\pi}\right)^2 \sum_{m=0}^{\infty} \sum_{k=0}^{\infty} \epsilon_m \frac{(-1)^k k!}{(m+2k)!} (\alpha^2 x^2 + \alpha^2 y^2)^{\frac{m}{2}} L_k^m(\alpha^2 x^2 + \alpha^2 y^2) \cdot \left[ B_{m+2k}^m(\alpha) \cos(m\phi) + D_{m+2k}^m(\alpha) \sin(m\phi) \right] e^{-(\alpha^2 x^2 + \alpha^2 y^2)} \quad (21)$$

where:

$$B_{m+2k}^m(\alpha) = \int_{-\pi}^{\pi} \int_{-\infty}^{\infty} g(y', \xi) \cos(m\xi) H_{m+2k}(\alpha y') dy' d\xi \quad (22)$$

$$D_{m+2k}^m(\alpha) = \int_{-\pi}^{\pi} \int_{-\infty}^{\infty} g(y', \xi) \sin(m\xi) H_{m+2k}(\alpha y') dy' d\xi \quad (23)$$

Equations (21), (22) and (23) represent the fundamental inversion by Maldonado's method. Both analytical and numerical inversions were demonstrated in his series of three papers.

The method applies quite directly to density fields. The zero



value of the function  $\Delta\varphi$  studied in interferometry is arbitrary and can always be chosen such that the function is zero outside of a given circular boundary. Singularities do not occur in real density fields except for the spaces occupied by opaque objects. Cases with simple solid objects appear amenable to this method, but will not be discussed here.

#### b. The Numerical Procedure

Since experimental data are not obtained in analytical form, the indicated operations must be performed numerically. The contractual report resulting from the investigation by Olsen, et. al. [1966], included a computer program. However, it appeared more prudent to reprogram the basic equations to fit the available computer, and to more closely meet the needs of the particular application.

The form of equation (24) is a truncated form of equation (21):

$$f(x,y) = \left(\frac{\alpha}{\pi}\right)^2 \sum_{m=0}^M \sum_{k=0}^K \epsilon_m \frac{(-1)^k k!}{(m+2k)!} (\alpha^2 x^2 + \alpha^2 y^2)^{\frac{m}{2}} L_k^m (\alpha^2 x^2 + \alpha^2 y^2) \quad (24)$$

$$\cdot \left[ B_{m+2k}^m(\alpha) \cos(m\phi) + D_{m+2k}^m(\alpha) \sin(m\phi) \right] e^{-(\alpha^2 x^2 + \alpha^2 y^2)}$$

The numerical evaluations of the coefficients from equations (22) and (23) are accomplished approximately. Since the function is known to be zero outside of the circular domain of Figure (5), the integration over  $y'$  need only be made over finite limits, defined here as  $-S/2$  to  $+S/2$ . The function  $g$ , which is always single-valued, is assumed to be constant within the discrete areas of the data plane represented



in Figures (6) and (7). This permits the integrals to be represented as a finite sum of integrals over the subregions:

$$B_{m+2k}^m(\alpha) = \sum_{i=1}^{IMAX} \sum_{j=1}^{JMAX} g(y'_j, \xi_i) \int_{\xi_{i-\frac{1}{2}}}^{\xi_{i+\frac{1}{2}}} \cos(m\xi) d\xi \int_{y'_{j-\frac{1}{2}}}^{y'_{j+\frac{1}{2}}} H_{m+2k}(\alpha y') dy' \quad (25)$$

$$D_{m+2k}^m(\alpha) = \sum_{i=1}^{IMAX} \sum_{j=1}^{JMAX} g(y'_j, \xi_i) \int_{\xi_{i-\frac{1}{2}}}^{\xi_{i+\frac{1}{2}}} \sin(m\xi) d\xi \int_{y'_{j-\frac{1}{2}}}^{y'_{j+\frac{1}{2}}} H_{m+2k}(\alpha y') dy' \quad (26)$$

The integrals are then evaluated over the sub-intervals with  $\xi_{\frac{1}{2}} \equiv -\pi$ ,

$$\xi_{IMAX+\frac{1}{2}} \equiv +\pi, \quad y'_{\frac{1}{2}} \equiv -\frac{S}{2}, \quad \text{and} \quad y'_{JMAX+\frac{1}{2}} \equiv +\frac{S}{2}$$

The integrals over  $\xi$  are elementary, and the integrals over  $y'$  are evaluated by use of the derivative formula for Hermite polynomials [Erdelyi,

et. al., 1953]. The resulting general formulae for B and D are:

$$B_{m+2k}^m(\alpha) = \frac{1}{2\alpha(m+2k+1)} \sum_{i=1}^{IMAX} \sum_{j=1}^{JMAX} g(y'_j, \xi_i) \left[ \frac{\sin(m\xi_{i+\frac{1}{2}}) - \sin(m\xi_{i-\frac{1}{2}})}{m} \right] \cdot \left[ H_{m+2k+1}(\alpha y'_{j+\frac{1}{2}}) - H_{m+2k+1}(\alpha y'_{j-\frac{1}{2}}) \right] \quad (27)$$

$$D_{m+2k}^m(\alpha) = \frac{-1}{2\alpha(m+2k+1)} \sum_{i=1}^{IMAX} \sum_{j=1}^{JMAX} g(y'_j, \xi_i) \left[ \frac{\cos(m\xi_{i+\frac{1}{2}}) - \cos(m\xi_{i-\frac{1}{2}})}{m} \right] \cdot \left[ H_{m+2k+1}(\alpha y'_{j+\frac{1}{2}}) - H_{m+2k+1}(\alpha y'_{j-\frac{1}{2}}) \right] \quad (28)$$

which are valid for  $m > 0$ . The special case of  $m = 0$  represents the axisymmetric solution. The terms within the brackets  $\left[ \right]$  are evaluated by l'Hospital's rule:  $D_{0+2k}^0 = 0$ , and





$$\lim_{m \rightarrow 0} \left\{ \frac{\sin(m\xi_{i+\frac{1}{2}}) - \sin(m\xi_{i-\frac{1}{2}})}{m} \right\} = \xi_{i+\frac{1}{2}} - \xi_{i-\frac{1}{2}} = \Delta\xi \quad (29)$$

### c. The Computer Program - Holofer

In order to perform the inversions a FORTRAN IV computer program called HOLOFER, which includes a large number of variable parameters and optional modes of operation, was written. The complete program, with input parameter descriptions and the working data, is included in appendix C.

(1) The Basic Program. The data plane, called the G-array, consists of a discrete set of values of the function  $g$  of equation (11) taken over regular intervals of  $y'$  and  $\xi$ , of size IMAX by JMAX (Figure 7). The G-array is obtained in one of three modes. Mode one computes the G-array that corresponds to an optional test function by the numerical integration of equation (11) at regular intervals of  $y'$  and  $\xi$ . By generating its own data from a test function, mode one provides the basic program testing capability. In mode two operation, HOLOFER interpolates a regular G-array from an irregularly entered set of values such as those normally obtained in holographic interferometry. Mode three operation reads in a regular array of input values directly.

Next, equations (27) and (28) are evaluated for each set of coefficients B and D up to the series truncation values of  $m = \text{MLIMIT}$



and  $k = \text{KLIMIT}$ . These B and D values are stored on external (DISK) storage.

Having computed the B and D coefficients, HOLOFER next evaluates equation (24) for each point in the test section individually. Either a cartesian or a cylindrically aligned array of spatial coordinates can be accommodated by choice of input parameters. In the evaluation of equation (24), truncation of each series is performed by first specifying an input parameter epsilon. If a certain number of terms in a row remain less than epsilon times the existing partial sum, the series is truncated. If the index values reach the limiting available set of B and D coefficients before the series has converged, the most recent few values of the partial sum are averaged.

(2) Add-On Functions. A second G-array may be computed and added to the original G-array prior to the inversion. The array is computed in the mode one operation from any given function. In addition, a gaussian random number of specified standard deviation may be added to the second G-array. The first feature provides the capability of adding a smoothing function to data with severe properties, such as from shock waves or opaque discontinuities in the interferograms. Peripheral information about the function may be used to determine a desirable function. The known add-on function is then automatically subtracted from the solution. The second feature allows one first to perform the inversion



of a set of data with a known error size and then to compare the result with a previous solution in order to estimate the possible error in the solution.

(3) Shock Waves. The polynomial series representation of discontinuous or high gradient regions such as those from shock waves requires a large number of terms. Accordingly, the inversion routine requires a large index of  $m$  and  $k$  to represent steep gradients. If sufficiently many data points are entered on input to provide adequate significance in the high order terms, one can utilize rather large values of MLIMIT and KLIMIT to obtain reasonably accurate inversions.

If one has prior knowledge of the function to be inverted, such as an isentropic solution of a flow field, an add-on function can be added which will smooth the net function at such discontinuities, i.e. the subtraction of a "plug" function shape in Figure (12). Such modification enhances the convergence of the resulting function, if it is well matched, and it therefore improves the accuracy of the result. An analogous method applicable to the Abel axisymmetric inversion has been described by Bennet, Carter, and Bergdolt [1952], called the method of "reduced functions," which operates on the fringe curve directly.

#### d. Symmetry

HOLOFER is designed to invert an asymmetric field. There



are, however, several simplifications to the process that result from symmetry in the field.

(1) Axisymmetric Fields. For axisymmetric fields, the angular variations disappear with the result that only one view or one line of the G-array need be considered. The coefficient evaluation integrals over the angular domain thus become zero, for all except the  $m = 0$  case, and the summation process simplifies to a single series. Computation time in this mode is reasonably short, from 20 - 60 seconds on the IBM 360-67 digital computer for KLIMIT = 1000. The majority of program testing has been in this mode.

(2) With Planes of Symmetry. Planes of symmetry in the field reduces the angular requirements of the input data. In Figure (8), the data plane is shown divided into unique segments, only one of which need be supplied. Note that even in the asymmetric case, the data plane has two duplicate (though inverted) segments. The function looks the same from opposite sides of the domain, with reversed argument:

$$g(\gamma', \xi) = g(-\gamma', \xi + \pi) \quad .$$

Additionally, the domain of orthogonality is reduced for cases of planar symmetry greater than one. The regions which are not cross hatched, are subdomains of orthogonality. The region of integration for coefficient evaluation is reduced accordingly in the program. The index value  $m$  in the series representation corresponds to the Fourier mode of the expansion of the function  $f$  in the azimuthal





direction. Therefore, for cases of planar symmetry the coefficients are zero for certain values of  $m$ . To summarize:

Asymmetric:	uses all B and D coefficients:
One Plane:	uses B coefficients only, all
Two Planes:	uses B coefficients, $m = 0, 2, 4, 6,$
Three Planes:	uses B coefficients, $m = 0, 3, 6, 9 \dots$
Four Planes:	uses B coefficients, $m = 0, 4, 8, 12 \dots$
Five Planes:	uses B coefficients, $m = 0, 5, 10, 15 \dots$
etc.	

Axisymmetric corresponds to an infinite number of planes of symmetry: uses B coefficients  $m = 0$  only.

While the higher numbers of symmetry planes have little practical value, they are included automatically in the generalization of the program symmetry tests.

### 3. Theoretical Results

#### a. Artificial Data Generation

Mode one of the program generates the G-array for a specified function. Several functions are included in subroutine FUNCT for use as program tests or as add-on functions. Provision is also made to enter an arbitrary function in subroutine SPFUN by simply entering the Fortran cards describing the function. In addition, a set of numerical values may be read in and used as a function with linearly



interpolated values between the given points. The G-array is evaluated at each value of  $y'$  and  $\xi$  as shown in Figure (7). Simple summation of the function value at  $3 \cdot (IMAX)$  points along the line  $y' = \text{const.}$  is used to evaluate the integral. Once the data plane is filled, the inversion process makes no distinction between computed or experimental data in the G-array.

#### b. Test Inversions

(1) Axisymmetric. Figure (9) represents the function, computed fringe curve, and inverted solution of a gaussian function similar to Maldonado's test case:

$$f = e^{-\theta^2(x^2+y^2)} \quad (30)$$

The original analytical function is shown as a solid line, while the corresponding computed fringe curve is shown to a separate scale as a series of boxes. The greatest difference between the inverted solution and the original function was 0.001, or 0.1 percent of the maximum function value.

Figure (10) is a cosine-squared function:

$$f = \cos^2 \left( 2\pi (x^2+y^2)/3 \right) \quad (31)$$

The greatest inversion error was 0.5 percent of the maximum functional value.

To determine the capability of the program to invert shock-wave type discontinuities, a circular square wave, or "plug" function, was inverted. Figure (11) shows a rounding off of the discontinuity that is



typical of a truncated series representation. The maximum error that occurs in the nearby region is 6.2 percent. At the center of the function, at radius zero, the series does not converge. The resulting 8.6 percent error is typical of the center point of inverted functions containing discontinuities.

Winckler, in an extensive application of the Abel inversion method to free jets [1948], used a hypothetical test function that is shown in Figure (12). Plots of the solutions he obtained are shown for comparison of the two methods. The characteristic "overshoot" of the Abel method near the discontinuity is shown, where the largest error by the Maldonado inversion was 3.8 percent.

Figures (13) and (14) are inversions of typical axisymmetric density functions from the Winckler analysis of a free jet. They demonstrate the capability of the inversion routine with realistic types of functions. Both inversions were accurate to within 2.6 percent.

(2) Non-Axisymmetric. Figure (15) represents three cross-sections of the same gaussian function as before, now centered at  $x = .1, y = 0$ . cm. This corresponds to the test example that Maldonado used in the verification of his inversion scheme. The solution is everywhere accurate to within 0.8 percent with a very low number of series terms. The function is planar symmetric and thus tests only the cosine terms of the expansion.



Figure (16) represents three-cross-sections of an asymmetric test case. The function is an elliptical cone of base diameters  $0.7 \times 0.5$  cm., centered at  $x = 0.707$ ,  $y = 0.707$  cm. In the solution, the tip of the cone is rounded by the natural smoothing characteristics of the inversion method, but otherwise the maximum error is 1.5 percent. This test case represents a complete test of the inversion procedure, utilizing both B and D terms of both series expansions.

### III. EXPERIMENTAL APPROACH

#### A. DESCRIPTION OF THE APPARATUS

##### 1. The Holographic Table

A holographic work table was designed and constructed to provide optical bench facilities about a free jet, as shown in Figures (17) and (18). The table was designed to evaluate various arrangements of optical components to achieve a wide angle of holographic field of view, and to suppress the vibration caused by the free jet noise.

The table was made of pressed plywood laminate, two and one-half inches thick. The four by six foot table was mounted on a rotatable set of plywood boards, with a centerhole of eight inches diameter to accommodate the free jet. This arrangement provided the capability of rotating the entire table about the flow field. Below the rotating arrangement, the table rested on four small tire tubes to provide





structural vibration isolation from the building. For experiments conducted in C-W gas laser holography with up to thirty second exposure times (without the free jet) the arrangement was very successful. Beneath the inner-tube mounting, the table rested on four standard automobile type screw jacks. Recessed jack points allowed the table to be readily tilted to about  $15^{\circ}$  about the flow field.

A Korad K-1 pulsed ruby laser operating at a wavelength of 6941. Å. was employed with a Pockels cell Q switching device. The resultant effective hologram exposure time was about 20 ns., eliminating problems with vibration during the hologram exposure. There does remain the problem of vibratory misalignment of the optical components between the two exposures of the holographic interferogram. To help damp acoustically-caused vibration, the mirrors were all mounted on heavy metal blocks. The weakest link in the setup appeared to be the beam splitter holders. They were lightest of the table components, and as a result of their vibration, holographic interferograms obtained tended to have a finite fringe. Occasionally a hologram would be unusable because the fringe spacing became too fine to resolve.

## 2. The Test Section

The table was mounted around a standing free jet. The plenum chamber was about 45 cm. long by 30 cm. diameter. The jet extended 45 cm. above the plenum chamber with an inside diameter of 3.18 cm. and



a throat diameter of 2.0 cm. at the exit. The test section was defined by a square plexiglass enclosure, the four inside surfaces of which were inscribed with a one centimeter square grid. The grid box provided some vibration insulation for the jet, and also produced a self-contained coordinate system for the hologram and the corresponding photographs. The holograms were arranged about the grid box as shown in Figure (19), with the coordinate system established as shown. Commercial ground glass plate was used as the diffuser.

### 3. Laboratory Techniques

Alignment of the laser beam with the optical components was accomplished by aligning a continuous wave helium-neon gas laser through the rear mirror and along the ruby axis of the pulsed laser. A -20 cm. meniscus lens of inexpensive quality was used to diverge the beam. Care must be exercised in this arrangement to insure the convex side of the lens is towards the ruby laser. Concave surfaces in the near vicinity of a high power laser can themselves focus a high density of reflected energy, which might damage the laser itself or any near components.

Relative intensities of reference to object beams of about 4:1 were found to yield good holograms.

Since the arrangement of the several mirrors, beamsplitters, etc., so as to have the same optical path length from source to hologram for each beam is a tedious procedure, a cork pinboard was designed to



facilitate the table arrangements. Threads of the same length, each one representing a laser beam, were stretched from the laser source to their various holograms via different routes over a sketch of the table and held in position with pins. The table has a six inch grid painted on its surface to facilitate location of the components from the grid on the sketch. The pin board saved many hours of arrangement time.

Holograms were made on Agfa-Gaefert 8E75 holographic plates. Development was five minutes in Kodak D-19 developer, 30 seconds in acetic acid stop bath of standard dilution, five minutes in standard fixer, one minute water wash, followed by immersion in wetting agent (Kodak PhotoFlo) prior to drying. It was observed that good reconstructions of restricted field of view could be obtained immediately after developing, while the plate was still wet. Normal reconstructions were made with the continuous wave gas laser at 6328Å. The resulting image magnification from reconstruction at a different wavelength was not considered deleterious. The technique used in making photographs for data extraction will be discussed in the next section.

## B. HOLOGRAPHIC EXPERIMENTAL RESULTS

### 1. Non-Flow Holographic Experiments

Holographic experience was gained with a Spectra-Physics model 124 gas laser. Both back-lighted scenes and diffuse objects were recorded.



Real time interferometry of a test area was demonstrated and surface deformation interferometry was obtained. Figure (20) shows the interference pattern on the surface of a small clamping device under strain. Figure (21) is one view of the interference pattern about a cigarette. Between exposures of the hologram, the cigarette had been radiantly heating the platform below it for about three minutes, and the platform shows the interference pattern caused by the resulting thermal expansion. The gas laser was used to confirm the optical arrangement of Figure (19) for multiple hologram viewing of the free jet test scene. Successful holographic interferograms were obtained of cigarettes at all hologram positions.

## 2. Free Jet Experimentation

The Korad giant pulse laser was installed on the table and holograms taken of the free jet exhausting to the atmosphere. Figure (22) shows a shadowgram taken at 35 psig plenum pressure. A shadowgram is produced directly on the hologram plate when the holographic image is recorded by a single exposure of the dark field technique (with the ground-glass diffuser absent).

Figures (23) and (24) show two views obtained from the same holographic interferogram of jet flow at 60 psig. The interferometric data from this hologram were inverted to provide an axisymmetric solution. The results of the solution follow in section D. Holographic





interferograms were also taken at 25, 40, 45, and 50 psig. , but were not reduced. Turbulent flow perturbations became more predominant as the pressure was reduced.

To provide a non-axisymmetric test of the method, the table was tilted  $11^{\circ}$  clockwise about the y axis of the table. As a result of the tilt, horizontal cross sections through the field became planar symmetric about the x-z plane. The solution of planar symmetric fields require a  $90^{\circ}$  field of view. Three simultaneous holographic interferograms were taken about the tilted jet at 60 psig. with the arrangement shown in Figure (19). Each of the three holograms provided a field of view of about  $15^{\circ}$ , one of which had several degrees obscured by the corner of the box. To provide more complete coverage, the table was rotated and additional holograms taken. Two rotations were required. Figures (25) and (26) show the interferograms taken at  $5^{\circ}$  and  $85^{\circ}$  which were used in the data reduction.

### 3. Experimental Techniques and Considerations

Previous work at this laboratory [Sullivan, 1968] had shown the intensity transmission of collimated laser light beyond commercial ground glass falls below 30 percent of the incident intensity beyond viewing angles of about  $\pm 8^{\circ}$ . Since the diffraction capability of a holographic plate exceeds  $\pm 8^{\circ}$ , the ground glass represents the limiting factor to the field of view. In fact, usable holographic interferograms were obtainable with from  $\pm 5^{\circ}$  to  $\pm 10^{\circ}$  field of view, centered about the object beam direction,



the field size being a function of the ratio of the intensities of object beam and reference beam.

The holographic interferogram appears as a completely three-dimensional set of fringes to the observer. Only special cases of the fringe pattern can be localized, those corresponding to Young's fringes (the finite fringe background pattern), or those corresponding to regions of spherical or cylindrical density variations. To obtain usable data from the fringe number function, one must sample discrete segments of the information. This is done by recording a series of photographic interferograms at regular angles about the test section. For a completely general field one requires  $180^{\circ}$  field of view, while the planar symmetric case studied required  $90^{\circ}$ .

There are two basic methods of obtaining sufficient angular coverage of the field. The first is to take several individual holograms, rotating the relative angle between the hologram setup and the test section for each hologram. Unsteadiness in the flow between the exposures will introduce errors. The second method involves arranging a series of holograms about the test section for simultaneous exposure. Intervals in the data from the second method are filled by interpolation. Interpolation over large angles requires that the function vary slowly in the angular direction. This experiment utilized a combination of both methods.



#### a. Photographic Technique

A normal photograph of the hologram records an image of the focus plane as shown in Figure (28). Each position on the photograph represents the line of sight from the image to the aperture (Figure 27). All of these lines of sight will represent a non-parallel set of lines. For reasonable camera focus distances, the deviation from parallelism is small and may be neglected. The spatial filtering technique shown in Figure (29) allows the selection of parallel sets of lines of sight for the recorded fringe pattern. The aperture stop at the focal plane of the lens filters out all but the lines parallel to the central angle. The resulting photographs are simpler to analyze since the angles are constant. In addition, fringe data from any  $z$  plane may be obtained from the single photograph. Mach-Zehnder interferograms, because of their single collimated source, provide the same type of interferogram.

The technique utilized for this investigation was an application of the lensless focusing capability of the hologram and is easier to achieve than the previous two methods. Figure (29a) shows a hologram being re-illuminated by a conjugate reference beam of small diameter. The real image of the test scene is formed in the same position as shown in Figure (3). Because the reconstruction beam is of small size, the illuminated portion of the hologram represents a small aperture. The resulting image has a large depth of field and a photographic film placed at the



image records the test scene. Additionally the rays may be focused in the most desirable plane by positioning the film plane, usually near the center of the disturbance. The lines of sight recorded represent the diverging bundle passing through the aperture position from the diffuser. The maximum angle of divergence at the edge of the test field encountered was  $\pm 5^\circ$ . For resolution greater than  $\pm 5^\circ$ , one must compensate for the variation. A subroutine of the computer program was written to accomplish this compensation, but the errors introduced by neglecting the bundle divergence have been acceptably small, and use of the routine has not been required.

The specular interference of coherent light from a diffuse surface causes a film graininess that is inversely proportional to recording aperture size [Tanner, 1967]. Although recording apertures of one millimeter were used, the speckle created no problems.

#### b. Data Reduction

To obtain the photographic interferograms, a camera back with viewing screen was placed in the position of the real image of the hologram as previously described (Figure 29a). The illumination of each position on the hologram corresponds to a particular effective aperture position. The hologram was positioned such that the desired set of front and rear grid lines lined up on the camera back viewing screen corresponding to the desired elevation and angle of view for the picture. Reference





to Figures (23) and (24) show grid alignments at  $z = 3. \text{ cm.}$ ,  $\xi = 0^\circ$  and  $z = 1. \text{ cm.}$ ,  $\xi = 0^\circ$  respectively. Polaroid P/N 55 film was used to record the image.

To obtain the graphical plot of the fringe number function, the negative was used in a photo enlarger to image directly upon graph paper. With the enlargement adjusted to match the scale of the paper, the positions of the maxima and minima of the fringes along the desired cross section were determined visually. The fringes were counted, and given a graphical elevation according to their number. Initial fringe numbering was arbitrary, commencing with a fringe well to one side of the field and proceeding across the field, the light regions representing integer values of the fringe number.

Figure (30) shows a typical working graph that was used for the  $\xi = 5^\circ$  view of the tilted jet. The finite fringe reference line was drawn from the field edges and the curve was transcribed. Numerical values were then read from the curve at regular increments of radius ( $y'$ ) corresponding to the G-array size IMAX.

For the axisymmetric case the entire procedure was repeated for each level  $z$  plane to be solved. Since each aperture position on the hologram corresponds to a particular elevation and angle of view, a new picture was made for each horizontal  $z$  plane through the field.



For the asymmetric case, a new picture was taken for each angle  $\xi$  desired. When the angle desired was not available because of gaps in the holographic coverage, the curve was graphically interpolated from nearby curves on either side. Fringe curves were obtained in the standard manner for angles on each side. The two curves were then overlaid on a light table and an intermediate curve drawn at the proper relative distance.

#### IV. THE APPLICATION OF THE INTEGRAL INVERSION TECHNIQUE TO THE EXPERIMENTAL RESULTS

##### A. AXISYMMETRIC SOLUTION

The interferometric data from the hologram of the free jet at 60 psig. were reduced at eight positions out to  $z = 2.0$  cm. in the manner described previously. Figure (31) shows the fringe curves obtained at  $z = 0.5$  cm. and  $z = 1.5$  cm. with their corresponding density solutions. The complete set of solutions are shown topologically in Figure (32). The solution compares quite well with the topological features of the free jet solutions obtained by Ladenberg, Van Voorhis, and Winckler [1949] in their very extensive interferometric analysis of free jets of one centimeter diameter. Figure (33) is an isodensity line plot of the obtained data. Qualitatively, the densities compare very well with the similar plot of the Winckler solution (Figure 34). Exhaust density in the central region



of the exit plane agrees within 0.2 mg/cc (5.3 percent of the maximum field density) and in the central region at  $z/d=1$ . ( $d$ = nozzle diameter) within about 0.1 mg/cc (2.8 %), rising to a maximum of 0.4 gm/cc (10.6%) between. At a relative radius of one-half, the difference in the two solutions runs from about 0.05 mg/cc (1.4%) at  $z/d=0$ . rising to about 0.2 mg/cc at  $z/d=0.25$  and falling to 0.1 mg/cc at  $z/d=1$ . At the jet radius, the maximum differences fall to about 0.05 mg/cc.

## B. NON-AXISYMMETRIC SOLUTION

Figure (35) shows the measured fringe curves obtained for the free jet at 60 psig. and eleven degrees of tilt, on a horizontal plane which intersects the jet axis at a point 0.5 cm from the nozzle. A total of nine angular positions were sampled, every other one being shown in the figure. The significant trend in these data is the shoulder increasing with decreasing angle on the left-hand side and with increasing angle on the right-hand side. A contour map of the data surface from  $\xi = 0^\circ$  to  $\xi = 90^\circ$  is shown in Figure (36). Since not all data could be obtained simultaneously, the run number from which the holograms used were obtained is shown. The non-regularities appear to be the effects of errors introduced in the correlation of angular views taken at different times. A data smoothing technique used by Maldonado, et. al. on this data plane was that of fitting smooth curves to the plotted points and adjusting the data to fit the



smoothed curves. For this experiment, however, the data were used without smoothing. Figure (37) shows a sketch of the tilted plane through the jet, with the five lines shown along which solutions were obtained. Figure (38) shows the solution at the five diametric cross sections from  $\xi = 0^\circ$  to  $\xi = 90^\circ$ . The effects of the shoulder variation in the input data show up here as variations in the position and size of the density "valley" which one can see in the axisymmetric topological plot of Figure (32). The comparison of the solution from the tilted plane at  $\xi = 0^\circ, 45^\circ$ , and  $90^\circ$  is made with the solutions taken from the axisymmetric experiment in common plots of the two functions. The shoulder and valley features of the two solutions appear consistent. The central "hill," is consistent in the two solutions, to the point of showing a common inflection in the slope near radius  $\pm 0.5$ . The outer five points on either side of the  $90^\circ$  curve include convergence errors arising from failure of their series evaluations to converge. The maximum difference in the two solutions is about 8 percent, although the mean deviation is much less.

## C. DISCUSSION OF THE ERRORS

### 1. Numerical Inversion Errors

Several function shapes were investigated with the axisymmetric inversion to determine the effect of inversion parameters upon the accuracy of the inversion. Errors resulted from two basic causes: one





was the failure of the series evaluation to converge within the maximum number of terms for which computed coefficients B and D were available; the other was the approximation caused by representation of the continuous function  $g$  by a discrete set of values.

Convergence of the series evaluation is fastest in regions where the functional shape matches a gaussian. As few as five terms of the K series were sufficient to evaluate the gaussian function to within one percent everywhere. The asymmetric test of Figure (15) of the displaced gaussian used only a maximum of 25 terms, corresponding to  $MLIMIT=5$ ,  $KLIMIT=5$  to achieve accuracy to within 0.8 percent. The opposite extreme occurs when functions with steep gradients or discontinuities are inverted. For example, in the test of Winckler's function (Figure 12), the region near the discontinuity required up to 1700 terms for convergence; at the discontinuity itself, convergence was not achieved with 2000 terms. For functions with such discontinuities, or for experimental data inversions where there are normal irregularities in the data, the center position (at radius zero) often fails to converge, resulting in error at that position of up to 10 percent. When convergence has failed, however, the index count of the output information clearly indicates the failure, and this point value may be simply neglected. Interpolation of the missing value from nearby convergent points normally reduces the error to within two percent.



Decreasing the number of points of the data plane reduces the significance of the higher order modes of the series expansion. This rounds normally smooth functions, and causes oscillations in functions with discontinuities. For example, the step function of Figure (11) had a maximum error of 6.2 percent with  $IMAX = 200$ , and maximum error of 12.7 percent with  $IMAX = 100$ . Additionally, the inversion at  $IMAX = 100$  caused a severe oscillation over most of the step.

Since there is no mathematical requirement in the inversion for regular spacing of the data grid, modification of the numerical equations could be made to accommodate finer mesh sizes in the regions of special interest.

## 2. Errors in the Data

The errors in the final solution are mostly due to errors in the data. There are several independent sources of data errors, covered here individually.

Probably the greatest source of error in the data arises from the unsteadiness of the jet flow. The three apparent perturbations in the solution of Figure (33) correspond to 0.1 mg/cc and 0.2 mg/cc respectively. Based upon the maximum density in the field, these correspond to 2.8 and 5.6 percent errors. Variations in the flow between the runs are considered responsible for the major fluctuations evident on the data plane shown in Figure (36). The asymmetric solution tends to spread



errors over the whole field, reducing their effect by statistical averaging.

Graphical positioning of the interferogram and scale matching in the photo-enlarger to graph paper step is accurate to within two percent. However, a two percent position error might be magnified to a five percent density error in regions of normally high density gradient. The accuracy to which one can determine the fringe number position in reading the interferogram is within  $\pm 1/8$ th. of a fringe, or within about 1.5 percent of the maximum fringe number of the flow interferograms studied. Winckler has provided an analysis of the relative merits in reading several different fringe arrangements to minimize the fringe number error. Figure (39) shows the inverted solution of the axisymmetric test case at  $z = 0.75$  cm. with a second solution superimposed. The second solution has been made from data with added random error of 0.0625 standard deviation, corresponding to  $\pm 1/8$ th. fringe number error in reading the data. The resulting error varies with a maximum of 2.1 percent.

The background finite fringe spacing is assumed to be constant through the field. Figure (40) illustrates the type of error that could exist by the failure of linearity. An error curve that starts at zero at the boundaries of the flow and rises to one-half fringe in the number



would yield a maximum solution error of 0.18 mg/cc at the center, or about 5.0 percent for the axisymmetric solution.

It is estimated in the solution presented herein that probable errors are less than 8 percent everywhere, corresponding to the maximum difference in comparison of the two solutions in Figure (38).

## V. SUMMARY

### A. CONCLUSIONS

A self-consistent method has been demonstrated for the acquisition of interferometric data about a three-dimensional density field of one plane of symmetry. The data set has been successfully inverted by the application of a recently developed mathematical inversion scheme and shown to be reliable to within eight percent of the density range. The mathematical model has been tested for realistic density patterns, representing supersonic wakes and jets. The pulsed laser method of holographic interferometry can be successfully applied in environments relatively hostile to normal interferometry. There are no inherent restrictions to the application of the method to generally asymmetric fields. The optical arrangement of the system is highly flexible and can be modified for interferometric studies of wakes, rockets, turbo-machinery flows and other hostile, or highly transient events.





## B. RECOMMENDATIONS

Most of the errors introduced in the solution were the results of the data-reduction methods used. The use of an appropriately designed densitometer for determining fringe locations on the negatives might improve the accuracy of fringe location and merits investigation. Measurable features on some object in the test area should be incorporated for accurate scaling and positioning of the data coordinates.

Experimental improvements could be accomplished as follows.

An effort should be made to increase the field of view from the diffuser plate to provide increased angular coverage. The use of heavy, naturally damped mounts should be provided for the beam splitters for better control of the spacing of finite background fringes.

## C. ACKNOWLEDGEMENTS

The writer wishes to gratefully acknowledge Dr. D. J. Collins for his sponsorship, guidance and assistance during the course of this investigation; Dr. A. E. Fuhs for his initial encouragement in the field; Drs. R. L. Kelly, T. H. Gawain, L. V. Schmidt, and G. D. Sackman for their time and support during the period; Dr. A. B. Witte, of TRW Systems, Inc., for his initial mention of Maldonado's work; the technical staff of the Department of Aeronautics under R. Besel and T. Dunton, particularly N. Leckenby and G. Gulbranson, for their able assistance; B. Taylor, of



the Department of Physics, for the loan of many little lenses and mirrors; Mrs. Kathryn Todd, for her considerable effort in the final preparation; and my wife and family for their noble patience and encouragement.



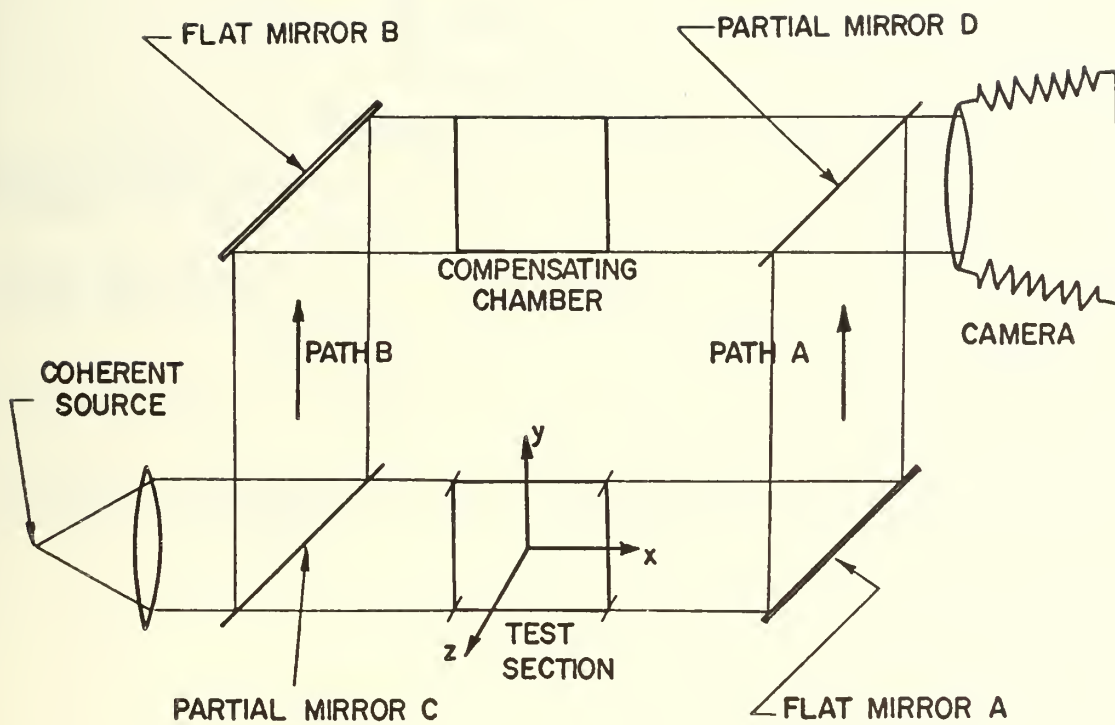


FIGURE 1: THE SCHEMATIC ARRANGEMENT OF A MACH ZEHNDER INTERFEROMETER.



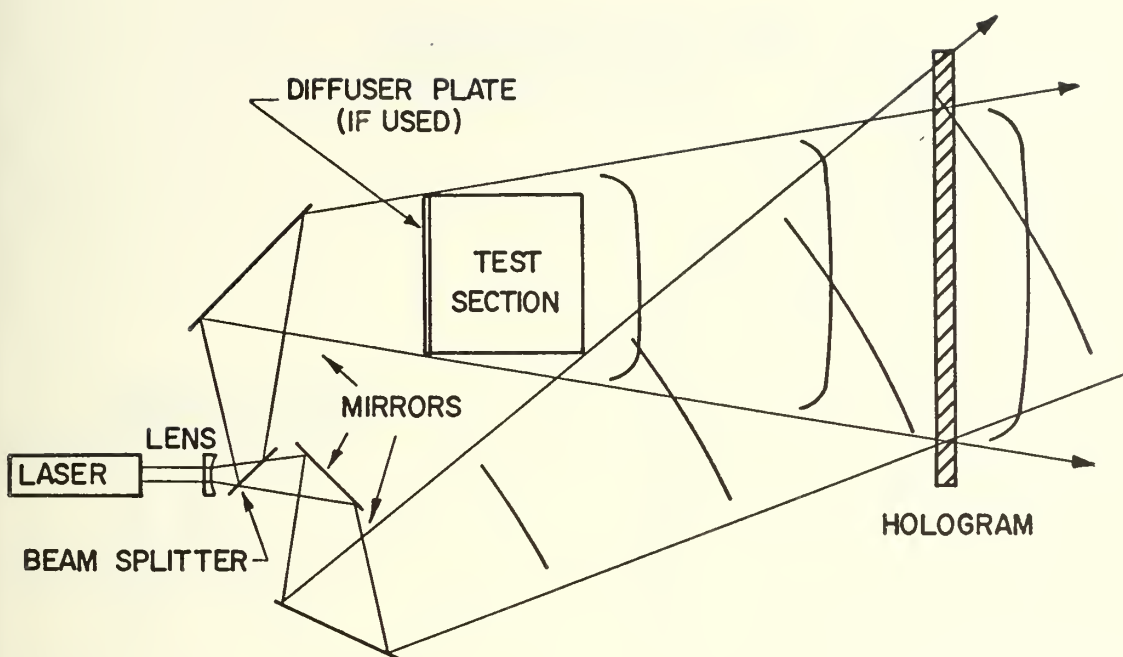


FIGURE 2: PRODUCTION OF A HOLOGRAM OF A TRANSILLUMINATED OBJECT.

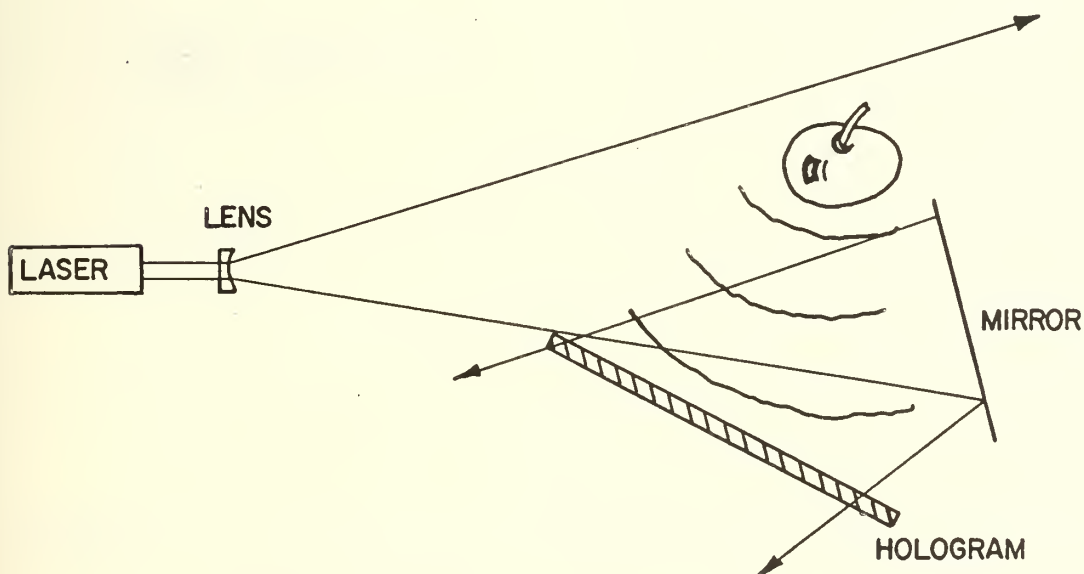


FIGURE 2a: PRODUCTION OF A HOLOGRAM OF A DIFFUSELY REFLECTING OBJECT.





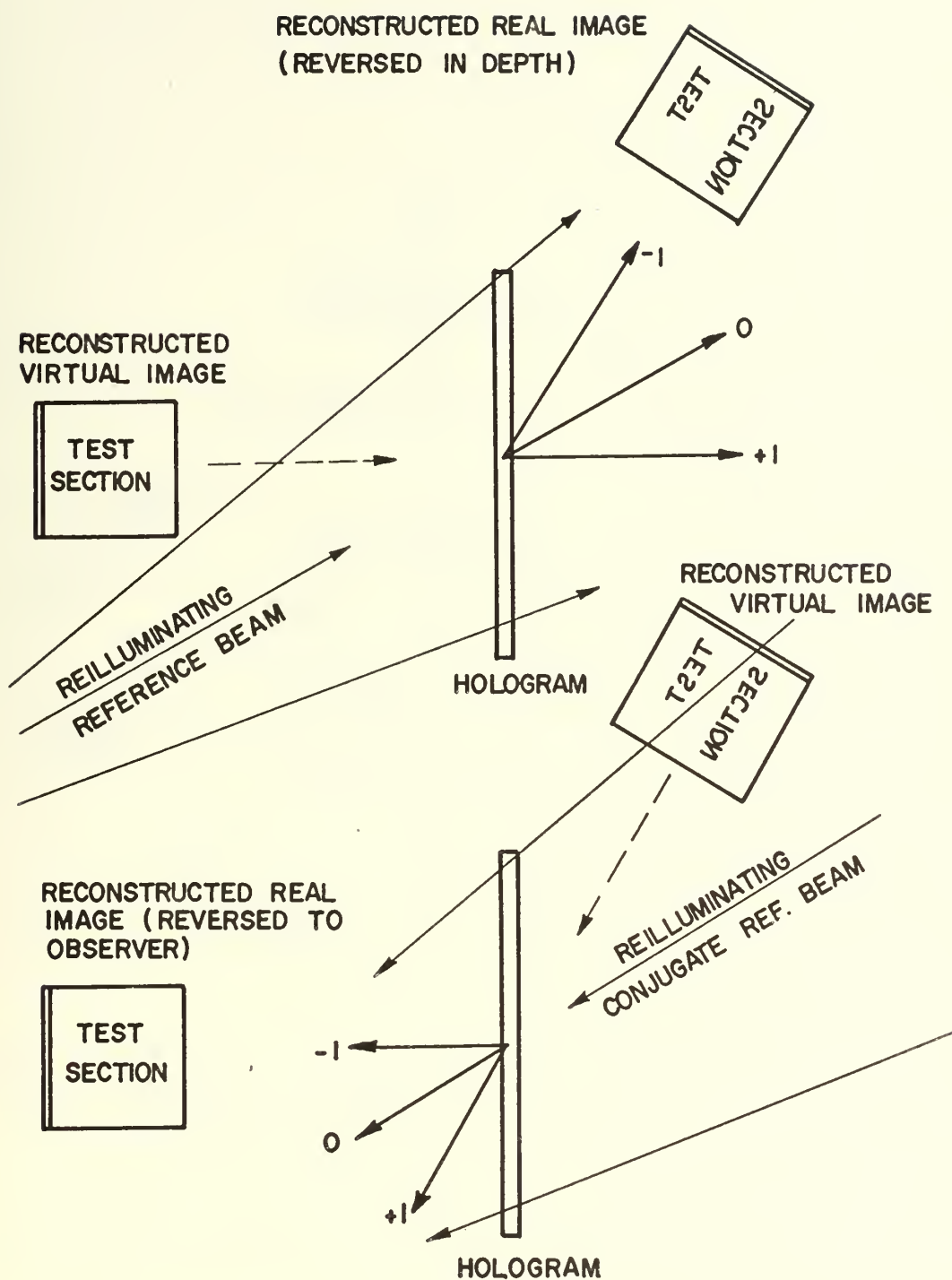


FIGURE 3: SHOWING IMAGES CREATED BY RECONSTRUCTION FROM EITHER SIDE.



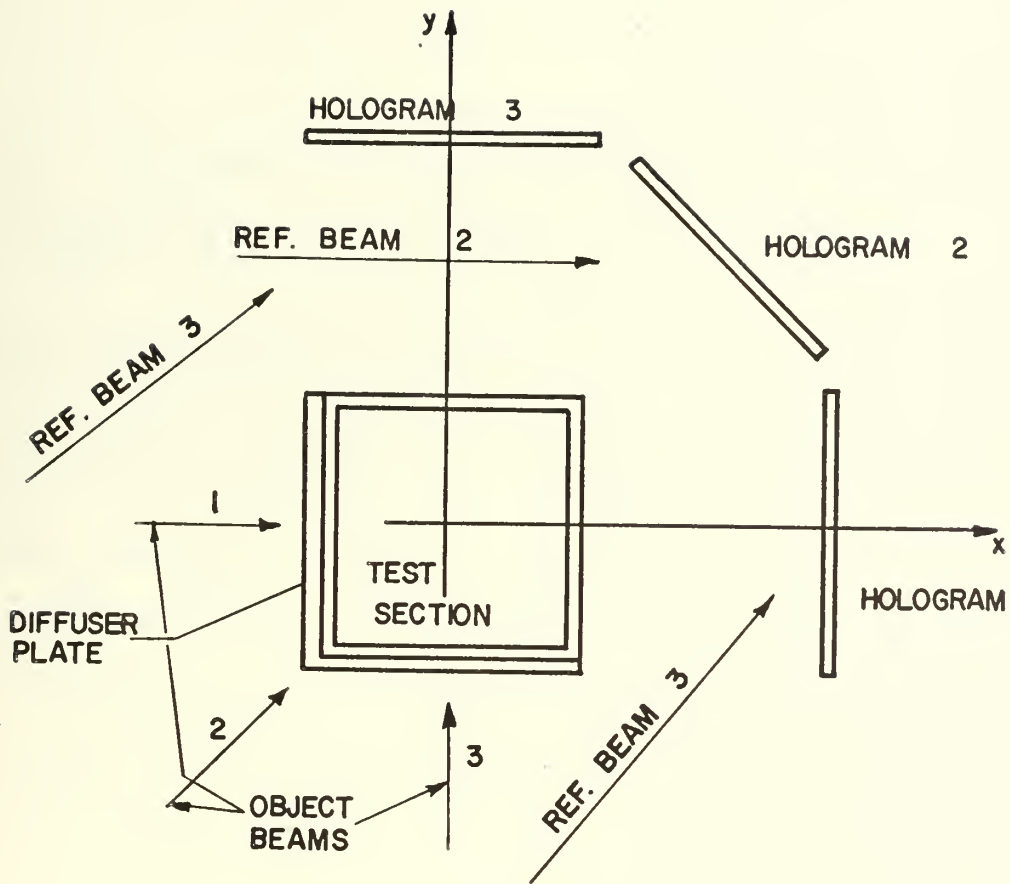


FIGURE 4: HOLOGRAM ARRANGEMENT FOR WIDE ANGULAR RANGE OF VIEWS.



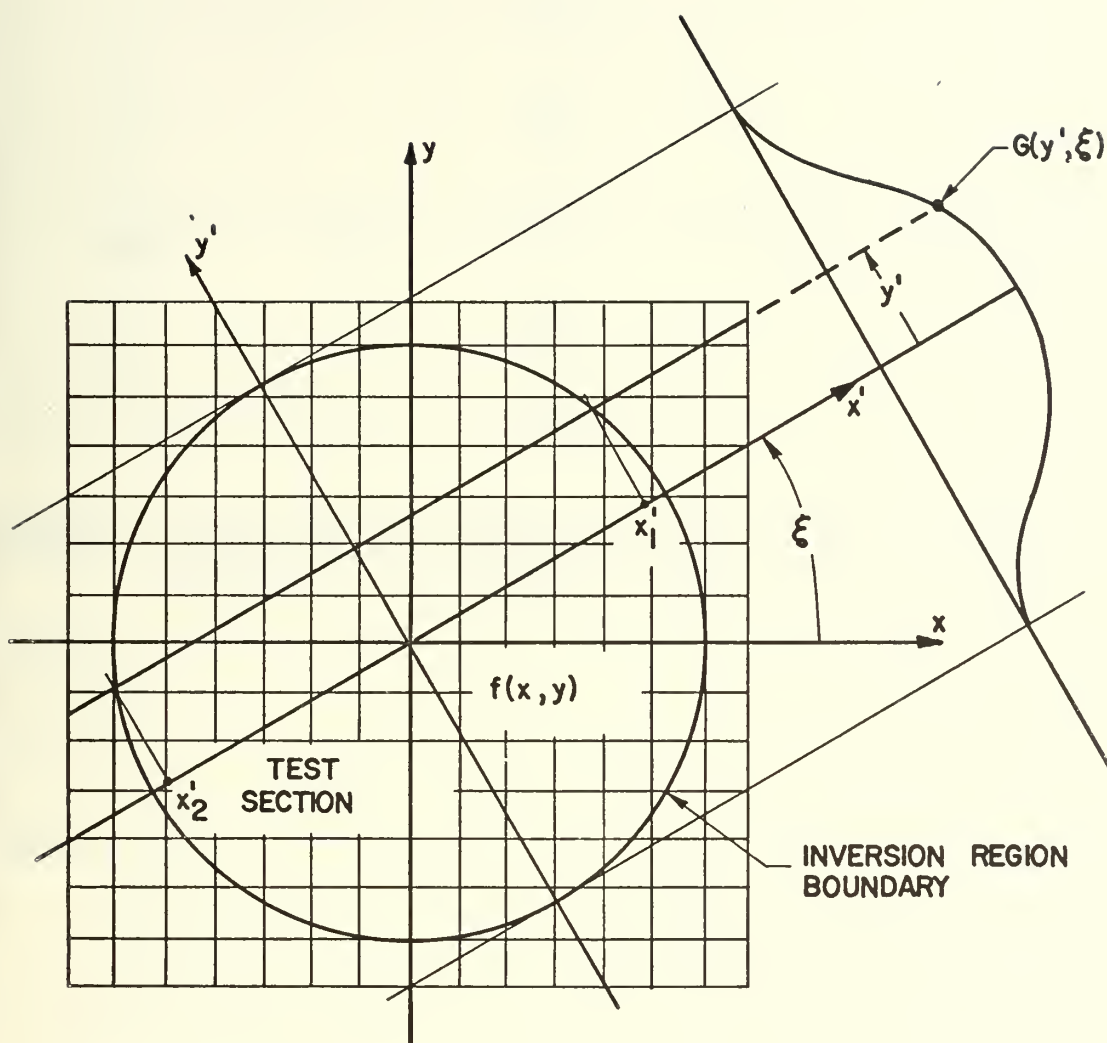


FIGURE 5: BASIC COORDINATE SYSTEM OF INVERSION PROCESS.



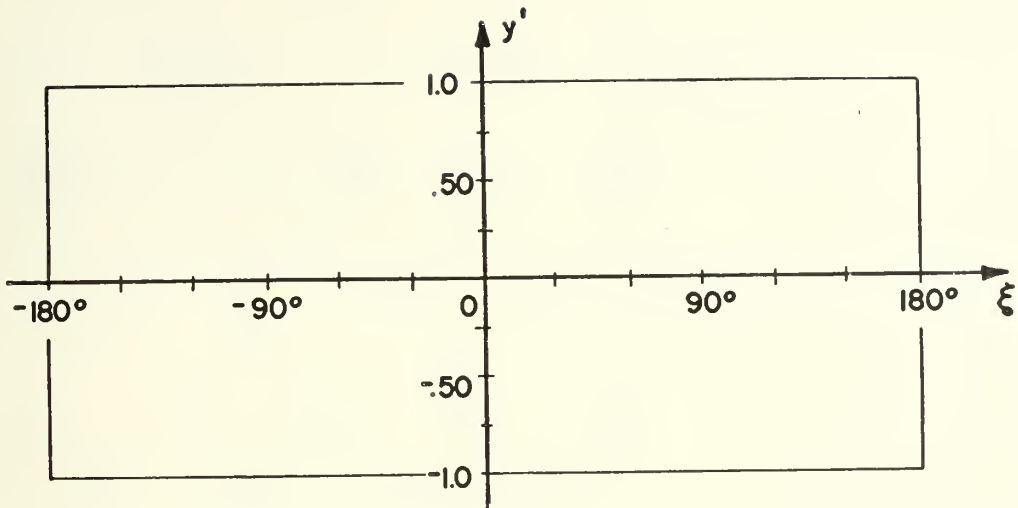


FIGURE 6 : DOMAIN OF THE FUNCTION G OVER WHICH ORTHOGONAL INVERSION IS PERFORMED IN THE GENERAL CASE :

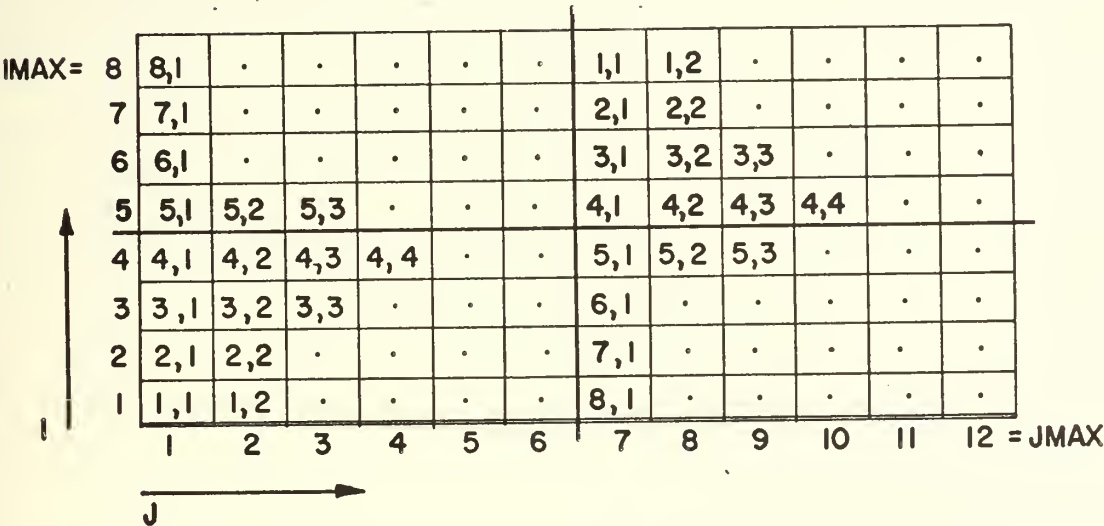


FIGURE 7 : DISCRETE ARRAY OF G VALUES CORRESPONDING TO DOMAIN OF FIGURE 6. SHOWING DUPLICATION OF THE FUNCTION.





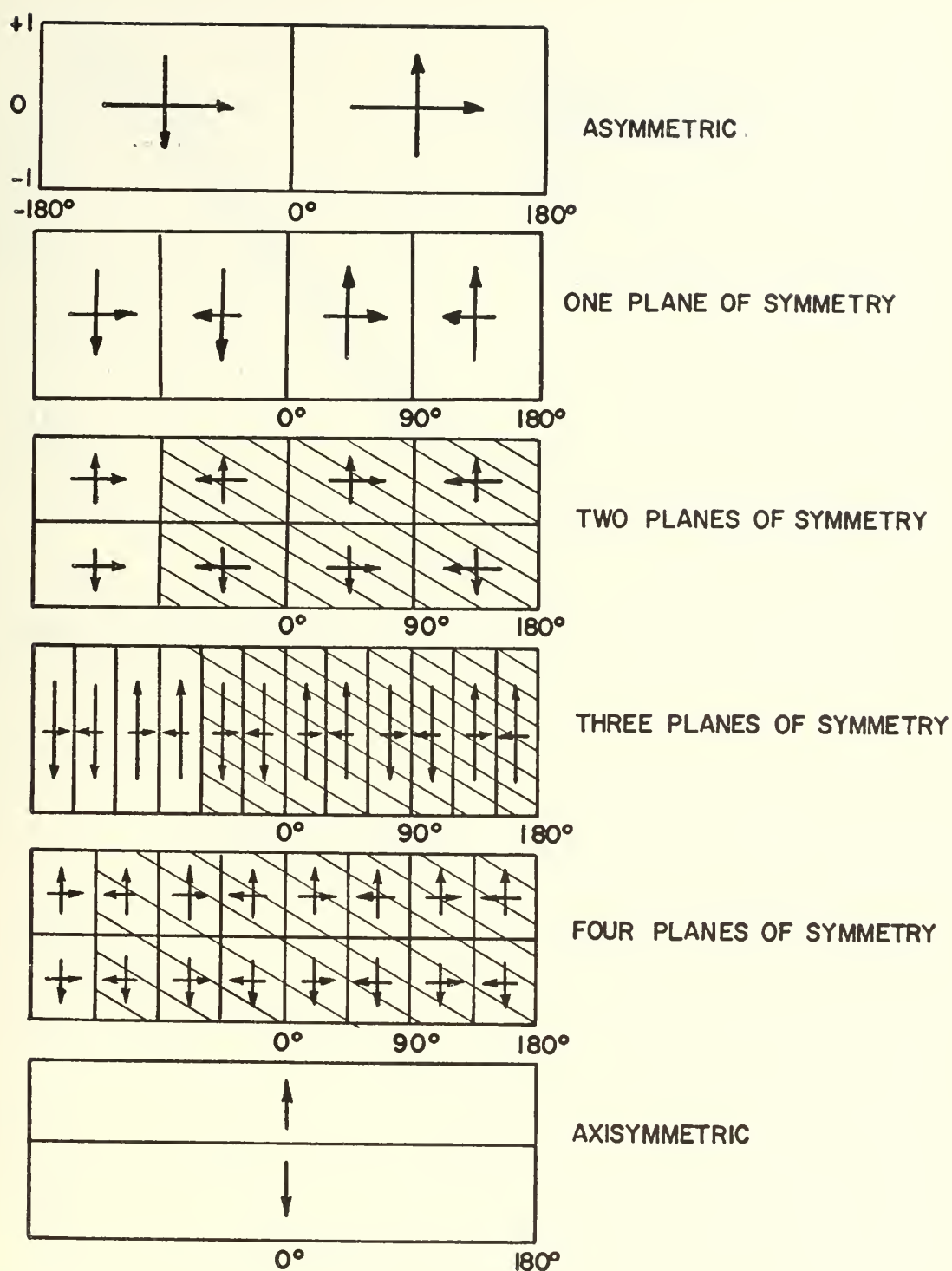


FIGURE 8. THE EFFECTS OF SYMMETRY OF THE FUNCTION  $F$  UPON THE REPEATABLE CHARACTER AND INTERVAL OF ORTHOGONALITY IN THE  $G$  FUNCTION.



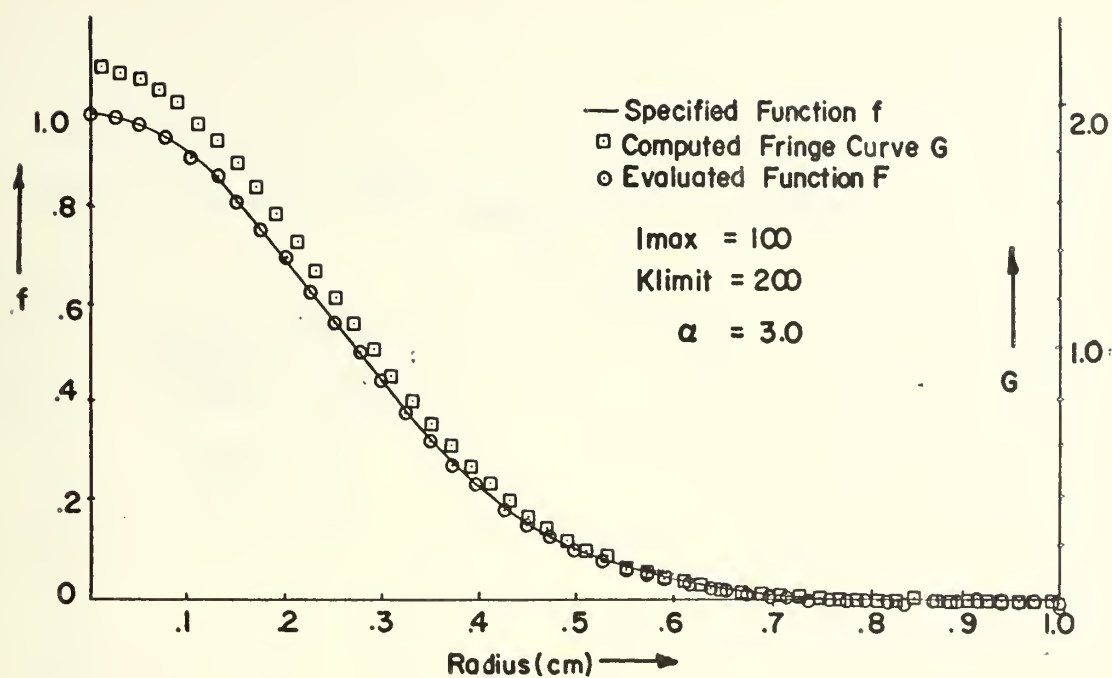


FIGURE 9. AXISYMMETRIC TEST CASE — GAUSSIAN FUNCTION

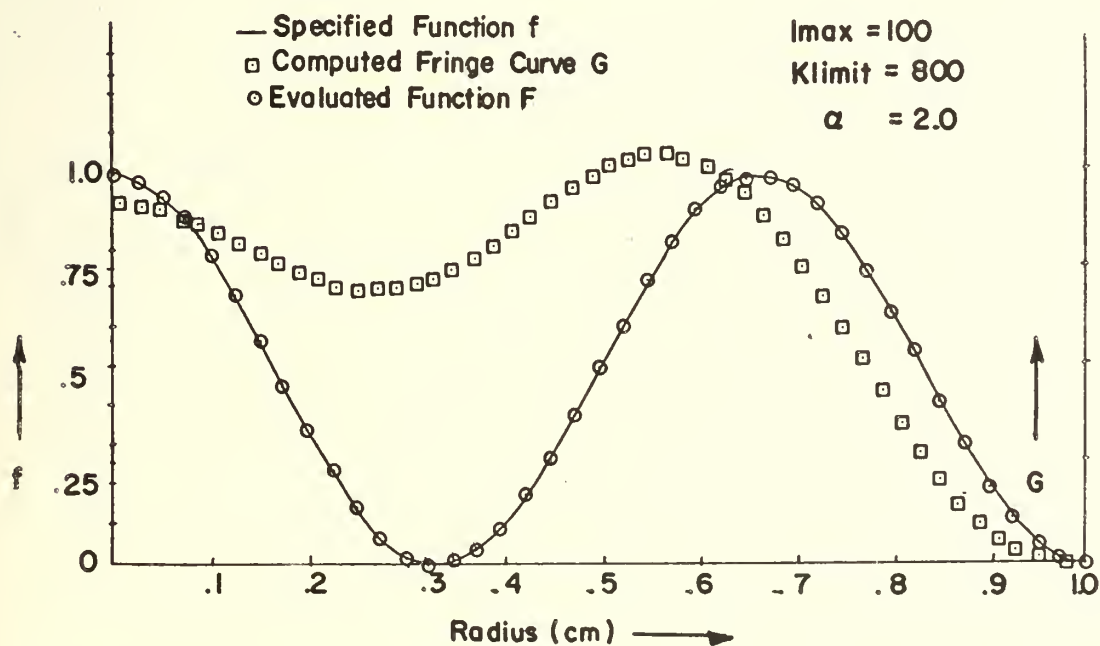


FIGURE 10. AXISYMMETRIC TEST CASE —  $(\text{COSINE})^2$  FUNCTION



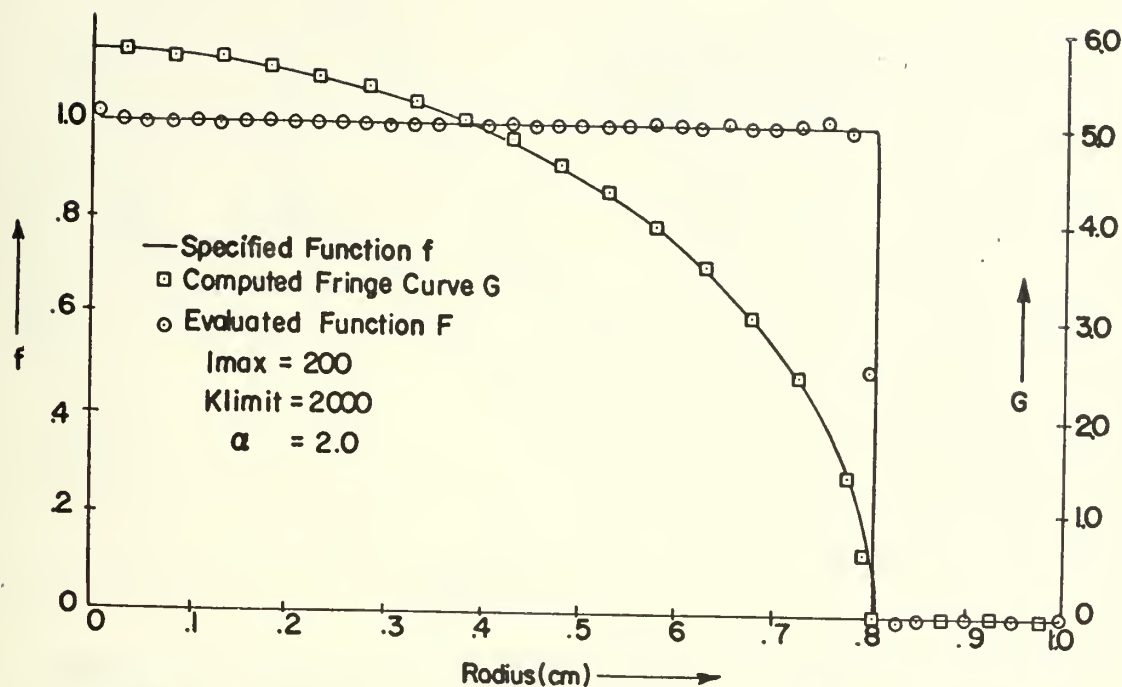


FIGURE 11. AXISYMMETRIC TEST CASE — STEP FUNCTION

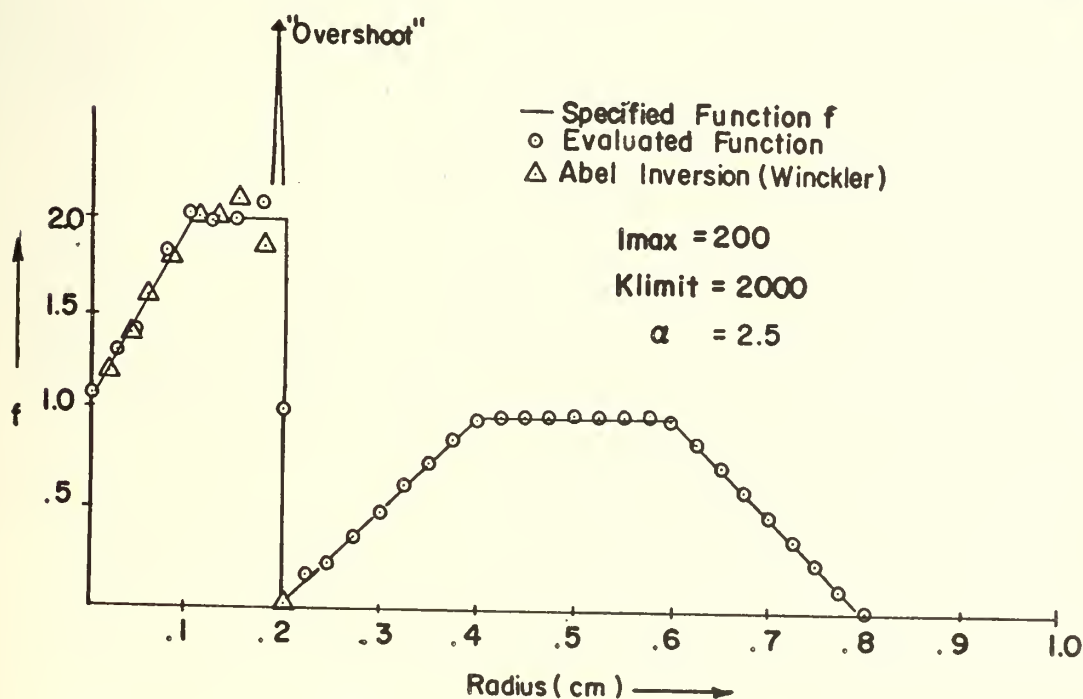


FIGURE 12. AXISYMMETRIC TEST CASE — WINCKLER'S TEST



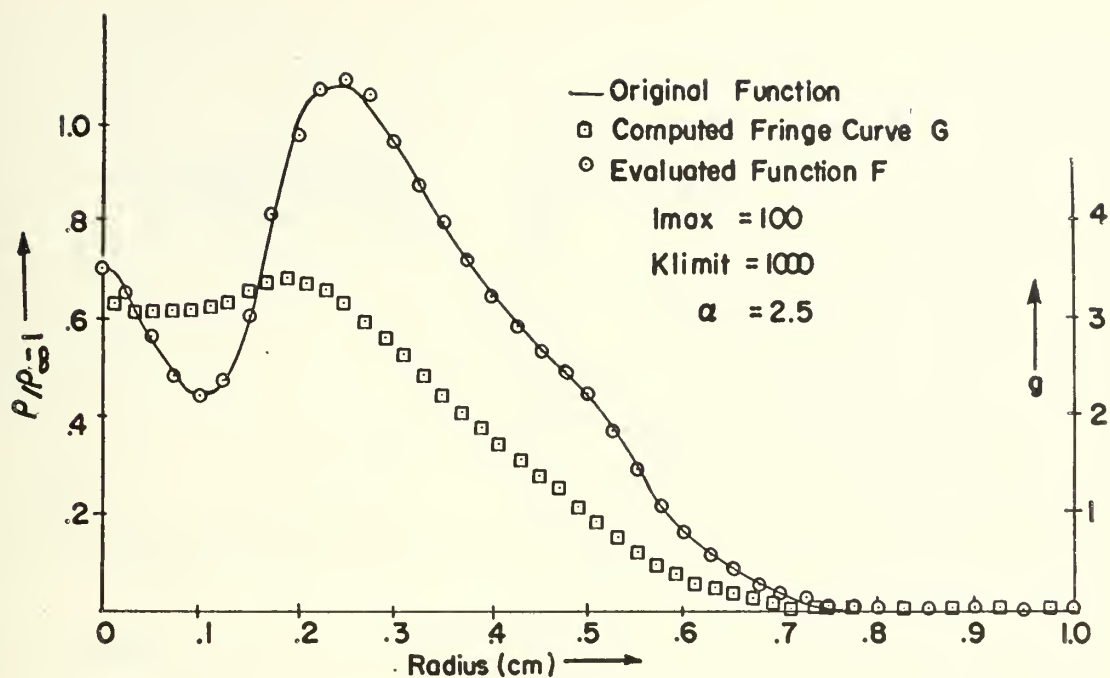


FIGURE 13. AXISYMMETRIC TEST CASE — FREE JET FLOW #1

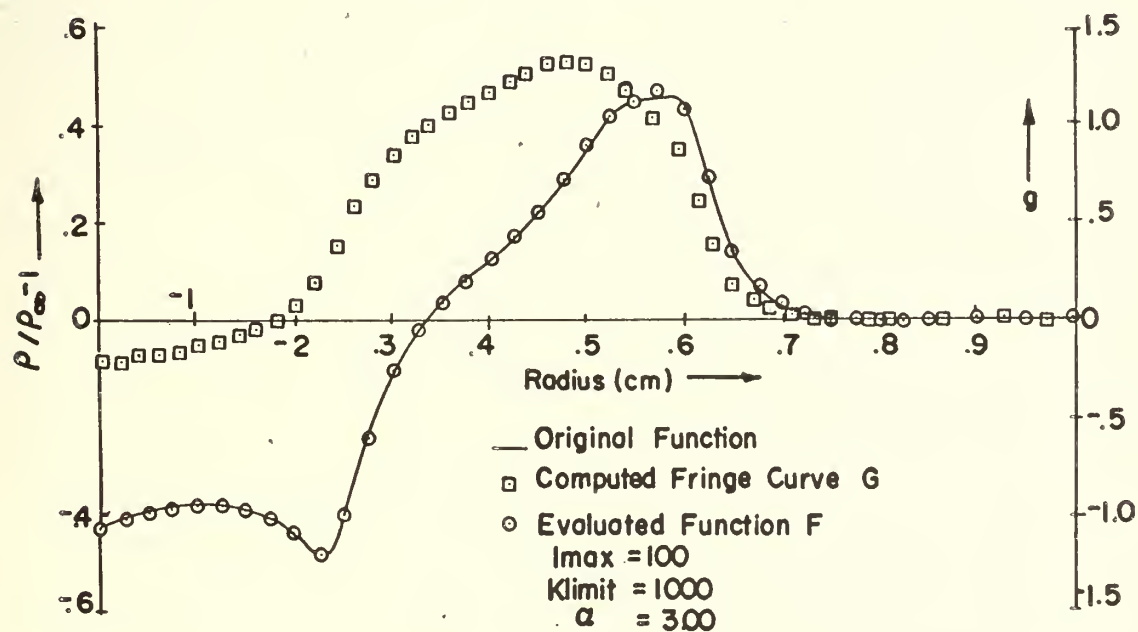


FIGURE 14. AXISYMMETRIC TEST CASE — FREE JET FLOW #2





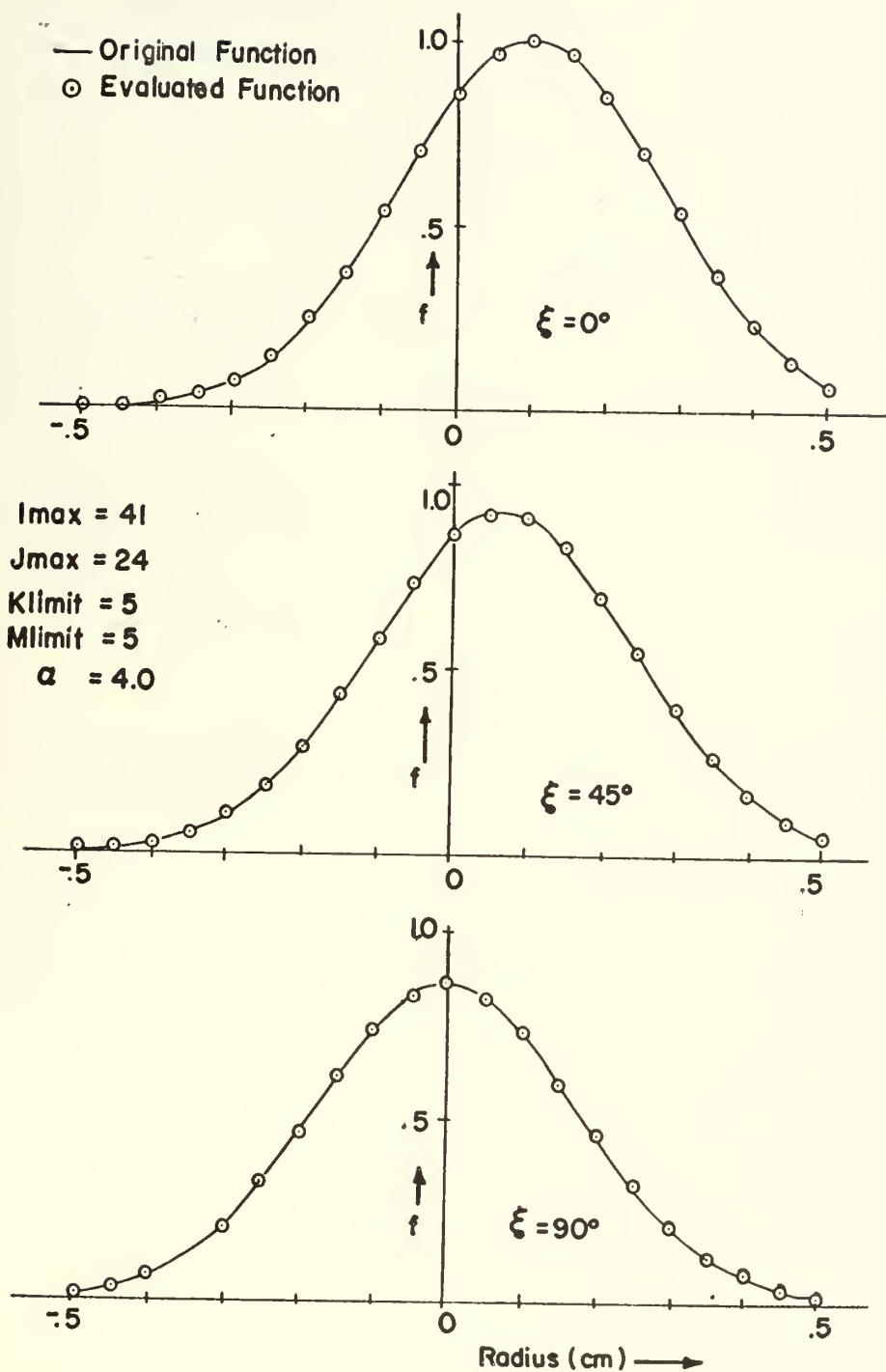


FIGURE 15. TEST INVERSION — DISPLACED GAUSSIAN



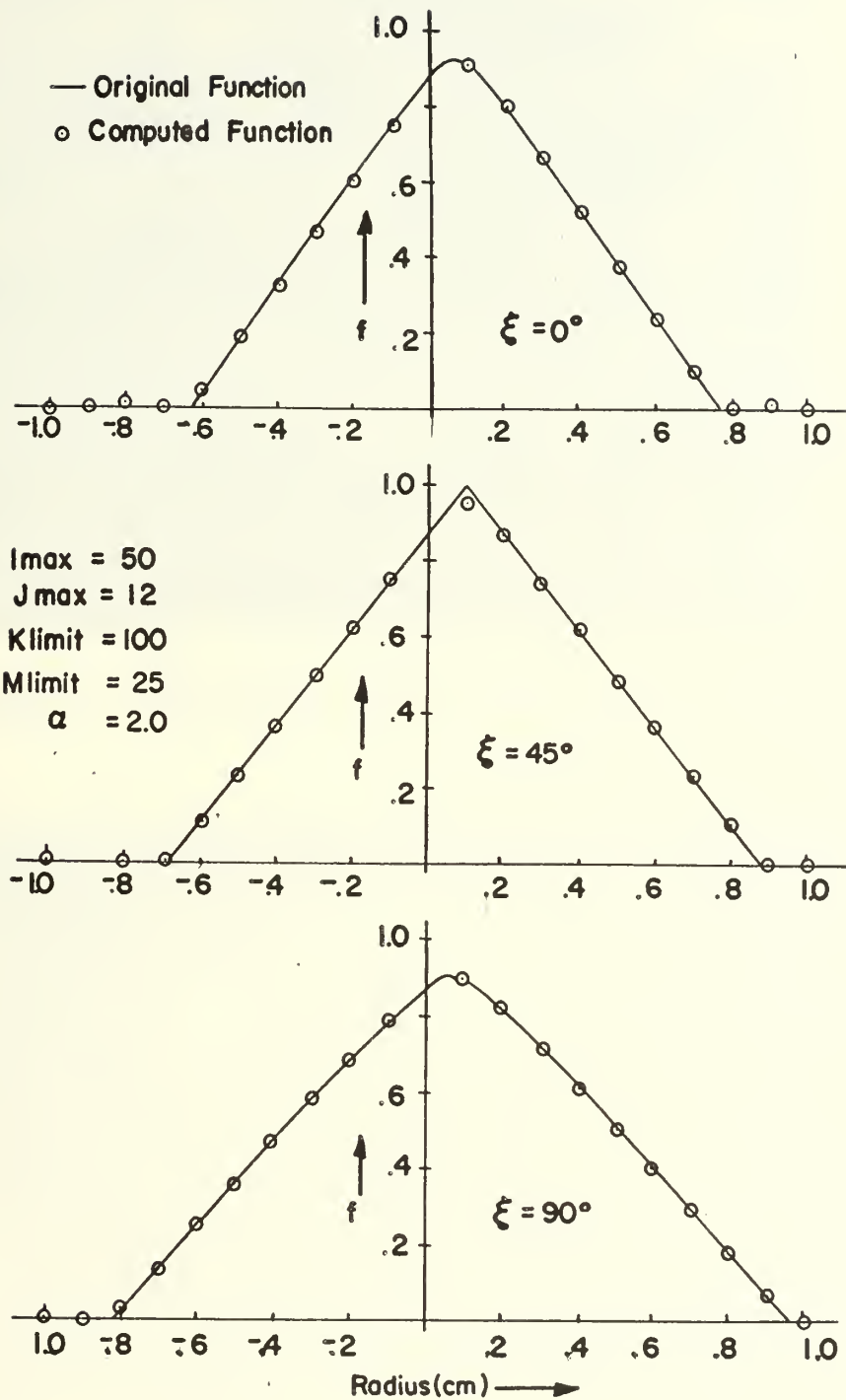


FIGURE 16 ASYMMETRIC TEST CASE—ELLIPTICAL CONE,



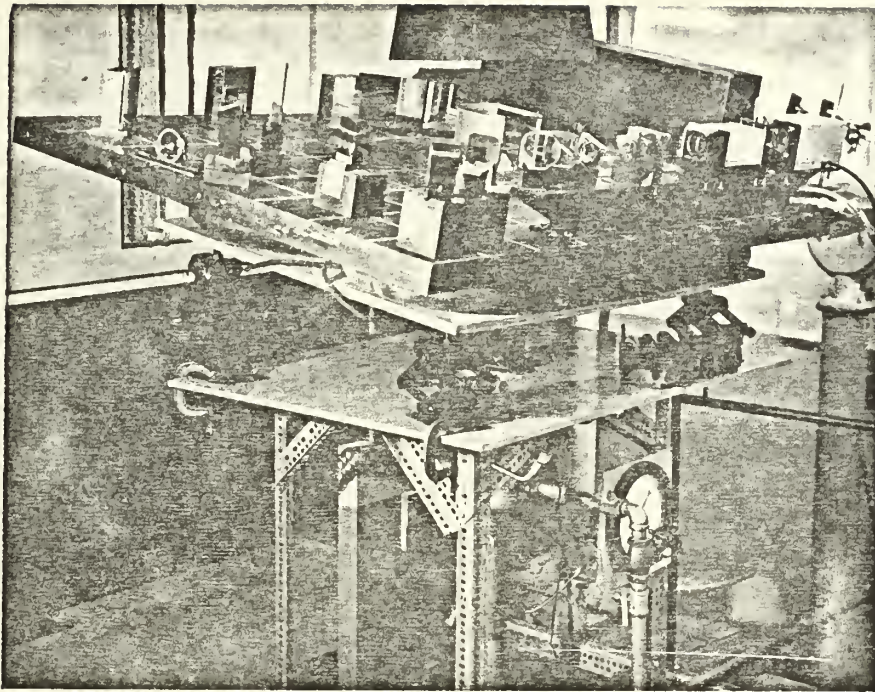


FIGURE 17. PHOTOGRAPH OF THE HOLOGRAPHIC TABLE

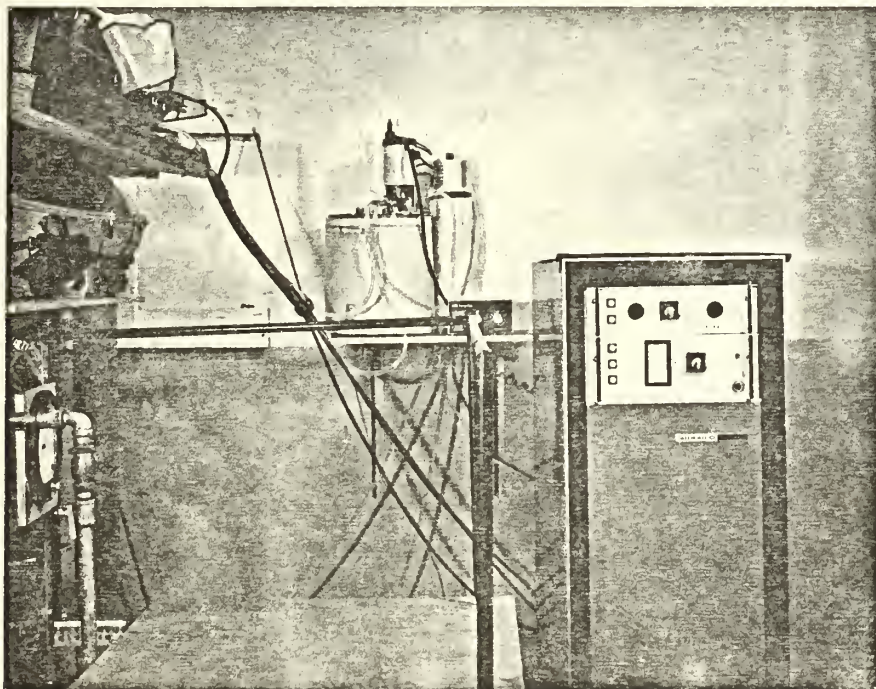


FIGURE 18. PHOTOGRAPH OF THE LASER POWER SUPPLY





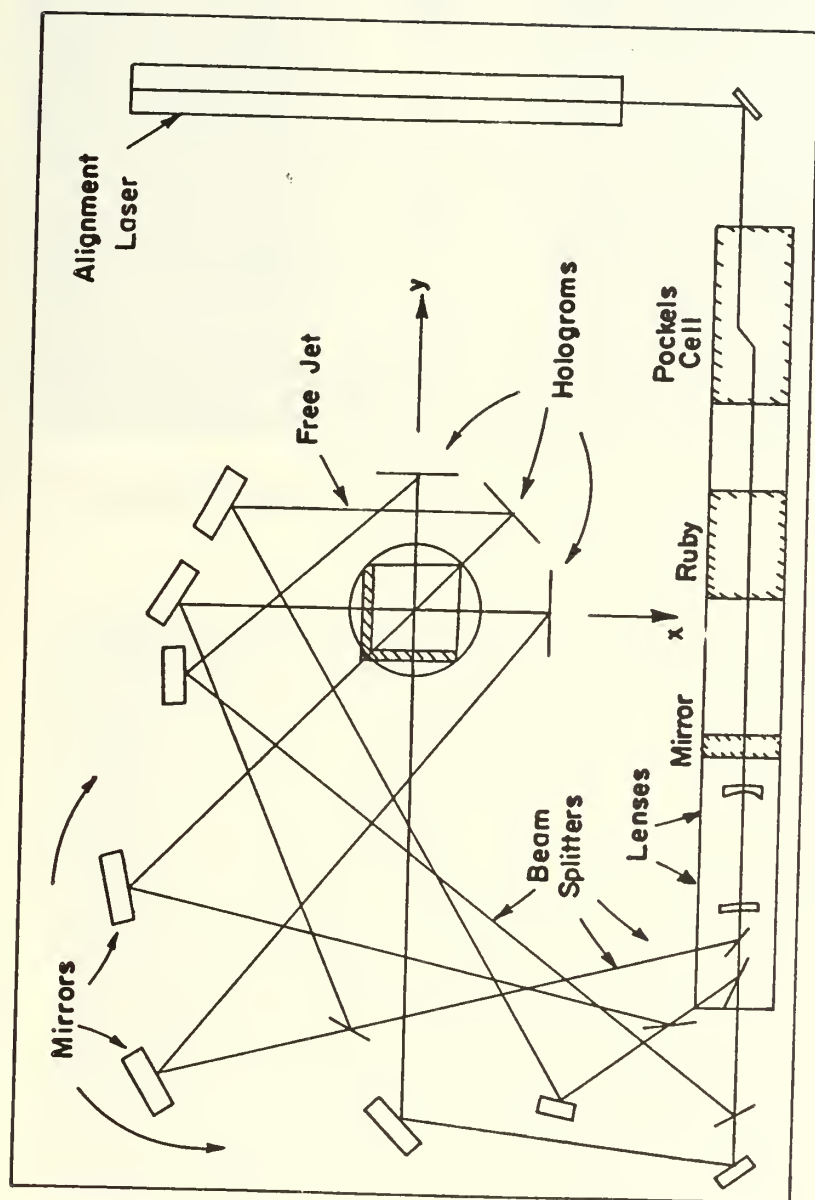


FIGURE 19. SCHEMATIC ARRANGEMENT OF HOLOGRAPHIC TABLE





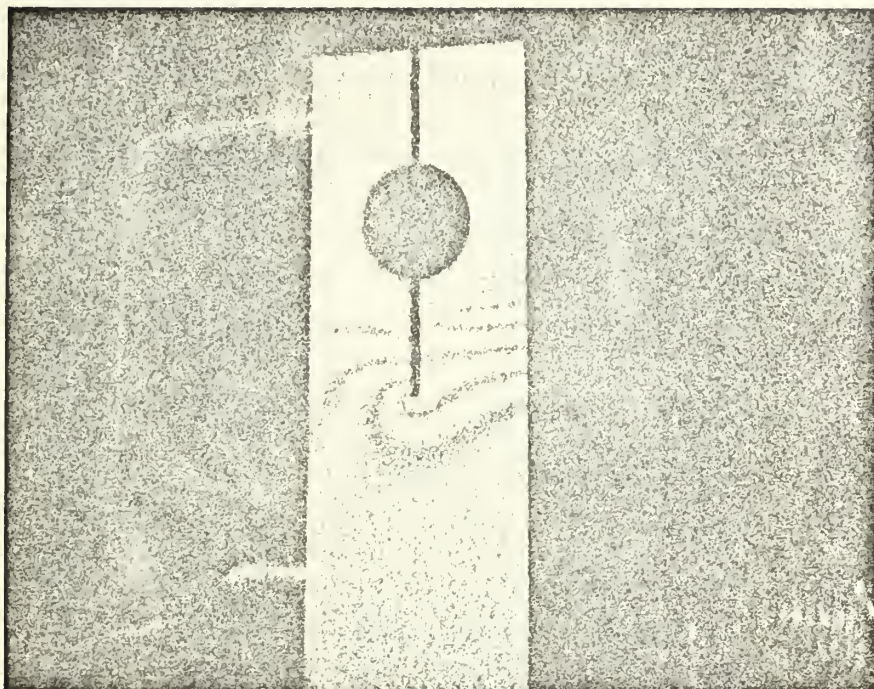


FIGURE 20. SURFACE INTERFEROGRAM OF A CLAMP UNDER STRAIN.

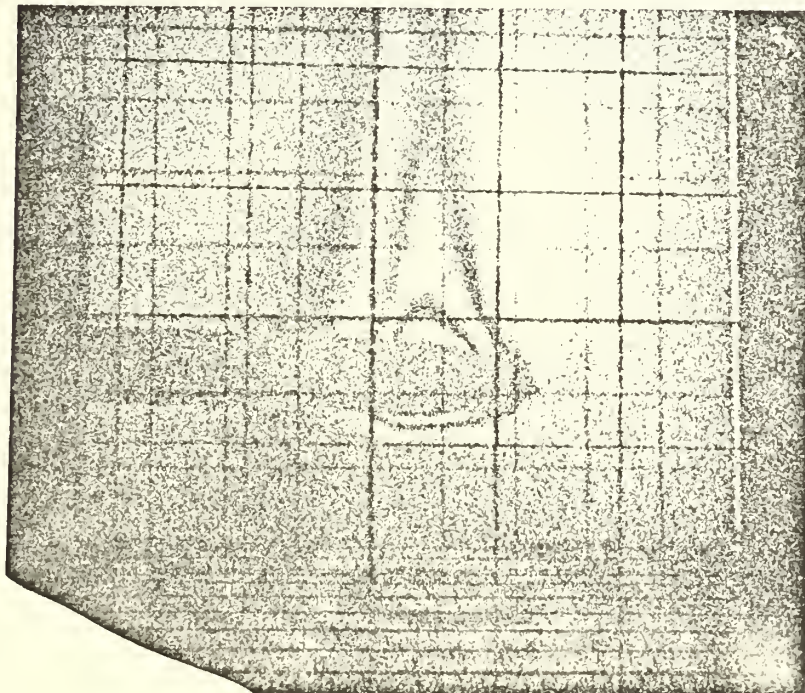


FIGURE 21. INTERFEROGRAM OF A CIGARETTE.



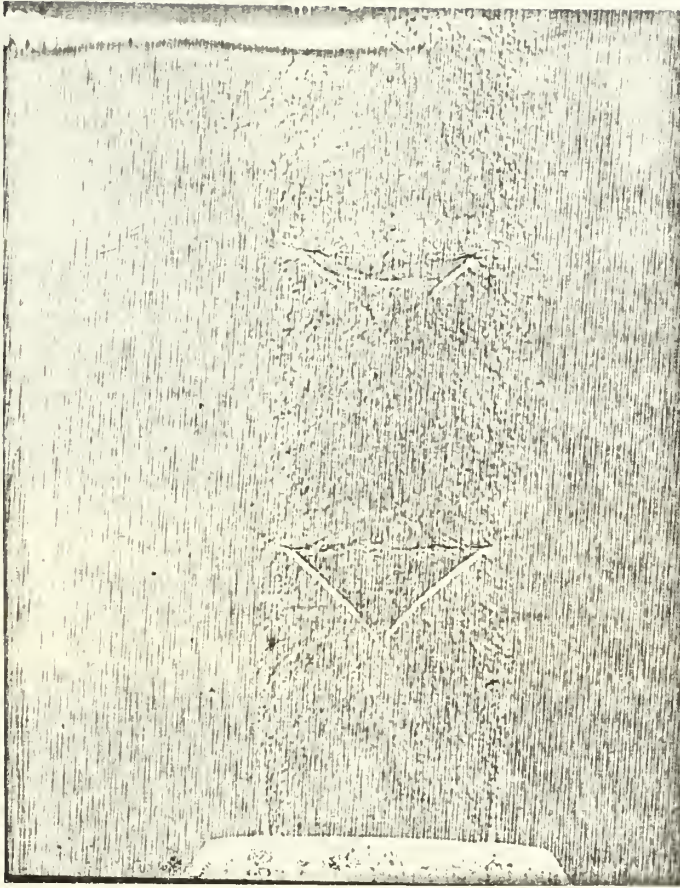


FIGURE 22. DIRECT PRINT OF A HOLOGRAM (DARK FIELD)  
SHOWING SHADOWGRAPH OF A FREE JET AT  
35 PSIG.







FIGURE 23. AXISYMMETRIC FREE JET, 60 PSIG.  $Z=3.0$  CM

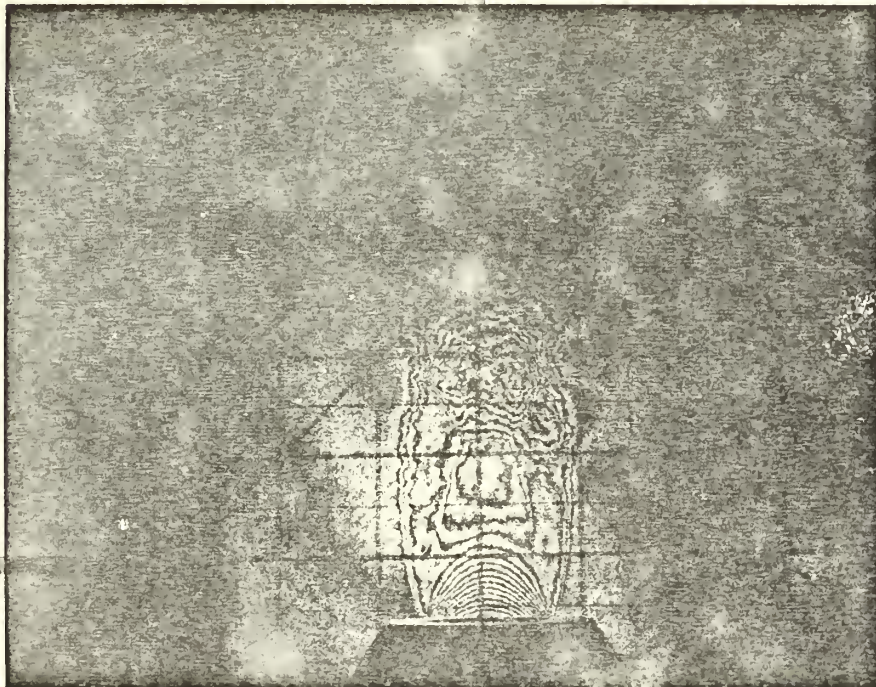


FIGURE 24. AXISYMMETRIC FREE JET, 60 PSIG.  $Z=1.0$  CM.





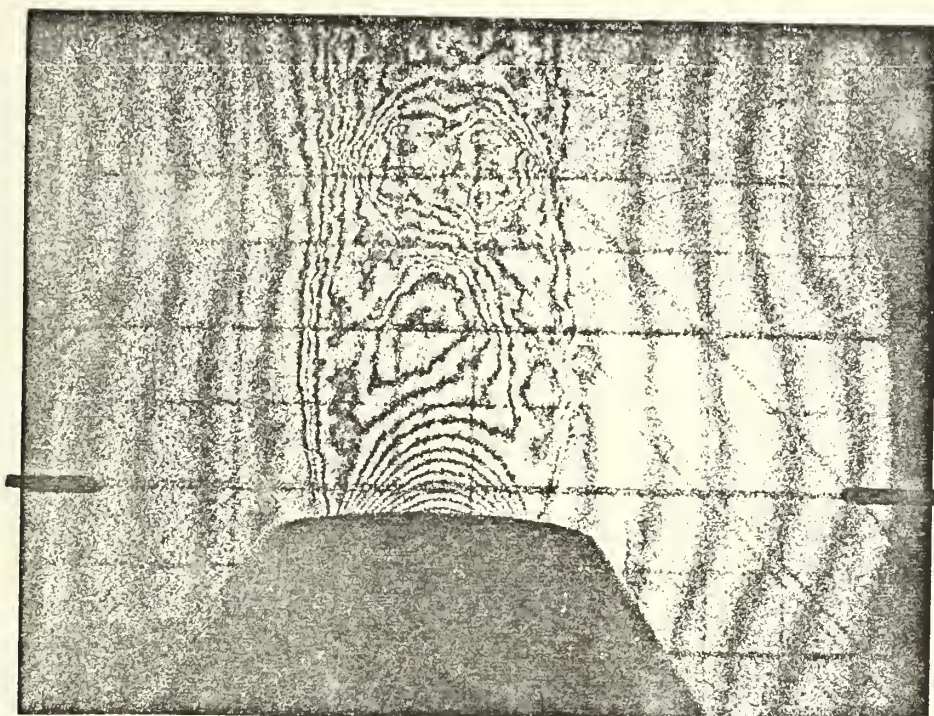


FIGURE 25. ASYMMETRIC SECTION OF A FREE JET, 60 PSIG.,  
 $Z = .5 \text{ CM.}$ ,  $11^\circ$  TILT,  $\xi = 5^\circ$



FIGURE 26. ASYMMETRIC SECTION OF A FREE JET, 60 PSIG.,  
 $Z = .5 \text{ CM.}$ ,  $11^\circ$  TILT,  $\xi = 85^\circ$





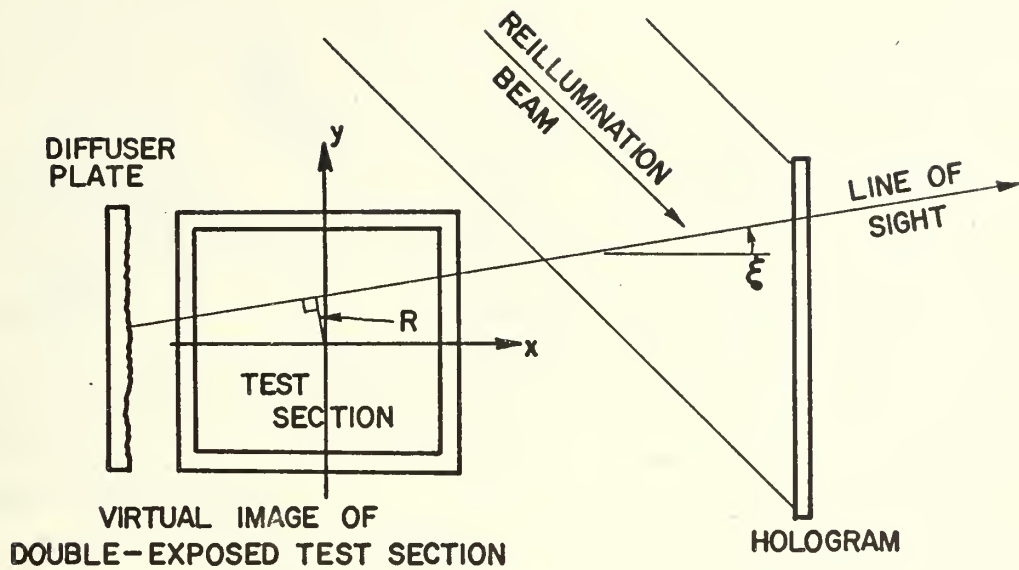


FIGURE 27:  $(R, \xi)$  COORDINATES FOR A LINE OF SIGHT THROUGH THE RECONSTRUCTED TEST SECTION

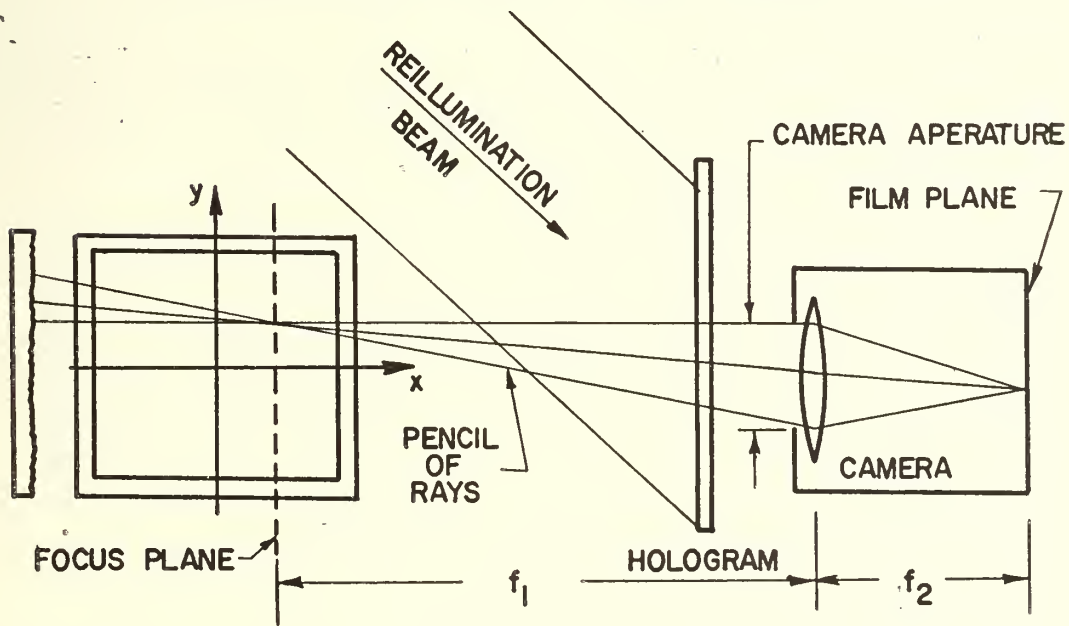


FIGURE 28: EFFECT OF APPERATURE SIZE AND FOCUS PLANE POSITION ON PENCIL SIZE OF RAYS ABOUT A LINE-OF-SIGHT RECORDED BY CAMERA.



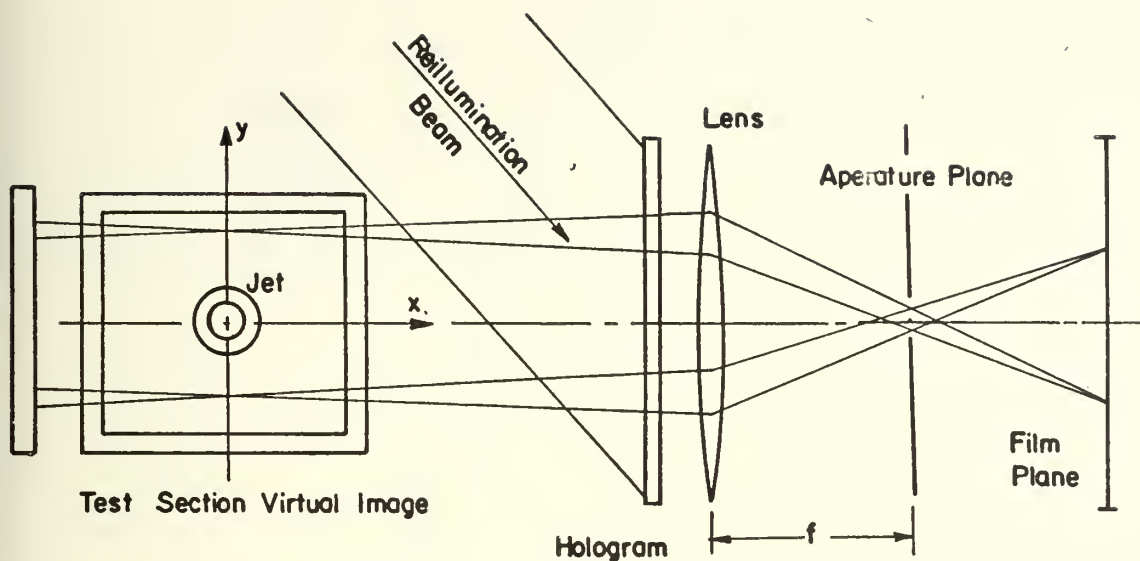


FIGURE 29 SPATIAL FILTERING TECHNIQUE FOR SELECTING PHOTOGRAPH OF CONSTANT ANGLE LINES OF SIGHT

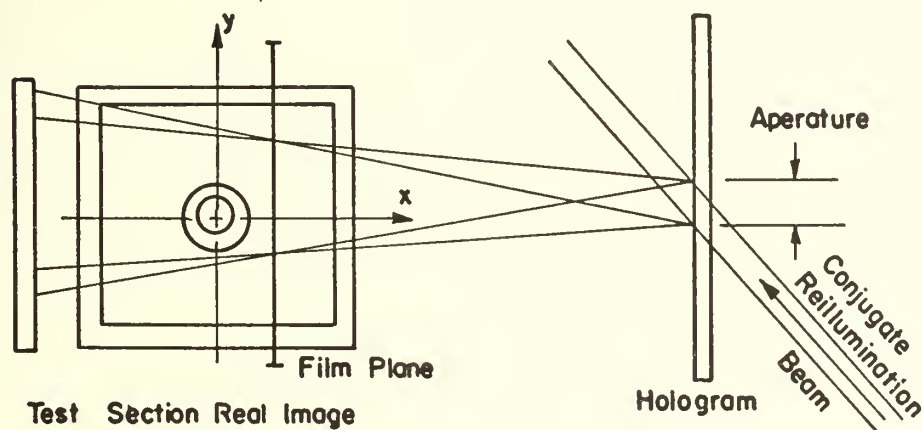


FIGURE 29a LENSELESS PHOTOGRAPHIC TECHNIQUE USING CONJUGATE REILLUMINATION BEAM OF SMALL DIAMETER



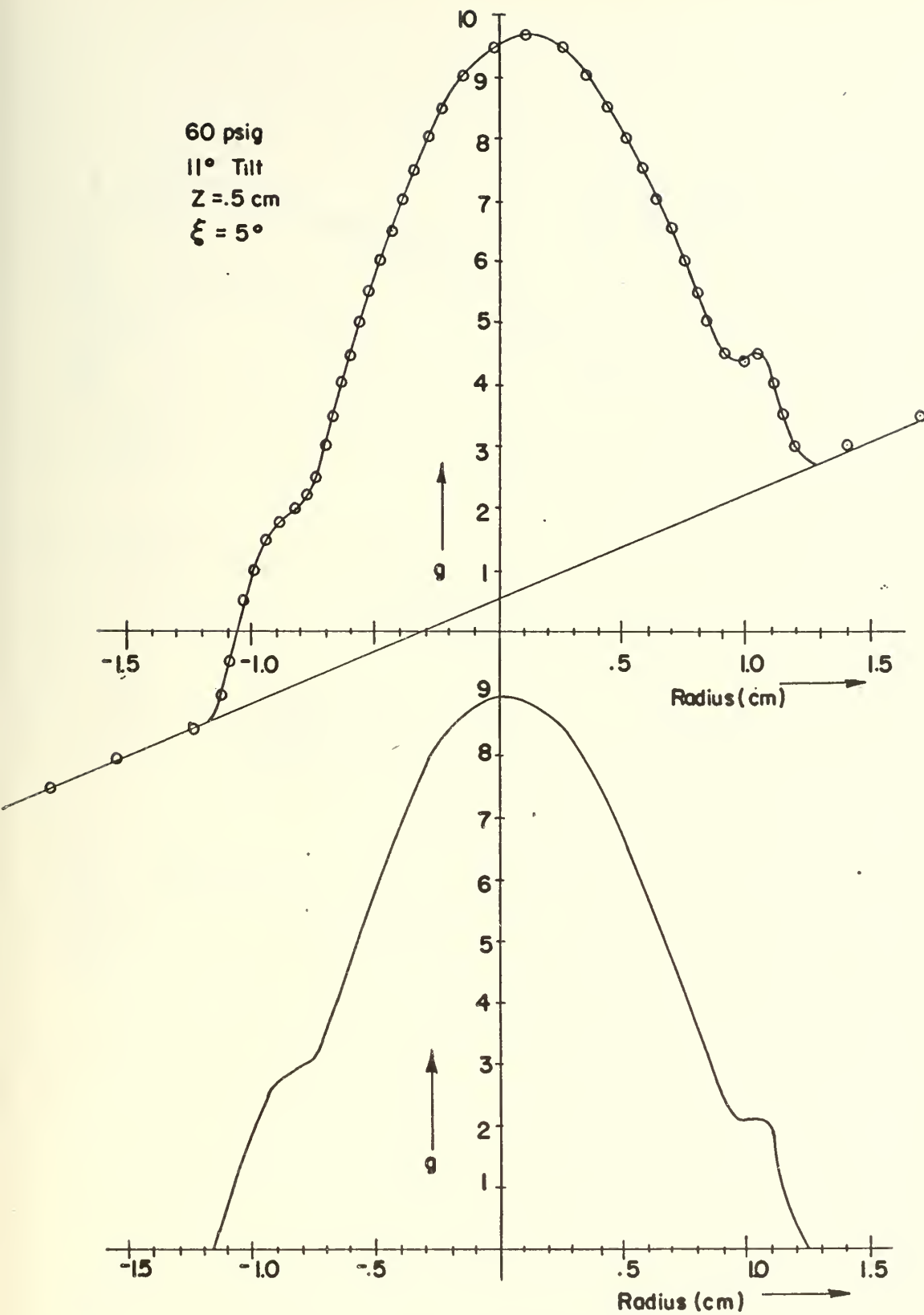


FIGURE 30 EXAMPLE GRAPHICAL WORK SHEET CURVES



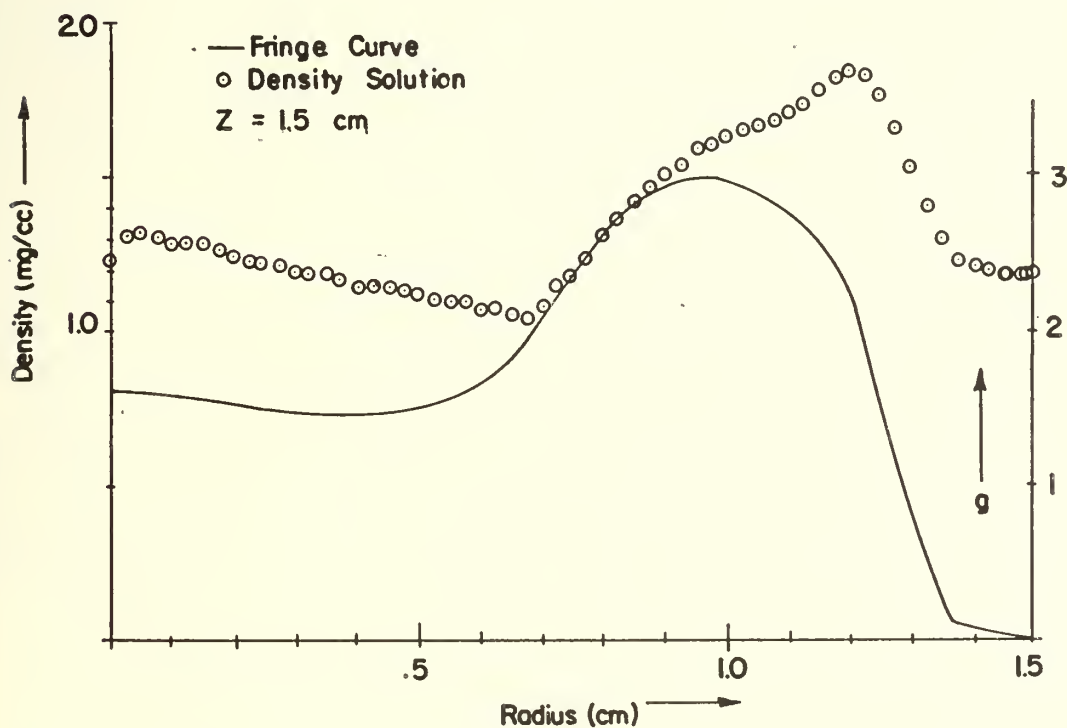
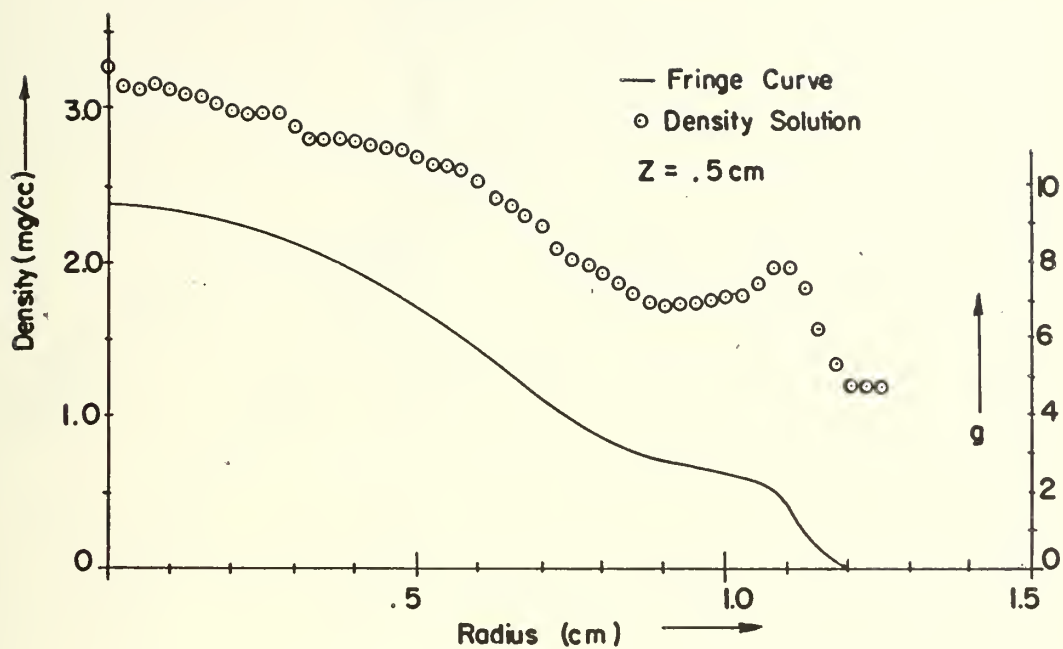


FIGURE 31 FRINGE CURVES AND CORRESPONDING SOLUTIONS FOR TWO STATIONS, AXISYMIC FREE JET, 60 PSIG





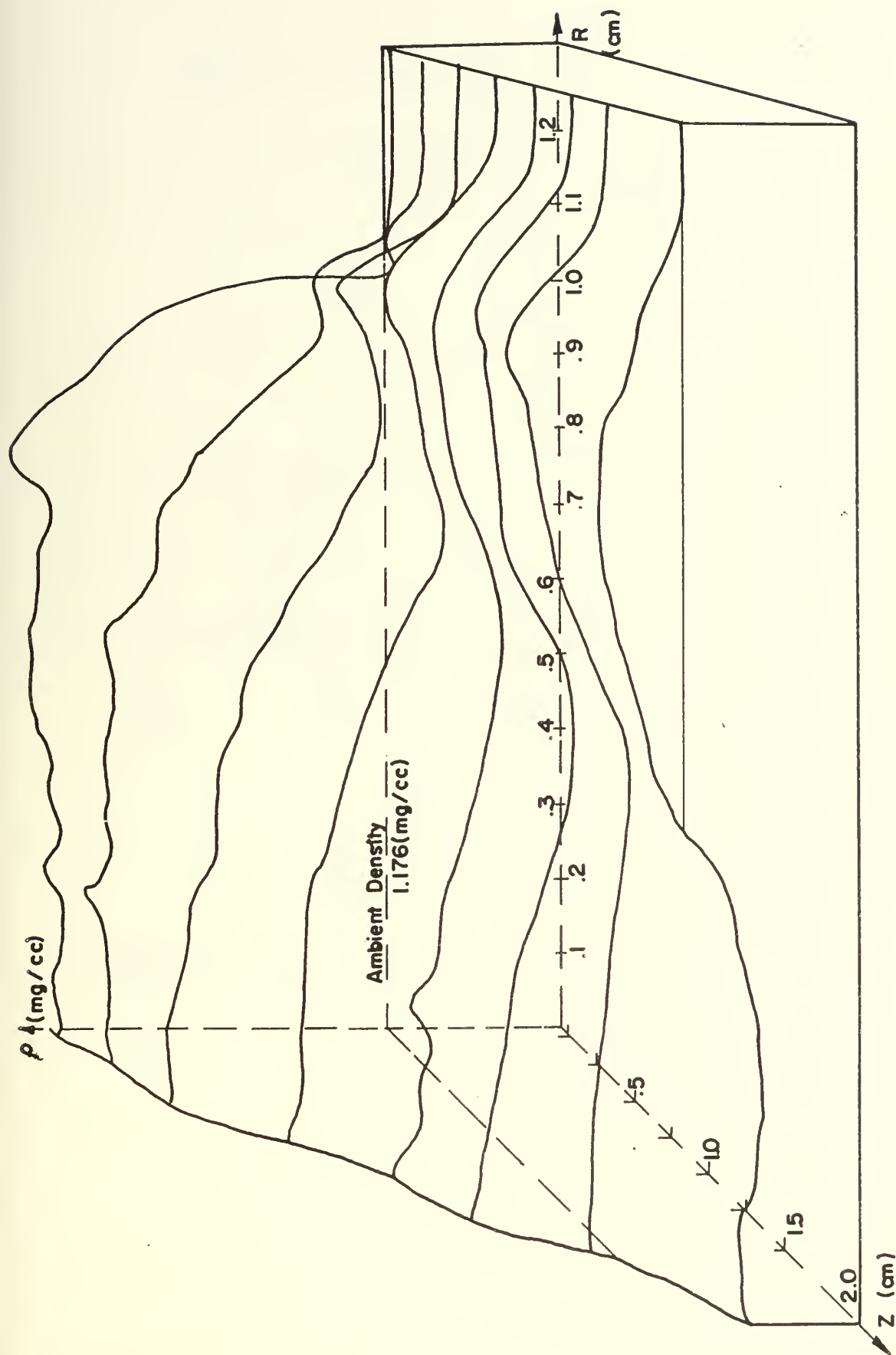


FIGURE 32 TOPOGRAPHICAL PLOT OF THE AXISYMMETRIC DENSITY SOLUTION OF A FREE JET AT 60 PSIG.



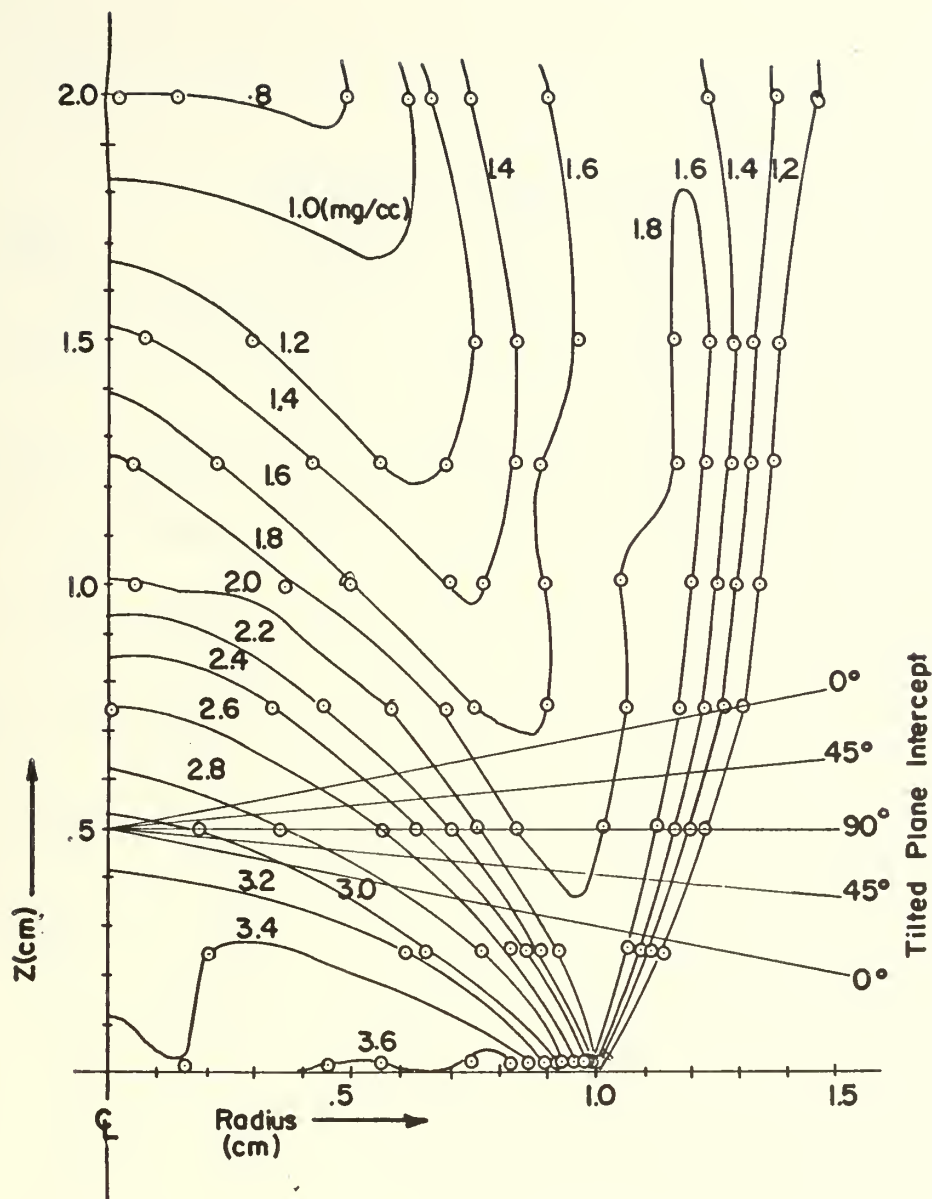


FIGURE 33. ISODENSITY LINE PLOT OF THE AXISYMMETRIC SOLUTION, 60 PSIG



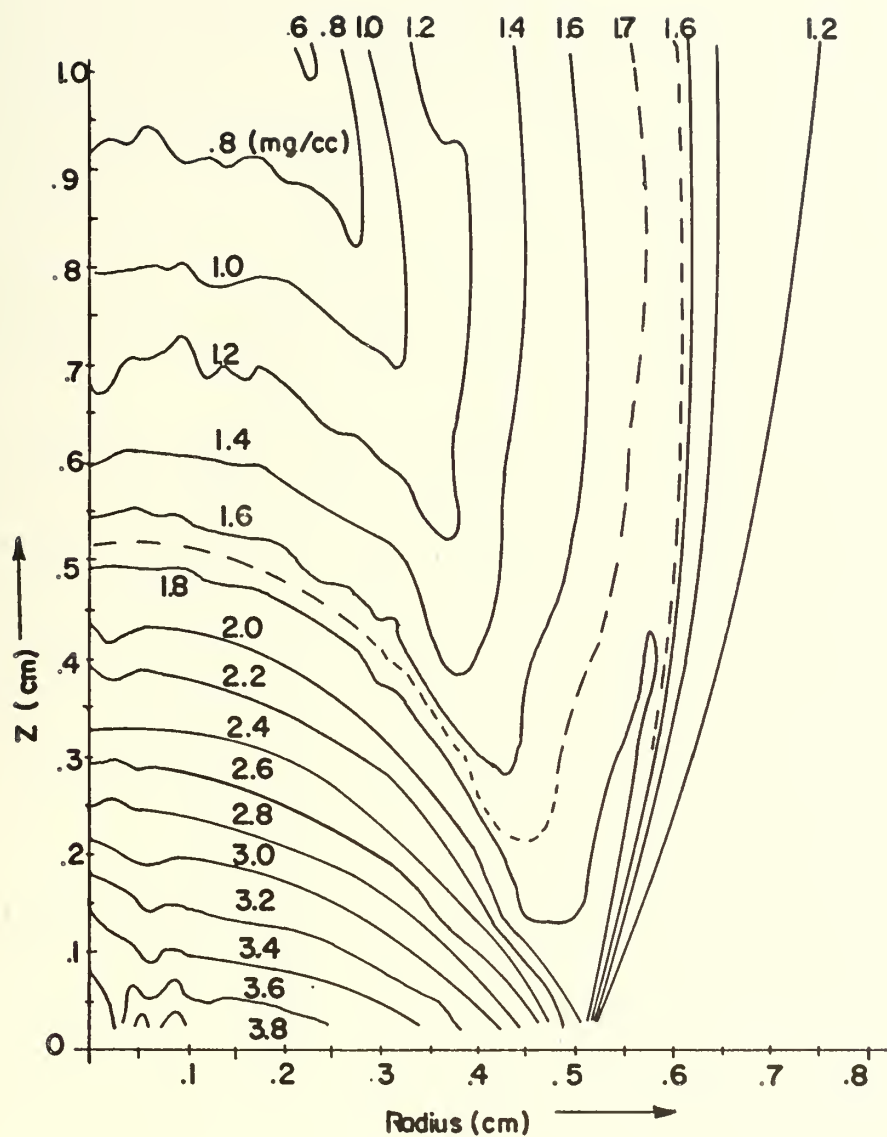


FIGURE 34 SKETCH OF THE AXISYMMETRIC DENSITY SOLUTION OF A 1.0 CM DIAMETER FREE JET AT 60 PSIG, FROM WINCKLER.



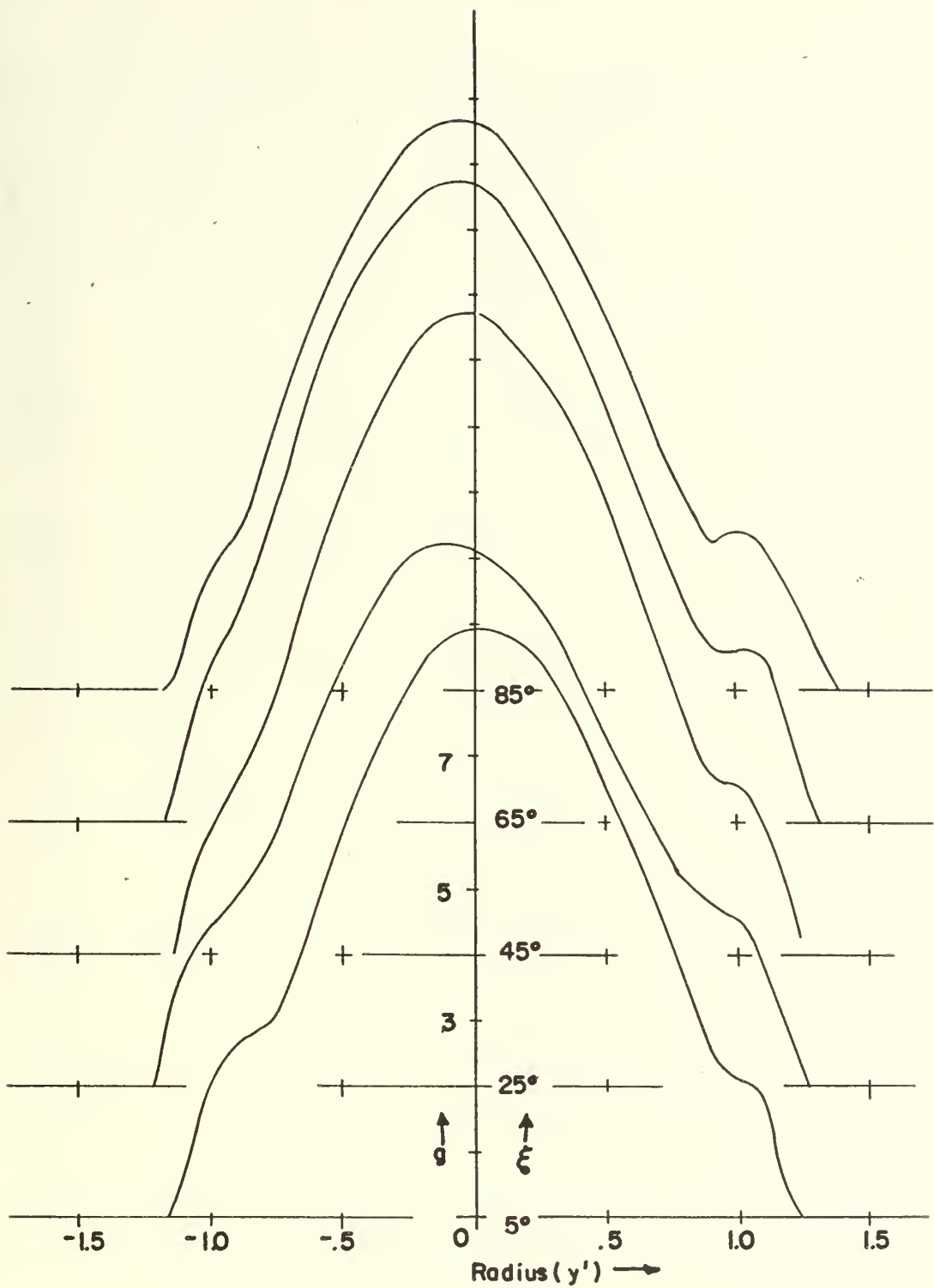


FIGURE 35. FRINGE NUMBER  $G$  CURVES OBTAINED FOR THE  $11^\circ$  TILT FREE JET AT 60 PSIG.





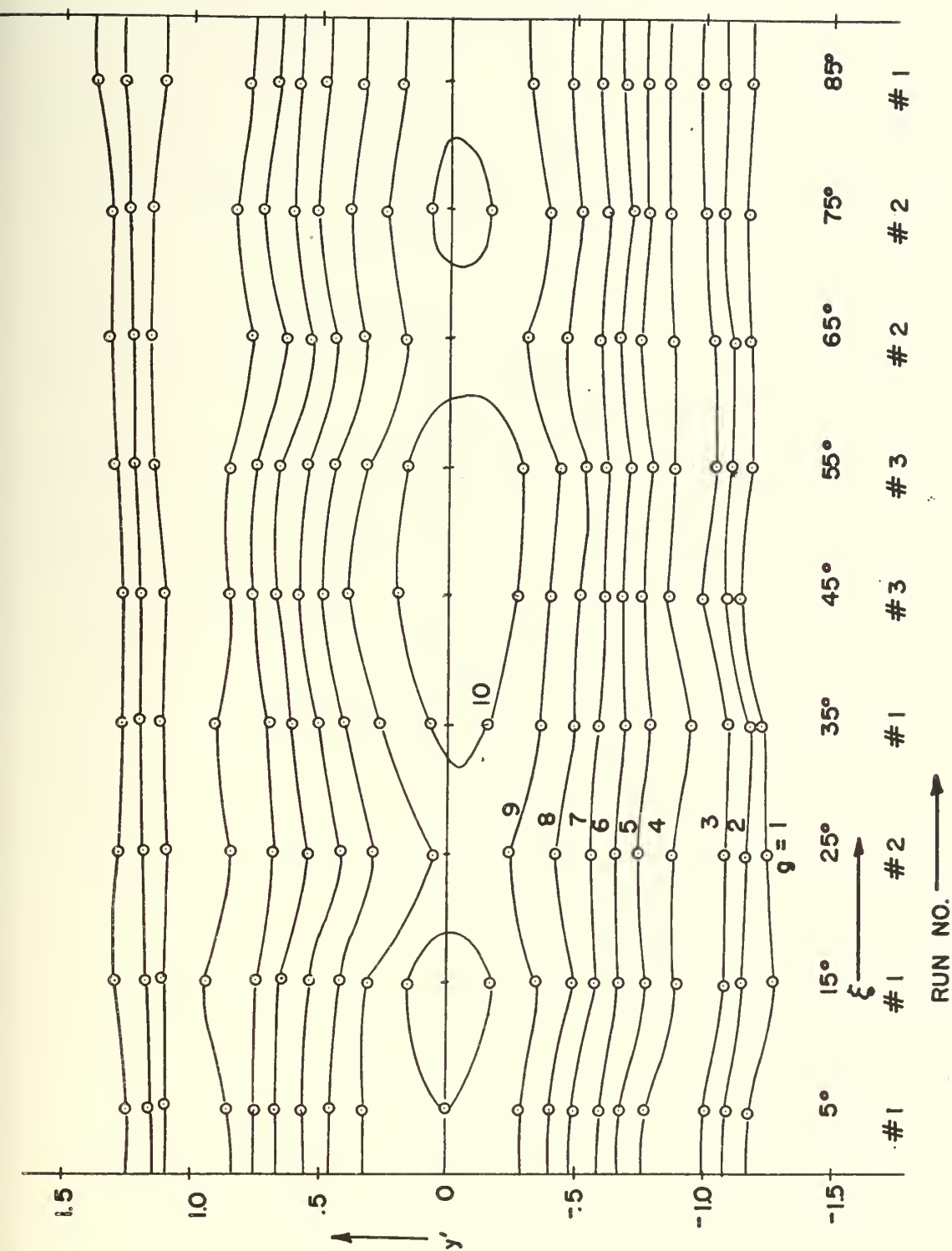


FIGURE 36. CONTOUR MAP OF THE FUNCTION  $G$ , 60 PSIG, 11° TILT



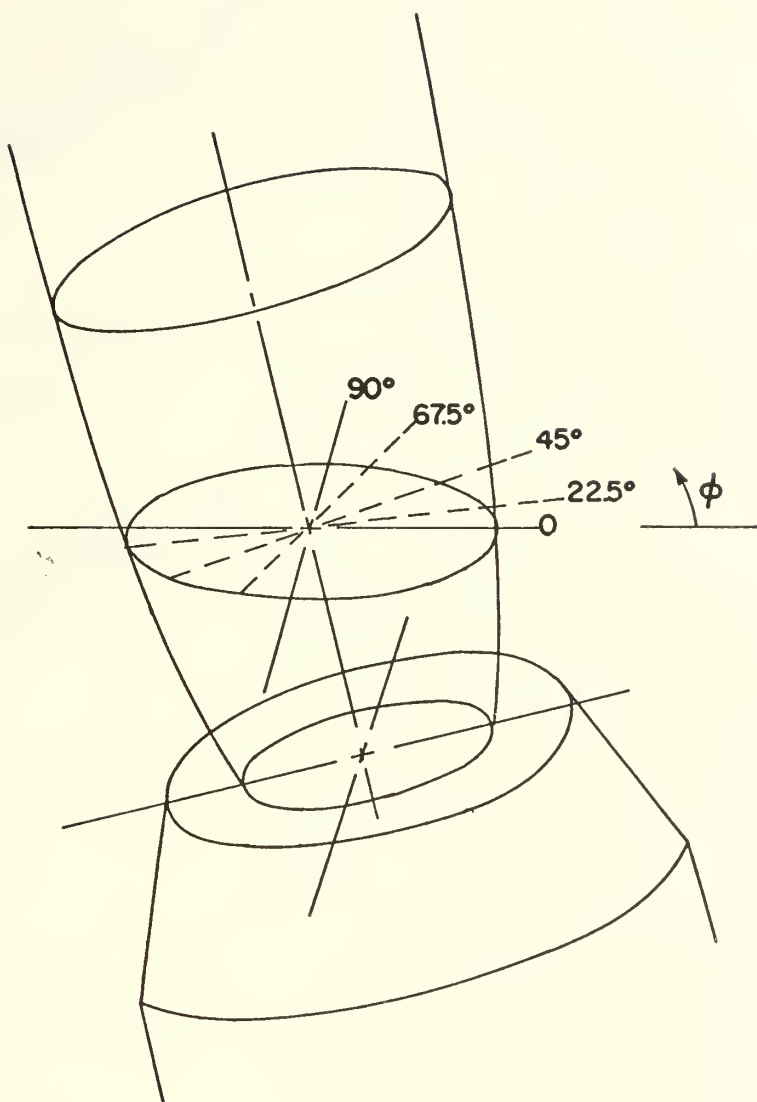


FIGURE 37 SKETCH OF TILTED PLANE SHOWING SOLUTION LINES.



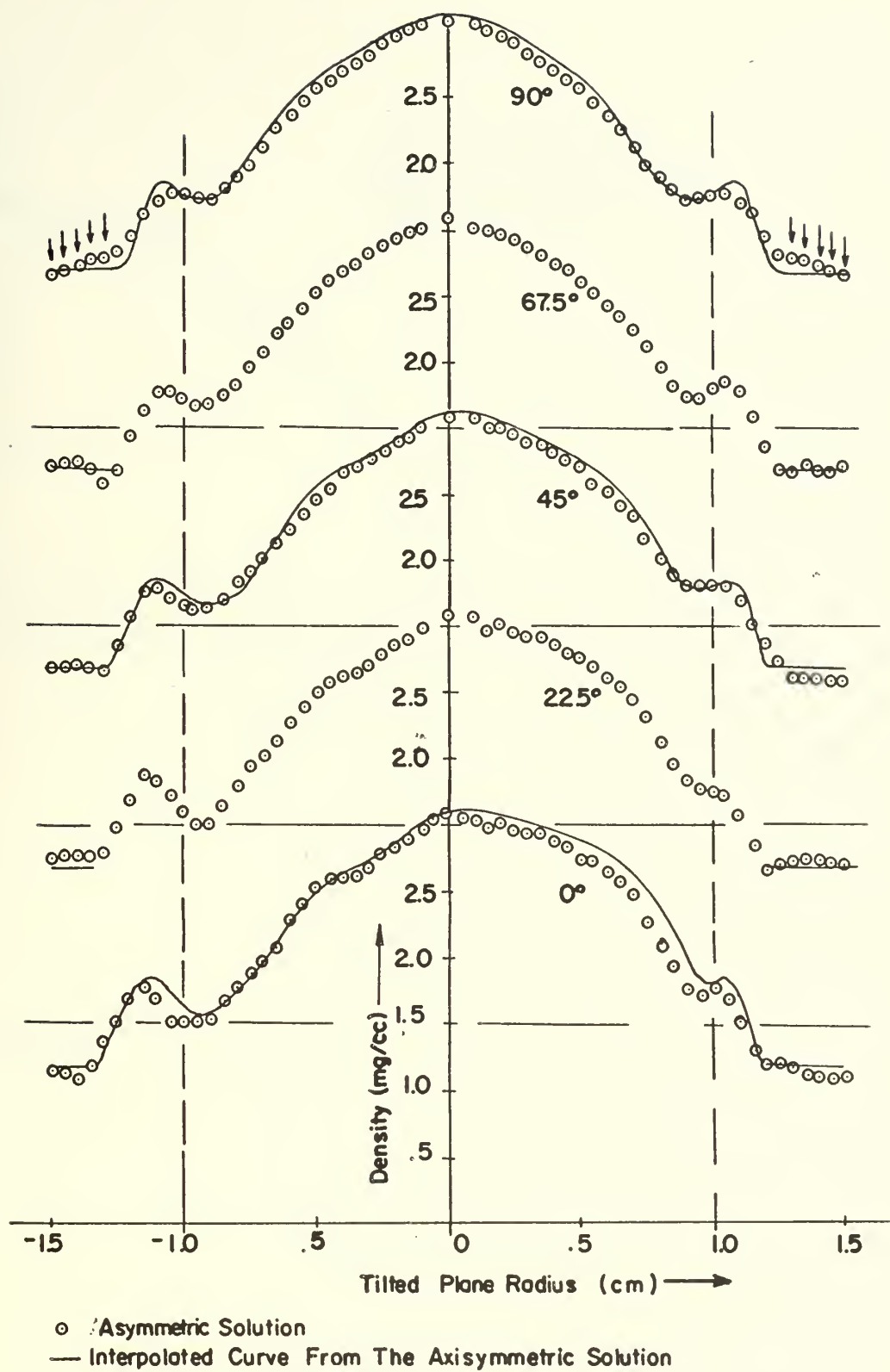


FIGURE 38 SOLUTION OF THE TILTED PLANE DENSITY ON FIVE DIAMETER LINES, 60 PSIG



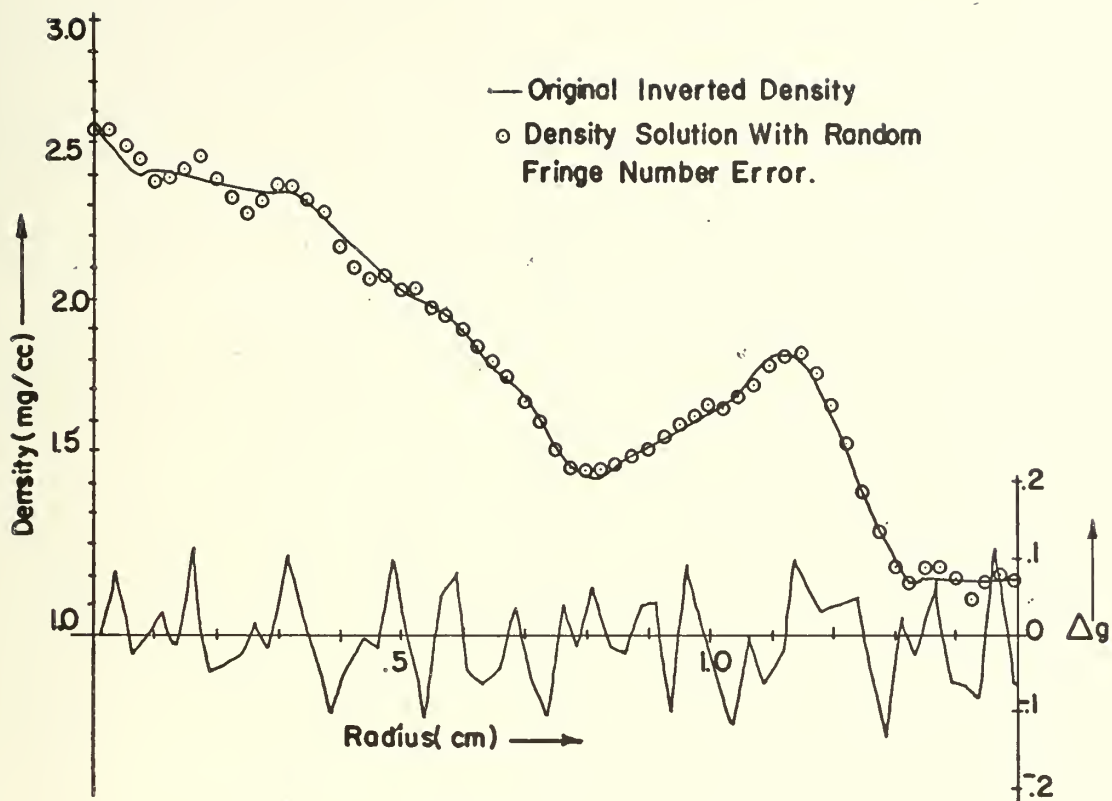


FIGURE 39 THE EFFECT OF RANDOM ERROR  $\Delta g$  ON THE AXISYMMETRIC SOLUTION AT  $Z = .75$  CM





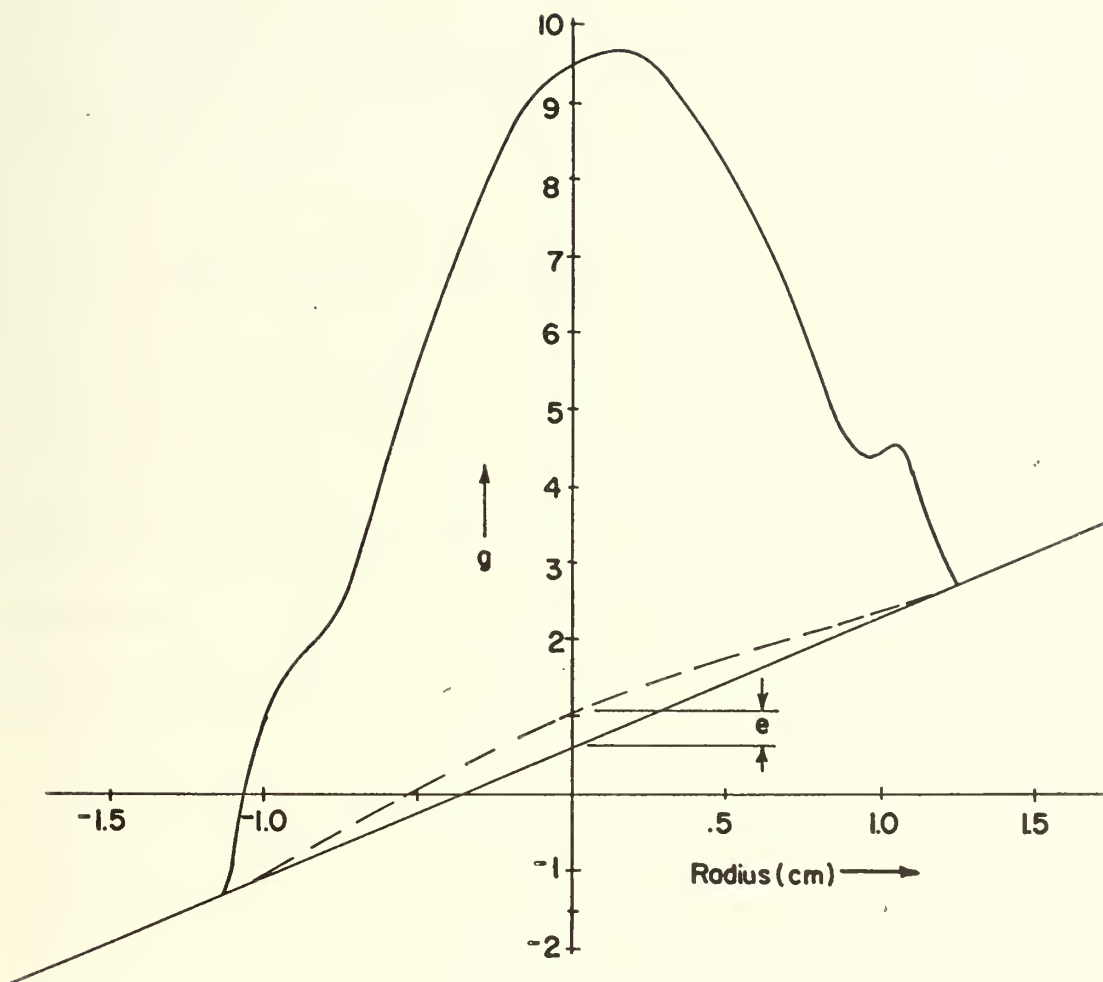


FIGURE 40 ILLUSTRATING POSSIBLE ERROR DUE TO NON-LINEAR BACKGROUND FRINGE.



## APPENDIX A

### OTHER INVERSION METHODS

#### 1. The Abel Inversion

For the case of axisymmetry, the function  $f$  becomes invariant to a rotation of the coordinate system, and equation eleven reduces to:

$$g(y) = 2Q \int_y^{s/2} \frac{r f(r) dr}{(r^2 - y^2)^{1/2}} \quad (A1)$$

where  $r = (x^2 + y^2)^{1/2}$ , which is a form of Abel's integral equation with a well known solution. The Abel inversion has long been the standard method for reducing the data from axisymmetric interferograms. [Ladenberg, ed. 1954]. It has been well studied and optimized. Unmodified, the Abel solution overshoots the correct values when crossing shock wave discontinuities. Iterative methods have been developed which reduce this problem [Sangster and Shaw 1968]. In addition, there is the "reduced function" method previously mentioned.

#### 2. The Generalized Abel Inversion

Recently a generalization of the Abel inversion by A. Pal has been reported [Cavanaugh, et.al. 1969] which applies to the two-dimensional function of equation eleven. It is in the process of being applied and evaluated at another laboratory. The method appears to have very similar application as the method utilized in this investigation.



### 3. Discrete Cubes

By representing the two-dimensional domain as a region of  $N \times N$ , discrete cubes of constant values (see figure five), one can represent equation eleven as a set of  $N^2$  linear equations in  $N^2$  unknown cube densities. The complexity of the resulting matrix inversion problem increases with the increasing size of the  $N^4$  matrix of coefficients, however, and the method is not presently competitive.

### 4. Rowley's Method

An analytical method involving a two-dimensional fourier transform has been reported recently [Rowley, 1969], but no application of the method is known to have been attempted.



## APPENDIX B MATHEMATICAL FOUNDATIONS

The selection of a set of functions which are orthogonal and defined over the domain has been made on the assumption that there exists a polynomial transform relationship which corresponds to the relationship between the functions  $f$  and  $g$ . Consider the operator notation of equation (11):

$$g = T f \quad (B1)$$

which has an inverse operation:

$$f = T^{-1} g \quad (B2)$$

One seeks a pair of orthogonal polynomial sets which, with an appropriate weighting function  $w$ , will satisfy the same transform operations.

Herlitz [1963], following a procedure from the diffraction theory of aberrations [Born and Wolf, 1959], for the cylindrically symmetric form of equation (11), and for the domain  $r \leq 1$ , used the Chebyshev functions [Madelung, 1953]:

$$V_k(\gamma) = \sin^{-1}(k \cos^{-1} \gamma) \quad (B3)$$

which satisfy the orthogonality relation

$$\int_{-1}^{+1} V_k(\gamma) V_l(\gamma) (1-\gamma^2) d\gamma = \int_{-\pi}^{\pi} \sin(k\theta) \sin(l\theta) d\theta = \frac{\pi}{2} \delta_{kl} \quad (B4)$$

and the Zernike polynomials, which have the form of the Legendre polynomials of argument  $t = 2r^2 - 1$ , and are orthogonal over the unit circle:

$$2(2k+1) \int_0^1 P_k(t) P_l(t) r dr = \delta_{kl} \quad (B5)$$





Using the Mehler integral [Whittaker and Watson, 1927]:

$$P_k(\cos \phi) = \frac{2^{\frac{1}{2}}}{\pi} \int_0^\phi \frac{\cos(k + \frac{1}{2}) \psi d\psi}{(\cos \psi - \cos \phi)} \quad (B6)$$

where  $\cos \frac{\phi}{2} = r$  and  $\cos \frac{\psi}{2} = \gamma$ , Herlitz reports the transform pair:

$$T P_k(t) = \frac{2}{2k+1} V_{2k+1}(\gamma) \quad (B7)$$

and

$$P_k(t) = \frac{2}{2k+1} T^{-1} V_{2k+1}(\gamma) \quad (B8)$$

Thus, by expanding  $f(r)$  in the Zernike polynomials with unknown coefficients

$$f(r) = \sum_{k=0}^{\infty} A_k P_k(t) \quad (B9)$$

and applying the transform relation (B1), one gets:

$$g(\gamma) = \sum_{k=0}^{\infty} \frac{2 A_k}{2k+1} V_{2k+1}(\gamma) \quad (B10)$$

The orthogonality relationship (B4) allows the determination of the unknown coefficients

$$A_k = \frac{2k+1}{\pi} \int_{-1}^1 g(\gamma) V_{2k+1}(\gamma) (1-\gamma^2)^{\frac{1}{2}} d\gamma \quad (B11)$$

Application of the evaluated coefficients  $A_k$  to the expansion of equation (B9) yields the desired solution for the density.

Maldonado [1965], in a similar analysis for the axisymmetric case over the entire domain  $r \leq \infty$ , using a generating procedure attributed to Bhatia and Wolf [1954], obtained the orthogonal polynomials:

$$U_{2k}(\alpha x, \alpha y) = (-1)^k \frac{\alpha}{\pi^{1/2}} L_k(\alpha^2 x^2 + \alpha^2 y^2) \quad (B12)$$

in which  $L_k$  are the Laguerre polynomials, defined over the interval  $r \leq \infty$ ,



which have a transform relationship with gaussian weighting function:

$$\int_{-\infty}^{\infty} U_{2k}(\alpha x, \alpha y) e^{-\alpha^2 x^2} dx = \frac{1}{k! 2^{2k}} H_{2k}(\alpha y) \quad (B13)$$

where  $H_{2k}(\alpha y)$  are the Hermite polynomials.

Hermite polynomials have the following orthogonality relationship:

$$\int_{-\infty}^{\infty} H_{2k}(\alpha y) H_{2l}(\alpha y) e^{-\alpha^2 y^2} dy = \frac{\delta_{kl}}{\alpha} \left[ \pi 2^{2k} 2^{2l} (2k)! (2l)! \right]^{\frac{1}{2}} \quad (B14)$$

Expanding the function  $f$  in terms of the polynomials  $U$ :

$$f(x, y) = \sum_{k=0}^{\infty} C_{2k}(\alpha) U_{2k}(\alpha x, \alpha y) e^{-(\alpha^2 x^2 + \alpha^2 y^2)} \quad (B15)$$

and applying the transform  $g = T f$ , one obtains:

$$g(y) = \sum_{k=0}^{\infty} \frac{1}{k! 2^{2k}} C_{2k}(\alpha) H_{2k}(\alpha y) e^{-\alpha^2 y^2} \quad (B16)$$

Again, the application of the orthogonality relationship (B14) provides for the evaluation of the unknown expansion coefficients:

$$C_{2k}(\alpha) = \frac{\alpha k!}{(2k)! \pi^{\frac{1}{2}}} \int_{-\infty}^{\infty} g(y) H_{2k}(\alpha y) dy \quad (B17)$$

As one can see, the logical structure of the development is the same as the Herlitz expansion, with the exception that the domain is here defined over the entire  $x, y$  plane. The evaluation of the unknown density function is made by evaluating equation (B15) with the coefficients obtained from (B17).

The same procedure is used for the asymmetric case. The polynomials chosen are [Maldonado, 1966]:

$$U_{m+2k}^{\pm m}(\alpha x, \alpha y) = (-1)^k \frac{\alpha}{\pi^{\frac{1}{2}}} \left[ \frac{k!}{(m+k)!} \right]^{\frac{1}{2}} (\alpha^2 x^2 + \alpha^2 y^2)^{\frac{m}{2}} e^{\pm i m \phi} L_k^m(\alpha^2 x^2 + \alpha^2 y^2) \quad (B18)$$

which have been chosen to have the property of "invariance in form" to a rotation of the coordinate system [Maldonado, 1965].



The "invariance in form" is demonstrated: suppose one makes a rotation of the axis by angle  $\xi$ . The polynomial  $U_{m+2k}^{\pm m}$  becomes:

$$U_{m+2k}^{\pm m}(\alpha x', \alpha y') = (-1)^k \frac{\alpha}{\pi^{1/2}} \left[ \frac{k!}{(m+k)!} \right]^{1/2} (\alpha x'^2 + \alpha y'^2)^{\frac{m}{2}} e^{\pm i m (\phi - \xi)} L_k^m(\alpha x'^2 + \alpha y'^2) \quad (B19)$$

or:

$$U_{m+2k}^{\pm m}(\alpha x', \alpha y') = e^{\mp i m \xi} U_{m+2k}^{\pm m}(\alpha x, \alpha y) \quad (B20)$$

Clearly, the form of the polynomial has remained unchanged.

The polynomials,  $U_{m+2k}^{\pm m}(\alpha x, \alpha y)$  have a gaussian transform of:

$$\begin{aligned} I_{m+2k}^{\pm m}(\xi, dy') &= \int_{-\infty}^{\infty} U_{m+2k}^{\pm m}(\alpha x, \alpha y) e^{-\alpha^2 x'^2} dx' \\ &= \int_{-\infty}^{\infty} U_{m+2k}^{\pm m}(\alpha x', \alpha y') e^{\mp i m \xi} e^{-\alpha^2 x'^2} dx' \\ &= \frac{e^{\pm i m \xi} H_{m+2k}(\alpha y')}{\left[ k! (m+k)! \right]^{1/2} 2^{m+2k}} \end{aligned} \quad (B21)$$

where the orthogonality relationship becomes:

$$\begin{aligned} \int_{-\pi}^{\pi} e^{\pm i m \xi} e^{\mp i n \xi} d\xi \int_{-\infty}^{\infty} H_{m+2k}(\alpha y') H_{n+2l}(\alpha y') e^{-\alpha^2 y'^2} dy' &= \\ \frac{2\pi}{\alpha} \left[ \frac{3/2}{(m+2k)! (n+2l)! 2^{m+2k} 2^{n+2l}} \right] \delta_{mn} \delta_{(m+2k)(n+2l)} \end{aligned} \quad (B22)$$

The property of "invariance in form" preserves the form of the relationships for both the transform operation (B21) and the orthogonality condition (B22) during arbitrary rotations of the axes,  $\xi$ .



A similar expansion of the function  $f$  in terms of the polynomial

$U_{m+2k}^{\pm m}$  is:

$$f(x, y) = \sum_{m=0}^{\infty} \sum_{k=0}^{\infty} \epsilon_m C_{m+2k}^{\pm m}(\alpha) U_{m+2k}^{\pm m}(\alpha x, \alpha y) e^{-(\alpha^2 x^2 + \alpha^2 y^2)} \quad (B23)$$

followed by a similar application of the transform operator  $g = Tf$  yields:

$$g(y', \xi) = \sum_{m=0}^{\infty} \sum_{k=0}^{\infty} \epsilon_m \left[ k! (m+k)! 2^{2(m+2k)} \right]^{-\frac{1}{2}} C_{m+2k}^{\pm m}(\alpha) e^{\pm i m \xi} H_{m+2k}(\alpha y') e^{-\alpha^2 y'^2} \quad (B24)$$

from which an application of the orthogonality relationship yields an

evaluation of the unknown coefficients  $C_{m+2k}^{\pm m}$  :

$$C_{m+2k}^{\pm m} = \frac{\alpha}{2\pi^{3/2}} \left[ \frac{[k! (m+k)!]^{1/2}}{(m+2k)!} \right] \int_{-\pi}^{\pi} \int_{-\infty}^{\infty} g(y', \xi) H_{m+2k}(\alpha y') e^{\mp i m \xi} dy' d\xi \quad (B25)$$

which allow the evaluation of the expanded function  $f$  of equation (B23).

The progressive application of the same logical sequence, which has been given, demonstrates the development of this method of inversion by orthogonal polynomial expansion.





## APPENDIX C

### HOLOFER,

A FORTRAN IV COMPUTER PROGRAM FOR INVERTING THE  
LINE INTEGRAL DATA OF HOLOGRAPHIC INTERFEROMETRY  
FOR ASYMMETRIC FIELDS

1. The Description of Input Parameters
2. A Sample Terminal Dialogue
3. The Terminal Executive Files
4. The Program
5. The Input Data Files Used in the Experiment



## 1. The Description of Input Parameters:

CMS	selects CP/CMS (terminal) or OS/MVT (batch) computer operation of the program. The selection is made by choice of the proper CMS definition card in the calling routine HOLOVERT.
IMAX	is the number of intervals of the input data in the radial direction, from $y' = -S/2$ to $+S/2$ . 1 IMAX 201.
JMAX/2	is the number of intervals of the input data in the azimuthal direction, from $\xi = 0^\circ$ to the edge of the orthogonal subinterval. $0 \leq JMAX/2 \leq 36$ , if JMAX/2 is set to zero, the value of JMAX will default to 1. This applies to the axisymmetric case where only one line of data is needed.
NOTE:	The dimension statements for G and GA in HOLOVERT set a limiting value of IMAX*JMAX at 5151. This would be exceeded if both values were individually set to their maximum. Only the dimension statements in HOLOVERT need be changed to change program dimensions.
KLIMIT	sets the number of B and D coefficients which will be computed corresponding to each k index of the double series. $1 \leq KLIMIT \leq 1000$ for asymmetric (SYM = 0) $1 \leq KLIMIT \leq 2000$ for symmetric (SYM = 0)
MLIMIT	sets the number of KLIMIT sets of B and D coefficients which will be computed corresponding to each m index of the double series. $1 \leq MLIMIT$ . MLIMIT may be any size, limited only by the disk space available for storage. Values greater than 50 are not desirable, however.
KEXTRA	is the number of extra terms that will be included in the evaluation of the k series after the term size has failed the epsilon criterion. $0 \leq KEXTRA \leq KLIMIT$ . This value insures that the term size has stabilized at a small value prior to truncating the evaluation. When the evaluation fails to converge prior to reaching KLIMIT terms, the last KEXTRA terms are averaged.



- MEXTRA the number of extra M series that will be evaluated after the K series evaluations have become small. MEXTRA has the same effect upon the m term evaluation as does KEXTRA on the K series.  $0 \leq \text{MEXTRA} \leq \text{MLIMIT}$ .
- ALPHA the scale factor for the Hermite and Laguerre polynomials.  $1.0 \leq \text{ALPHA} \leq 5.0$   
Maldonado, et.al. have shown that the factor Alpha has a significant effect upon the convergence criteria of the series. The guide line given is to match the edge slopes of the G function to a gaussian curve:  $G = e^{-\alpha^2 y^2}$   
Then one uses the value  $\alpha$  which matches. For the G functions used in this investigation, the variable SIZE has been adjusted to keep the function edges near .8 on the unit circle. ALPHA = 2.0 has been satisfactory for the experimental inversions.
- SIZE defines the diameter of the region from which data is taken, i.e. the diameter of the inversion circle. SIZE has been 2.5 or 3.0 for all experimental inversions, 2.0 for all mode 1 test runs.
- EPS is the convergence criterion. When the Nth term of the series becomes less than EPS times the partial sum to date, the KEXTRA or MEXTRA terms begin counting extra terms. If the (N+KEXTRA) term remains less than EPS\*SUM, the series is truncated. EPS=.0001 was used in most inversions.
- RHO-INF is the atmospheric density, in mg/cc., entered as an input for the density conversion of the output data. 1.176 mg/cc. was used for the experimental inversions.
- LAMBDA is the wavelength of the hologram source light in angstroms,  $\lambda = 6941.0 \text{ \AA}$  for ruby laser holograms.  $\lambda = 6328.0 \text{ \AA}$  for helium-neon holograms.
- BETA is the first term binomial expansion coefficient of the relation between index of refraction and density. BETA=.000291 for red light (6900A) BETA=.000293 for yellow-green light (5500A).



MODE selects the manner in which the G-array will be obtained. The three modes are described in the text and in the subroutine comment cards of the program. In addition to modes 1, 2, and 3, the parameter may be modified. Mode = -1, -2, or -3 will utilize subroutine FIELD2 which generates the B and D coefficients individually as needed. It requires much more time, but does not use offline disk space. MODE = 11, 12, or 13 will assume the B and D coefficients are already stored on the disk, will bypass subroutine BDGEN and use the previously computed coefficients. This provides a restart capability to the program. Once the coefficients have been generated, one can vary the output parameters for repeat inversions.

SYM selects the symmetry parameters of the field to be inverted. SYM is called JSYM in the program.  
 SYM = 0 - completely asymmetric field  
 SYM = 1,2,3,4,... - 1,2,3,4... regularly spaced planes of symmetry exist in the field, aligned with plane number one on the X-Z plane.  
 SYM > JMAX - an axisymmetric field.

POINTS is the number of points to be inverted on each sampling line. POINTS  $\geq 1$

LINES is the number of lines of points through the field to be inverted LINES  $\geq 1$

DIAGNOS provides a series of levels of diagnostic printout. It is helpful if errors show up in the program to printout the parameters as they are computed. No explanation will be made here, as the use of this parameter involves detailed study of the program anyway. DIAGNOS = 0. for normal operation.

STD.DEV. provides the ability to add a random error of given standard deviation to the add-on function G-array. The resulting inversion will reflect the effect of random errors to the data. This parameter allows some degree of error estimate to the experimental data.  
 STD.DEV. = 0.0 for normal operation  
 STD.DEV. = .0625 for  $\pm 1/8$  fringe number error in the data.

PHIZERO is the angle in degrees, which the first line to be inverted will make with the X axis. PHIZERO = 0.0 for most uses.





DELPHI is the angular incrementation, in degrees, that successive inversion lines will make with the X-axis. The second line will be at  $\text{PHI}=\text{PHIZERO}+\text{DELPHI}$ , etc.

YPZERO is the  $y'$  position of the first line to be inverted, in the primed coordinate system rotated by angle PHI

YPRANGE is the range over which  $y'$  will uniformly vary for the number of lines to be inverted. If one sets  $\text{DELPHI}=0$ . and  $\text{YPRANGE} \neq 0$ . A cartesian array of points will be selected, if  $\text{DELPHI} \neq 0$ . and  $\text{YPRANGE}=0$ . A cylindrical array of points will be selected.

XPZERO is the position of the beginning of each line to be inverted (in the primed coordinate system).

XPRANGE is the range over which the number of points selected will range, beginning at XPZERO.

TST.FUN is the number of the function to be inverted. In mode 1 this number corresponds to the function number in subroutine FUNCT. In modes 2 and 3 it serves as a run identifying number on the output.

ADD.FUN is the number of the function in FUNCT to be used as an add-on function.  $\text{ADD.FUN}=0$ . will default the use of an add-on function.

GARRAY is the output parameter for printout of the G-array used.  
GARRAY =

- 0. -- no printout.
- 1. -- prints the G-array.
- 2. -- prints the G-array with a pause for paper spacing on the terminal prior to printing.
- 3. -- prints both G-array and the add-on G-array.
- 4. -- prints both G-arrays with terminal pauses for spacing.
- 1. -- punches the G-array on a deck of cards and prints the G-array
- 3. -- punches the modified G-array sum of both on a deck of cards, then prints both G-arrays separately.



GRAPH        prints a graph of each line of the G-array.    GRAPH =

0. -- no graph.
1. -- a graph of G-array for each J.
2. -- same as 1. , with terminal pause.
3. -- both G-array and add-on G-array are on each graph.
4. -- same as 3. , with terminal pause.

LIN.PRT       prints the inversion results LIN.PRT =

0. -- G-array is set up, inversion results are not printed.  
Inversion is not performed unless MAP.BND=0.
1. -- prints the inversion results a line at a time.
2. -- prints the inversion results with a terminal pause  
prior to each line of points , for paper spacing.  
It also sets a terminal pause prior to MAP output ,  
if MAP is used.

MAP.BND       prints a map of the inversion array on the printer.    Uses  
library subroutine MTMPII.    MAP.BND=

0. -- map is not printed.
- ≠0. -- the number used defines the interval between con-  
tours of the function f on the map , e. g. 0.2.

A,B,C,D,E,P are variable function parameters for the functions in  
subroutine FUNCT , as used in mode 1 inversion.

S,T,U,V,W,Q are variable function parameters for the functions of sub-  
routine FUNCT , as used for the add-on function.

PHISYM        is an input angle entered in the data cards for mode 2 or 3  
operation that defines a rotation between the inversion  
coordinate system and the laboratory , or output coordinate  
system , e.g. if the plane of symmetry of the function was  
at 5° in the laboratory system , one would enter 5.0 in the  
data cards.    Output would then be in the laboratory coordinate  
system.    Raw data for mode 2 is entered in the laboratory  
coordinate system; G-array data for mode 3 is entered in the  
data plane coordinate system.

XO,YO        are the laboratory coordinates of the estimated center of the  
function , entered in the data cards used in mode 2 , to provide  
a well-centered inversion.    Output is in laboratory coordinates.



INPUT DATA for batch operation, input data cards are read in order:

- 1) 7 cards of input data, format 89 of calling program HOLOVERT; data corresponds exactly to parameters in the sample dialogue.
- 2) IF USED: data cards for numerical function, formats 88, 89 of subroutine FREAD.
- 3) IF USED: data cards for numerical add-on function, formats 88, 89 of subroutine FREAD.
- 4) input data for mode 2 or mode 3
  - mode 2: formats 59, 58 of subroutine SHEET;  
if NCODE.GE.1: format 29 of subroutine SIM.
  - mode 3: formats 39, 38 of subroutine READ.
- 5) a blank card if another data set follows, otherwise a FINISH card; format 60, HOLOVERT.

For terminal operation, input data 2), 3), and 4) are entered in the above formats in separate files and given optional filenames/filetypes. The organization of files for execution is handled by exec file HOLOFER.

A sample terminal dialogue follows.



2. A Sample Terminal Dialogue on the Cambridge Monitor System.

```
holofer
ERASE FILE FT03F001 *
ERASE FILE FT04F001 *
SPLIT INPUT DATA FILE FT04F001 1 EOF
EOF REACHED
FILE MODIFIED
```

ANSWER YES OR NO...

DO YOU WISH INFO TYPEOUT?  
no

DO YOU WISH INPUT DATA TYPED OUT OR CHANGED?  
yes

THE INPUT VALUES FOLLOW:  
--1) IF CHANGES ARE DESIRED TYPE NEW VALUE(S) UNDER OLD  
--2) IF NO CHANGES, HIT SPACE BAR AND RETURN  
--3) TO CHANGE A NON-ZERO NUMBER TO ZERO, TYPE "999."

\$ SETUP  
EXECUTION BEGINS...

```
*****
*   IMAX   * JMAX/2 * KLIMIT * MLIMIT * KEXTRA * MEXTRA *
*   60.    * 18.    * 250.    * 30.    * 5.      * 2.      *
*   41.    * 999.   *          * 1.      *          *          *
*   ALPHA  * SIZE   * EPS.   * RHO-INF * LAMBDA * BETA   *
*   2.000  * 3.000  * 0.000500 * 1.1760 * 6941.0 * 0.000291
*          * 2.      * .001     *          *          *
*****
```





```

)  * MODE * SYM. * POINTS * LINES * DIAGNOS * STD.DEV *
    3.      1.      31.      9.      0.0      0.0
    1.      100.     21.      1.
* PHIZERO * DELPHI * YPZERO * YPRANGE * XPZERO * XPRANGE *
    0.0      22.500    0.0      0.0      0.0      1.500
                                1.
* TST FUN * ADD FUN * GARRAY * GRAPH * LIN PRT * MAP BND *
    60.      0.0      1.      0.0      1.      0.0
    5.      999.
* A * B * C * D * E * P *
    1.000    0.700    0.900    0.071    0.071    0.0
    1.      1.
* S * T * U * V * W * Q *
    0.0      1.000    1.000    0.0      0.0      1.000

```

```

*****
IHC0021 STOP 0
ERASE INPUT DATA *
SPLIT FILE FT04F001 INPUT DATA 1 EOF
EOF REACHED
FILE MODIFIED
*****

```

```

DO YOU WISH THE TEST DATA READ IN?
no

```

```

WILL ADD-ON FUNCTION DATA BE READ IN? (EQ'N. NO. 8)
no

```

```

EXECUTE THE PROGRAM?
no
R; T=0.97/2.82 15.32.16

```

























100









[illegible]

```

(XP(I).EQ.0.) THT=C.
ISIG=TAL*FIE/2.+THT
IF (SIG.GT.PIE) SIG=SIG-TPIE
IF (SIG.LT.MPIE) SIG=SIG+TPIE
XS=RS*CS(SIG)
IF (DGN.GE.1) WRITE (6,44) SIG
FORMAT (1, SIG)
YS=RS*CS(SIG)
IF (DGN.GE.5) WRITE (6,57) PHI,DELPHI,PSI,TAU,THT,SIG,SIGI,XS,YS
I=1
R=1
IF (DGN.GE.2) WRITE (6,65) I
FUNCTION (XS,YS,FA(I,J),NAF,DGN,NTWO)
IF (I.EQ.1) CALL FUNCT (XS,YS,F,NCF,DGN,MONE)
IF (I.EQ.2) REWIND 3
IF (I.EQ.3) CALL FIELD (PS,SIGI,SOLN,NRD,BDA,DGN,KBD)
IF (I.EQ.4) CALL FIELD2 (RS,SIGI,SCLN,G,H,SCF,DGN)
IF (I.EQ.5) CALL FIEL3 (XS,YS,FA(I,J))
IF (I.EQ.6) CALL FIEL4 (XS,YS,FA(I,J))
IF (I.EQ.7) CALL FIEL5 (XS,YS,FA(I,J))
IF (I.EQ.8) CALL FIEL6 (XS,YS,FA(I,J))
IF (I.EQ.9) CALL FIEL7 (XS,YS,FA(I,J))
IF (I.EQ.10) CALL FIEL8 (XS,YS,FA(I,J))
IF (I.EQ.11) CALL FIEL9 (XS,YS,FA(I,J))
IF (I.EQ.12) CALL FIEL10 (XS,YS,FA(I,J))
IF (I.EQ.13) CALL FIEL11 (XS,YS,FA(I,J))
IF (I.EQ.14) CALL FIEL12 (XS,YS,FA(I,J))
IF (I.EQ.15) CALL FIEL13 (XS,YS,FA(I,J))
IF (I.EQ.16) CALL FIEL14 (XS,YS,FA(I,J))
IF (I.EQ.17) CALL FIEL15 (XS,YS,FA(I,J))
IF (I.EQ.18) CALL FIEL16 (XS,YS,FA(I,J))
IF (I.EQ.19) CALL FIEL17 (XS,YS,FA(I,J))
IF (I.EQ.20) CALL FIEL18 (XS,YS,FA(I,J))
IF (I.EQ.21) CALL FIEL19 (XS,YS,FA(I,J))
IF (I.EQ.22) CALL FIEL20 (XS,YS,FA(I,J))
IF (I.EQ.23) CALL FIEL21 (XS,YS,FA(I,J))
IF (I.EQ.24) CALL FIEL22 (XS,YS,FA(I,J))
IF (I.EQ.25) CALL FIEL23 (XS,YS,FA(I,J))
IF (I.EQ.26) CALL FIEL24 (XS,YS,FA(I,J))
IF (I.EQ.27) CALL FIEL25 (XS,YS,FA(I,J))
IF (I.EQ.28) CALL FIEL26 (XS,YS,FA(I,J))
IF (I.EQ.29) CALL FIEL27 (XS,YS,FA(I,J))
IF (I.EQ.30) CALL FIEL28 (XS,YS,FA(I,J))
IF (I.EQ.31) CALL FIEL29 (XS,YS,FA(I,J))
IF (I.EQ.32) CALL FIEL30 (XS,YS,FA(I,J))
IF (I.EQ.33) CALL FIEL31 (XS,YS,FA(I,J))
IF (I.EQ.34) CALL FIEL32 (XS,YS,FA(I,J))
IF (I.EQ.35) CALL FIEL33 (XS,YS,FA(I,J))
IF (I.EQ.36) CALL FIEL34 (XS,YS,FA(I,J))
IF (I.EQ.37) CALL FIEL35 (XS,YS,FA(I,J))
IF (I.EQ.38) CALL FIEL36 (XS,YS,FA(I,J))
IF (I.EQ.39) CALL FIEL37 (XS,YS,FA(I,J))
IF (I.EQ.40) CALL FIEL38 (XS,YS,FA(I,J))
IF (I.EQ.41) CALL FIEL39 (XS,YS,FA(I,J))
IF (I.EQ.42) CALL FIEL40 (XS,YS,FA(I,J))
IF (I.EQ.43) CALL FIEL41 (XS,YS,FA(I,J))
IF (I.EQ.44) CALL FIEL42 (XS,YS,FA(I,J))
IF (I.EQ.45) CALL FIEL43 (XS,YS,FA(I,J))
IF (I.EQ.46) CALL FIEL44 (XS,YS,FA(I,J))
IF (I.EQ.47) CALL FIEL45 (XS,YS,FA(I,J))
IF (I.EQ.48) CALL FIEL46 (XS,YS,FA(I,J))
IF (I.EQ.49) CALL FIEL47 (XS,YS,FA(I,J))
IF (I.EQ.50) CALL FIEL48 (XS,YS,FA(I,J))
IF (I.EQ.51) CALL FIEL49 (XS,YS,FA(I,J))
IF (I.EQ.52) CALL FIEL50 (XS,YS,FA(I,J))
IF (I.EQ.53) CALL FIEL51 (XS,YS,FA(I,J))
IF (I.EQ.54) CALL FIEL52 (XS,YS,FA(I,J))
IF (I.EQ.55) CALL FIEL53 (XS,YS,FA(I,J))
IF (I.EQ.56) CALL FIEL54 (XS,YS,FA(I,J))
IF (I.EQ.57) CALL FIEL55 (XS,YS,FA(I,J))
IF (I.EQ.58) CALL FIEL56 (XS,YS,FA(I,J))
IF (I.EQ.59) CALL FIEL57 (XS,YS,FA(I,J))
IF (I.EQ.60) CALL FIEL58 (XS,YS,FA(I,J))
IF (I.EQ.61) CALL FIEL59 (XS,YS,FA(I,J))
IF (I.EQ.62) CALL FIEL60 (XS,YS,FA(I,J))
IF (I.EQ.63) CALL FIEL61 (XS,YS,FA(I,J))
IF (I.EQ.64) CALL FIEL62 (XS,YS,FA(I,J))
IF (I.EQ.65) CALL FIEL63 (XS,YS,FA(I,J))
IF (I.EQ.66) CALL FIEL64 (XS,YS,FA(I,J))
IF (I.EQ.67) CALL FIEL65 (XS,YS,FA(I,J))
IF (I.EQ.68) CALL FIEL66 (XS,YS,FA(I,J))
IF (I.EQ.69) CALL FIEL67 (XS,YS,FA(I,J))
IF (I.EQ.70) CALL FIEL68 (XS,YS,FA(I,J))
IF (I.EQ.71) CALL FIEL69 (XS,YS,FA(I,J))
IF (I.EQ.72) CALL FIEL70 (XS,YS,FA(I,J))
IF (I.EQ.73) CALL FIEL71 (XS,YS,FA(I,J))
IF (I.EQ.74) CALL FIEL72 (XS,YS,FA(I,J))
IF (I.EQ.75) CALL FIEL73 (XS,YS,FA(I,J))
IF (I.EQ.76) CALL FIEL74 (XS,YS,FA(I,J))
IF (I.EQ.77) CALL FIEL75 (XS,YS,FA(I,J))
IF (I.EQ.78) CALL FIEL76 (XS,YS,FA(I,J))
IF (I.EQ.79) CALL FIEL77 (XS,YS,FA(I,J))
IF (I.EQ.80) CALL FIEL78 (XS,YS,FA(I,J))
IF (I.EQ.81) CALL FIEL79 (XS,YS,FA(I,J))
IF (I.EQ.82) CALL FIEL80 (XS,YS,FA(I,J))
IF (I.EQ.83) CALL FIEL81 (XS,YS,FA(I,J))
IF (I.EQ.84) CALL FIEL82 (XS,YS,FA(I,J))
IF (I.EQ.85) CALL FIEL83 (XS,YS,FA(I,J))
IF (I.EQ.86) CALL FIEL84 (XS,YS,FA(I,J))
IF (I.EQ.87) CALL FIEL85 (XS,YS,FA(I,J))
IF (I.EQ.88) CALL FIEL86 (XS,YS,FA(I,J))
IF (I.EQ.89) CALL FIEL87 (XS,YS,FA(I,J))
IF (I.EQ.90) CALL FIEL88 (XS,YS,FA(I,J))
IF (I.EQ.91) CALL FIEL89 (XS,YS,FA(I,J))
IF (I.EQ.92) CALL FIEL90 (XS,YS,FA(I,J))
IF (I.EQ.93) CALL FIEL91 (XS,YS,FA(I,J))
IF (I.EQ.94) CALL FIEL92 (XS,YS,FA(I,J))
IF (I.EQ.95) CALL FIEL93 (XS,YS,FA(I,J))
IF (I.EQ.96) CALL FIEL94 (XS,YS,FA(I,J))
IF (I.EQ.97) CALL FIEL95 (XS,YS,FA(I,J))
IF (I.EQ.98) CALL FIEL96 (XS,YS,FA(I,J))
IF (I.EQ.99) CALL FIEL97 (XS,YS,FA(I,J))
IF (I.EQ.100) CALL FIEL98 (XS,YS,FA(I,J))
IF (I.EQ.101) CALL FIEL99 (XS,YS,FA(I,J))
IF (I.EQ.102) CALL FIEL100 (XS,YS,FA(I,J))
IF (I.EQ.103) CALL FIEL101 (XS,YS,FA(I,J))
IF (I.EQ.104) CALL FIEL102 (XS,YS,FA(I,J))
IF (I.EQ.105) CALL FIEL103 (XS,YS,FA(I,J))
IF (I.EQ.106) CALL FIEL104 (XS,YS,FA(I,J))
IF (I.EQ.107) CALL FIEL105 (XS,YS,FA(I,J))
IF (I.EQ.108) CALL FIEL106 (XS,YS,FA(I,J))
IF (I.EQ.109) CALL FIEL107 (XS,YS,FA(I,J))
IF (I.EQ.110) CALL FIEL108 (XS,YS,FA(I,J))
IF (I.EQ.111) CALL FIEL109 (XS,YS,FA(I,J))
IF (I.EQ.112) CALL FIEL110 (XS,YS,FA(I,J))
IF (I.EQ.113) CALL FIEL111 (XS,YS,FA(I,J))
IF (I.EQ.114) CALL FIEL112 (XS,YS,FA(I,J))
IF (I.EQ.115) CALL FIEL113 (XS,YS,FA(I,J))
IF (I.EQ.116) CALL FIEL114 (XS,YS,FA(I,J))
IF (I.EQ.117) CALL FIEL115 (XS,YS,FA(I,J))
IF (I.EQ.118) CALL FIEL116 (XS,YS,FA(I,J))
IF (I.EQ.119) CALL FIEL117 (XS,YS,FA(I,J))
IF (I.EQ.120) CALL FIEL118 (XS,YS,FA(I,J))
IF (I.EQ.121) CALL FIEL119 (XS,YS,FA(I,J))
IF (I.EQ.122) CALL FIEL120 (XS,YS,FA(I,J))
IF (I.EQ.123) CALL FIEL121 (XS,YS,FA(I,J))
IF (I.EQ.124) CALL FIEL122 (XS,YS,FA(I,J))
IF (I.EQ.125) CALL FIEL123 (XS,YS,FA(I,J))
IF (I.EQ.126) CALL FIEL124 (XS,YS,FA(I,J))
IF (I.EQ.127) CALL FIEL125 (XS,YS,FA(I,J))
IF (I.EQ.128) CALL FIEL126 (XS,YS,FA(I,J))
IF (I.EQ.129) CALL FIEL127 (XS,YS,FA(I,J))
IF (I.EQ.130) CALL FIEL128 (XS,YS,FA(I,J))
IF (I.EQ.131) CALL FIEL129 (XS,YS,FA(I,J))
IF (I.EQ.132) CALL FIEL130 (XS,YS,FA(I,J))
IF (I.EQ.133) CALL FIEL131 (XS,YS,FA(I,J))
IF (I.EQ.134) CALL FIEL132 (XS,YS,FA(I,J))
IF (I.EQ.135) CALL FIEL133 (XS,YS,FA(I,J))
IF (I.EQ.136) CALL FIEL134 (XS,YS,FA(I,J))
IF (I.EQ.137) CALL FIEL135 (XS,YS,FA(I,J))
IF (I.EQ.138) CALL FIEL136 (XS,YS,FA(I,J))
IF (I.EQ.139) CALL FIEL137 (XS,YS,FA(I,J))
IF (I.EQ.140) CALL FIEL138 (XS,YS,FA(I,J))
IF (I.EQ.141) CALL FIEL139 (XS,YS,FA(I,J))
IF (I.EQ.142) CALL FIEL140 (XS,YS,FA(I,J))
IF (I.EQ.143) CALL FIEL141 (XS,YS,FA(I,J))
IF (I.EQ.144) CALL FIEL142 (XS,YS,FA(I,J))
IF (I.EQ.145) CALL FIEL143 (XS,YS,FA(I,J))
IF (I.EQ.146) CALL FIEL144 (XS,YS,FA(I,J))
IF (I.EQ.147) CALL FIEL145 (XS,YS,FA(I,J))
IF (I.EQ.148) CALL FIEL146 (XS,YS,FA(I,J))
IF (I.EQ.149) CALL FIEL147 (XS,YS,FA(I,J))
IF (I.EQ.150) CALL FIEL148 (XS,YS,FA(I,J))
IF (I.EQ.151) CALL FIEL149 (XS,YS,FA(I,J))
IF (I.EQ.152) CALL FIEL150 (XS,YS,FA(I,J))
IF (I.EQ.153) CALL FIEL151 (XS,YS,FA(I,J))
IF (I.EQ.154) CALL FIEL152 (XS,YS,FA(I,J))
IF (I.EQ.155) CALL FIEL153 (XS,YS,FA(I,J))
IF (I.EQ.156) CALL FIEL154 (XS,YS,FA(I,J))
IF (I.EQ.157) CALL FIEL155 (XS,YS,FA(I,J))
IF (I.EQ.158) CALL FIEL156 (XS,YS,FA(I,J))
IF (I.EQ.159) CALL FIEL15
```



```

14
3
4
5
14

```













[illegible]



```

      HB=2.*SQRT((PK+1.)*(RM+PK+1.))/(ORDER+1.)/((CORDER+2.))
      DO 5 I=1,IMX2
      IIM=IIMX-I+1
      H(I,1)=2.*(H(I,3)*H(I,2)-HA*H(I,1))
      H(I,1,1)=SIGN*H(I,1)
      H(I,1,2)=H(I,3)*H(I,1)-CORDER*H(I,2)
      ADVANCE 3 THE SIN/COS ARRAY FOR THE NEXT M:
      DO 3 J=1,JJMX
      IF (DGN.LE.-5) WRITE (5,87) (SCE(J,NT),NT=1,6)
      I FORMAT (1 SIN/COS MXI:9E10.3)
      STEMP=SCE(J,1)
      SCE(J,1)=SCE(J,2)*SCE(J,3)
      SCE(J,2)=SCE(J,4)+SCE(J,2)*SCE(J,3)
      SCE(J,3)=SCE(J,1)
      SCE(J,4)=SCE(J,1,1)-SCE(J,1)
      SCE(J,5)=SCE(J,1,2)-SCE(J,2)
      WRITE (5,88) (BDA(I),I=1,10)
      IF (DGN.LE.-3) WRITE (4,88) (BDA(I),I=1,10)
      IF (JSYN.GT.JMAX) RETURN
      RM=RM+1
      REGENERATE THE HERMITE ARRAY FOR NEW M, K=0:
      DO 7 IIMX-I+1
      IIV=IIMX-I+1
      H(I,1,4)=SQRT(RM)/((RM+1.))
      H(I,1,5)=H(I,1,4)*SQRT(2.)
      H(I,1,1)=H(I,1,5)*H(I,1)
      H(I,1,2)=-SIGN*H(I,1)
      H(I,1,3)=2.*SQRT(RM+1.)*H(I,1)-(RM+1.)*H(I,2)
      H(I,1,4)=H(I,1,2)
      H(I,1,5)=H(I,1,1)
      H(I,1,1)=H(I,1,4)
      H(I,1,2)=H(I,1,5)
      H(I,1,3)=H(I,1,1)
      H(I,1,4)=H(I,1,2)
      H(I,1,5)=H(I,1,3)
      FORMAT (14,1, P='E10.4', D='E10.4')
      FORMAT (2X,1CE10.3)
      RETURN
      END
CCCCC2

```

```

SUBROUTINE FIELD (RS,SIG,SCLN,NBD,BDA,DGN,KBD)
FIELD EVALUATES THE VALUE OF THE FIELD FUNCTION AT A PARTICULAR
POINT DESIGNATED IN CYLINDRICAL COORDINATES, BY USING THE INVERSION
EQUATION OF MAUDGNADG. THE FIELD USES THE ARRAY OF R & D
COEFFICIENTS GENERATED IN SUBROUTINE BDGEN.
COMMON IMAX,JMAX,IIMX,JJMX,ALPHA,SIZE,EPS,MODE,BDX,SD,IX,Z
COMMON /IAB/ INDEX,KEXTRA,VEXTRA,KLIMIT,NLIMIT,KOUT,MOUT
COMMON /SYN/ ISYN,JSYN,NSYN,FCU,IMS,JMS,OSYN

```





















SUBROUTINE FIELD2 (RS,SIG,SCLN,G,H,SCF,DGN)  
 FIELD2 COMPUTES THE SAME INVERSION AS SUBROUTINE FIELD, EXCEPT THAT  
 THE COEFFICIENTS R AND D ARE COMPUTED INDIVIDUALLY AS USED BY  
 CALLING ROUTINE. DISK STORAGE IS NOT REQUIRED, BUT COMPUTING TIME IS  
 MUCH GREATER. FIELD2 IS UTILIZED BY SPECIFYING A NEGATIVE MODE ON  
 THE INPUT PARAMETER. THE VALUE OF THE FIELD FUNCTION AT A PARTICULAR  
 POINT DESIGNATED IN CYLINDRICAL COORDINATES, BY USING THE INVERSION  
 EQUATION OF MALDONADO, ET AL. FIELD CALLS SUBROUTINES RC & GAPRAY.  
 COMMON IMAX,JMAX,IMX,JMX,IJMX,ALPHA,SIZE,EPS,MODE,POX,SD,IX,7  
 COMMON /TAB/ INDEX,KEXTRA,MEXTRA,KLIMIT,MLIMIT,OSYM  
 COMMON /SYM/ ISYM,JSYM,MSYM,FCL,IMS,JMS,OSYM  
 DIMENSION G(IJMX),H(IJMX,5),SCF(IJMX,6)  
 INITIALIZE THE VALUES:  
 IN INDEX=C  
 MTIME=C  
 KOUT=0  
 MOUT=0  
 MMAX=0  
 KUTAL=C  
 JIMX=JIMX\*5  
 JIMX2=(IIMX+1)/2  
 AR=ALPHA\*2  
 ARG=ARG\*2  
 ARGON=EXP(-ARG)  
 FIEP=2.141592653589793  
 APP=ALPHA/PIE/PIE  
 M=C  
 RM=M  
 RIM=1X=IMAX  
 RX=2./RIMAX  
 RJM=1X=JMAX

SUBROUTINE FIELD2 (RS,SIG,SCLN,G,H,SCF,DGN)  
 FIELD2 COMPUTES THE SAME INVERSION AS SUBROUTINE FIELD, EXCEPT THAT  
 THE COEFFICIENTS R AND D ARE COMPUTED INDIVIDUALLY AS USED BY  
 CALLING ROUTINE. DISK STORAGE IS NOT REQUIRED, BUT COMPUTING TIME IS  
 MUCH GREATER. FIELD2 IS UTILIZED BY SPECIFYING A NEGATIVE MODE ON  
 THE INPUT PARAMETER. THE VALUE OF THE FIELD FUNCTION AT A PARTICULAR  
 POINT DESIGNATED IN CYLINDRICAL COORDINATES, BY USING THE INVERSION  
 EQUATION OF MALDONADO, ET AL. FIELD CALLS SUBROUTINES RC & GAPRAY.  
 COMMON IMAX,JMAX,IMX,JMX,IJMX,ALPHA,SIZE,EPS,MODE,POX,SD,IX,7  
 COMMON /TAB/ INDEX,KEXTRA,MEXTRA,KLIMIT,MLIMIT,OSYM  
 COMMON /SYM/ ISYM,JSYM,MSYM,FCL,IMS,JMS,OSYM  
 DIMENSION G(IJMX),H(IJMX,5),SCF(IJMX,6)  
 INITIALIZE THE VALUES:  
 IN INDEX=C  
 MTIME=C  
 KOUT=0  
 MOUT=0  
 MMAX=0  
 KUTAL=C  
 JIMX=JIMX\*5  
 JIMX2=(IIMX+1)/2  
 AR=ALPHA\*2  
 ARG=ARG\*2  
 ARGON=EXP(-ARG)  
 FIEP=2.141592653589793  
 APP=ALPHA/PIE/PIE  
 M=C  
 RM=M  
 RIM=1X=IMAX  
 RX=2./RIMAX  
 RJM=1X=JMAX



[illegible]





```

IF (MS.EQ.NSYM) MS=0
ITOTAL=C.
MS=MS+1
IF (MS.NE.1) GO TO 7
IF (MS.EQ.1) GO TO 7
IF (MS.EQ.2) GO TO 7
IF (MS.EQ.3) GO TO 7
IF (MS.EQ.4) GO TO 7
IF (MS.EQ.5) GO TO 7
IF (MS.EQ.6) GO TO 7
IF (MS.EQ.7) GO TO 7
IF (MS.EQ.8) GO TO 7
IF (MS.EQ.9) GO TO 7
IF (MS.EQ.10) GO TO 7
IF (MS.EQ.11) GO TO 7
IF (MS.EQ.12) GO TO 7
IF (MS.EQ.13) GO TO 7
IF (MS.EQ.14) GO TO 7
IF (MS.EQ.15) GO TO 7
IF (MS.EQ.16) GO TO 7
IF (MS.EQ.17) GO TO 7
IF (MS.EQ.18) GO TO 7
IF (MS.EQ.19) GO TO 7
IF (MS.EQ.20) GO TO 7
IF (MS.EQ.21) GO TO 7
IF (MS.EQ.22) GO TO 7
IF (MS.EQ.23) GO TO 7
IF (MS.EQ.24) GO TO 7
IF (MS.EQ.25) GO TO 7
IF (MS.EQ.26) GO TO 7
IF (MS.EQ.27) GO TO 7
IF (MS.EQ.28) GO TO 7
IF (MS.EQ.29) GO TO 7
IF (MS.EQ.30) GO TO 7
IF (MS.EQ.31) GO TO 7
IF (MS.EQ.32) GO TO 7
IF (MS.EQ.33) GO TO 7
IF (MS.EQ.34) GO TO 7
IF (MS.EQ.35) GO TO 7
IF (MS.EQ.36) GO TO 7
IF (MS.EQ.37) GO TO 7
IF (MS.EQ.38) GO TO 7
IF (MS.EQ.39) GO TO 7
IF (MS.EQ.40) GO TO 7
IF (MS.EQ.41) GO TO 7
IF (MS.EQ.42) GO TO 7
IF (MS.EQ.43) GO TO 7
IF (MS.EQ.44) GO TO 7
IF (MS.EQ.45) GO TO 7
IF (MS.EQ.46) GO TO 7
IF (MS.EQ.47) GO TO 7
IF (MS.EQ.48) GO TO 7
IF (MS.EQ.49) GO TO 7
IF (MS.EQ.50) GO TO 7
IF (MS.EQ.51) GO TO 7
IF (MS.EQ.52) GO TO 7
IF (MS.EQ.53) GO TO 7
IF (MS.EQ.54) GO TO 7
IF (MS.EQ.55) GO TO 7
IF (MS.EQ.56) GO TO 7
IF (MS.EQ.57) GO TO 7
IF (MS.EQ.58) GO TO 7
IF (MS.EQ.59) GO TO 7
IF (MS.EQ.60) GO TO 7
IF (MS.EQ.61) GO TO 7
IF (MS.EQ.62) GO TO 7
IF (MS.EQ.63) GO TO 7
IF (MS.EQ.64) GO TO 7
IF (MS.EQ.65) GO TO 7
IF (MS.EQ.66) GO TO 7
IF (MS.EQ.67) GO TO 7
IF (MS.EQ.68) GO TO 7
IF (MS.EQ.69) GO TO 7
IF (MS.EQ.70) GO TO 7
IF (MS.EQ.71) GO TO 7
IF (MS.EQ.72) GO TO 7
IF (MS.EQ.73) GO TO 7
IF (MS.EQ.74) GO TO 7
IF (MS.EQ.75) GO TO 7
IF (MS.EQ.76) GO TO 7
IF (MS.EQ.77) GO TO 7
IF (MS.EQ.78) GO TO 7
IF (MS.EQ.79) GO TO 7
IF (MS.EQ.80) GO TO 7
IF (MS.EQ.81) GO TO 7
IF (MS.EQ.82) GO TO 7
IF (MS.EQ.83) GO TO 7
IF (MS.EQ.84) GO TO 7
IF (MS.EQ.85) GO TO 7
IF (MS.EQ.86) GO TO 7
IF (MS.EQ.87) GO TO 7
IF (MS.EQ.88) GO TO 7
IF (MS.EQ.89) GO TO 7
IF (MS.EQ.90) GO TO 7
IF (MS.EQ.91) GO TO 7
IF (MS.EQ.92) GO TO 7
IF (MS.EQ.93) GO TO 7
IF (MS.EQ.94) GO TO 7
IF (MS.EQ.95) GO TO 7
IF (MS.EQ.96) GO TO 7
IF (MS.EQ.97) GO TO 7
IF (MS.EQ.98) GO TO 7
IF (MS.EQ.99) GO TO 7
IF (MS.EQ.100) GO TO 7

```







[illegible]

```

COMMON IMAX,JMAX,IIMX,IJMX,ISYM,JSYM,MSYM,FCU,IMS,JMS,QSYM
COMMON /SYM/ ISYM,JSYM,MSYM,FCU,IMS,JMS,QSYM
COMMON /IO/ CMS,IN1,IN2,IN4
COMMON ION,G(IMAX,JMAX),G4(IMAX,JMAX)
PIE=3.141592653589793
P3=SIZE/2*GT.3) MODE=1
IF (MODE.GT.3) MODE=1
RIMX=IMAX
RJMXX=JMAX
LRLR=SIZE/RIMX
DELXI=2.*PIE/FCU
IF (MODE.GT.1) GO TO 2
DO 1 J=1,JMS
FJ=J
XI=(RJ-.5)*DELXI-PIE
J2=J+2*(JMS-J)
J3=J+JMAX/2
DO 1 I=1,IMS
PI=I
II=IMAX+I-1
R=(PI-.5)*DELX-HS
CALL GCLF (R,XI,GIJ,NCF,DGN,NUMB)
G(I,J)=GIJ
IF (ISYM.EQ.2) G(II,J)=GIJ
IF (ISYM.EQ.2) GO TO 1
G(II,J3)=GIJ
IF (JSYM.EQ.0) GO TO 1
G(II,J2)=GIJ
G(II,J4)=GIJ
CONTINUE
IF (MODE.GT.2) GO TO 3
CALL VSHEET (G,GA,XO,YO,PHISYM,NCF)
GO TO 4
CALL READ (Z,XO,YO,PHISYM,NCF,IMAX,JMAX,G)
CALL DGN.GE.2) WRITE (6,35)
RETURN
DEMAT ( ' GAPRAY RETURNS')
END
CCCCCCC

```



```

CCCC
SUBROUTINE GOLF (R,XI,GIJ,NCF,DGN,NUMB)
GOLF COMPUTES THE FUNCTION G(R,XI) FOR A PARTICULAR LINE OF SIGHT
FROM A KNOWN FUNCTION CONTAINED IN SUBROUTINE FUNCT.
COMMON IMAX,JMAX,IIMX,JJMX,IJMX,ALPHA,SIZE,EPS,MODE,BOX,SD,IX,Z
ZERO=0
LMAX=IMAX*3
RLMAX=LMAX
DELXP=SIZE/RLMAX
SXI=SIZE/RLMAX
CXI=SIZE/RLMAX
DELXS=DELXP*CXI
DELXS=DELXP*CXI
XS=DELXP*CXI
XS=XI-DELXP*CXI
XS=XI+DELXP*CXI
GIJ=0
DO I=1,LMAX
  RL=L
  FUNCT(XS,YS,F,NCF,DGN,NUMB)
  CALL GIJ+DELXS
  XS=XS+DELXS
  YS=YS+DELXS
  IF (GOLF.EQ.0.) GIJ=GIJ*DELXP*BOX
  IF (GOLF.EQ.0.) OR (NUMB.EQ.1) GC TO 2
  IF (DGN.GE.3) WRITE (3,28) IX
  CALL GALSS (IX,SD,ZERO,RV)
  GIJ=GIJ+RV
  IF (DGN.GE.3) WRITE (6,29) R,XI,GIJ
  RETURN
  IF (DGN.GE.3) R=1,FR.3,1, XI=1,FR.3,1, GIJ=1,FR.3,1
  FORMAT (1,1) GALSS, IX=1, I8)
END
CCCCC

```

```

CCCC
SUBROUTINE FUNCT (XS,YS,F,NCF,DGN,NUMB)
FUNCT EVALUATES AN INPUT FUNCTION AT POSITION (X,Y) IN THE TEST
SECTION COORDINATE SYSTEM. NCF IDENTIFIES THE EQUATION USED.
COMMON IMAX,JMAX,IIMX,JJMX,IJMX,ALPHA,SIZE,EPS,MODE,BOX,SD,IX,Z
COPAR/A,B,C,D,E,P,Q,S,T,U,V,W,RO,PA,NO,NA,N1,N2
CIMPANSION RO(101),RA(101)
A=1

```









```

5      IF (NCF.GT.6) GO TO 7
      RRC=SQRT(((XS-DD)/(RB)**2+((YS-EE)/(CC)**2)
      F=0
      IF (RBC.LT.1.) F=44
      GO TO 11
C C C C C
7.    CIRCULAR COSINE-SQUARED FUNCTION OF RB MAXIMA:
      IF (NCF.GT.7) GO TO 8
      F=44*CCS((2.*RB-1.)*PIE*R/2.):**2
      GO TO 11
C C C C C
8.    NUMERICAL FUNCTION:  REQUIRES AN INPUT ARRAY READ IN BY
      SUBROUTINE FREAD: N FOLLOWED BY N POINT VALUES. (101 MAX)
      A CONSTANT VALUE 44 IS ADDED TO THE FUNCTION.
      IF (NCF.GT.8) GO TO 9
      IF (NUMB.LE.1) N=NC
      IF (NUMB.GT.1) N=NA
      NM=N-1
      NM=N-2
      QN=NM
      QN=NM*(QN-1.)+1.
      RI=INT(RI)
      IR=FLCAT(IR)
      CIE=RI-IR
      IF (NUMB.LE.1) F=RQ(IR)
      IF (NUMB.GT.1) F=RA(IR)
      IF ((IR.NE.N).AND.(NUMB.LE.1)) F=F+DI*(RQ(IR+1)-RQ(IR))
      IF ((IR.NE.N).AND.(NUMB.GT.1)) F=F+DI*(RA(IR+1)-RA(IR))
      F=F+44+BB
      GO TO 11
C C C C C
9.    SPECIAL FUNCTION:  MAY BE WRITTEN FOR THE OCCASION AND
      INSERTED IN SUBROUTINE SPFUN
      IF (NCF.GT.9) GO TO 10
      CALL SPFUN (XS,YS,E)
      GO TO 11
C C C C C
      EQUATIONS NO. 10 AND BEYOND ARE SET TO ZERO.
      F=C.
      IF (DGN.GE.4) WRITE (6,99) XS,YS,E
      FORMAT (' XS=',F8.3,' YS=',F8.3,' F=',F8.3)
      RETURN
      ENDC
C C C C C

```



```

SUBROUTINE SPFUN (XS,YS,F)
C
C SPFUN IS A SPECIAL ROUTINE FOR EQ'N NO. 9. ANY FUNCTION MAY BE
C ENTERED.
C
COMMON /EQPARA/ A,B,C,D,E,P,Q,S,T,U,V,W,RO,RA,NC,NA,N1,N2
DIMENSION PO(101),RA(101)
F=C*(ABS(XS).LE.B).AND.(ARS(YS).LE.C) F=A
RETURN
END
C
C000000
C

```

```

SUBROUTINE SHEET (G,D,XG,YC,PHISYM,NCF)
C
C SHEET READS IRREGULARLY SPACED VALUES OF THE LINE INTEGRAL, AS MAY BE
C OBTAINED FROM HOLOGRAPHIC INTERFEROGRAMS. THE INTEGRAL AND RADIIUS
C OF THE LARGEST POSITIONAL INTERCEPTS, THE SYSTEM CENTER, LINES
C ABOUT 100 ENTERED IN CONSECUTIVE ORDER BY SPECIFYING NCONF=1,
C (PCS.) RADIUS. DATA MAY BE SIMULATED BY SPECIFYING NCONF=1,
C FOLLOWED BY APERTURE POSITIONS FOR A FUNCTION.
C
COMMON IMAX,JMAX,IMX,JMX,IJMX,IJMX,ALPHA,SIZE,EPS,MODE,BOX,SD,IX,Z
COMMON /SYM/ ISYM,JSYM,MSYM,FCU,IMS,JMS,QSYM
COMMON /IC/ CMS,INI,IN2,IN4
DIMENSION XG(303),XD(303),YG(303),YD(303),XI(303),RE(303)
NAPRE=303
NAPRE=2*PI*PI/2.
TRIPIT=PI*PI/2.
PLOT THE J=1, I=1, JMAX
Z=DO(I,J)=C.
DO(I,J)=C.
DO(I,J)=C.
XG(I)=C.
XG(I)=C.
XG(I)=C.
XG(I)=C.
XI(I)=C.

```

```

C
C 152653589793
C

```









00000      70

---

























```

1  IF (IT.GT.IMAX) IT=IMAX
    IBT=IT-1
    WRITE (6,98) (II,II=IB,IT)
    DO 2 I=1,IBT
    RI=I-1
    X(I)=SIZE/2.+(RI-.5)*DX
    LW=7*I
    WRITE (6,97) (X(I),I=1,IBT)
    WRITE (6,96) (HYP,L=1,LV),VERT
    JMH=JMH2+1
    DO 3 J=JMH,JMAX
    RJ=J
    XI=J-18C+CXI*(RJ-.5)
    IGR=(J-1)*IMAX+IB
    IGT=IGR-1
    WRITE (6,95) J,XI,(G(L),L=IGR,IGT)
    WRITE (6,94) (HYP,L=1,LV),VERT
    IPT=IGR+1
    ITO=IGR+INT RVL
    ITE=ITO-1
    IF (ITE.GT.IMAX) GO TO 1
    WRITE (6,93)
    I=1
    DO 4 I=1,IMAX
    WRITE (6,92) (I,II=I,IMAX)
    WRITE (6,91) (I,II=I,IMAX)
    WRITE (6,90) (I,II=I,IMAX)
    WRITE (6,89) (I,II=I,IMAX)
    WRITE (6,88) (I,II=I,IMAX)
    WRITE (6,87) (I,II=I,IMAX)
    WRITE (6,86) (I,II=I,IMAX)
    WRITE (6,85) (I,II=I,IMAX)
    WRITE (6,84) (I,II=I,IMAX)
    WRITE (6,83) (I,II=I,IMAX)
    WRITE (6,82) (I,II=I,IMAX)
    WRITE (6,81) (I,II=I,IMAX)
    WRITE (6,80) (I,II=I,IMAX)
    WRITE (6,79) (I,II=I,IMAX)
    WRITE (6,78) (I,II=I,IMAX)
    WRITE (6,77) (I,II=I,IMAX)
    WRITE (6,76) (I,II=I,IMAX)
    WRITE (6,75) (I,II=I,IMAX)
    WRITE (6,74) (I,II=I,IMAX)
    WRITE (6,73) (I,II=I,IMAX)
    WRITE (6,72) (I,II=I,IMAX)
    WRITE (6,71) (I,II=I,IMAX)
    WRITE (6,70) (I,II=I,IMAX)
    WRITE (6,69) (I,II=I,IMAX)
    WRITE (6,68) (I,II=I,IMAX)
    WRITE (6,67) (I,II=I,IMAX)
    WRITE (6,66) (I,II=I,IMAX)
    WRITE (6,65) (I,II=I,IMAX)
    WRITE (6,64) (I,II=I,IMAX)
    WRITE (6,63) (I,II=I,IMAX)
    WRITE (6,62) (I,II=I,IMAX)
    WRITE (6,61) (I,II=I,IMAX)
    WRITE (6,60) (I,II=I,IMAX)
    WRITE (6,59) (I,II=I,IMAX)
    WRITE (6,58) (I,II=I,IMAX)
    WRITE (6,57) (I,II=I,IMAX)
    WRITE (6,56) (I,II=I,IMAX)
    WRITE (6,55) (I,II=I,IMAX)
    WRITE (6,54) (I,II=I,IMAX)
    WRITE (6,53) (I,II=I,IMAX)
    WRITE (6,52) (I,II=I,IMAX)
    WRITE (6,51) (I,II=I,IMAX)
    WRITE (6,50) (I,II=I,IMAX)
    WRITE (6,49) (I,II=I,IMAX)
    WRITE (6,48) (I,II=I,IMAX)
    WRITE (6,47) (I,II=I,IMAX)
    WRITE (6,46) (I,II=I,IMAX)
    WRITE (6,45) (I,II=I,IMAX)
    WRITE (6,44) (I,II=I,IMAX)
    WRITE (6,43) (I,II=I,IMAX)
    WRITE (6,42) (I,II=I,IMAX)
    WRITE (6,41) (I,II=I,IMAX)
    WRITE (6,40) (I,II=I,IMAX)
    WRITE (6,39) (I,II=I,IMAX)
    WRITE (6,38) (I,II=I,IMAX)
    WRITE (6,37) (I,II=I,IMAX)
    WRITE (6,36) (I,II=I,IMAX)
    WRITE (6,35) (I,II=I,IMAX)
    WRITE (6,34) (I,II=I,IMAX)
    WRITE (6,33) (I,II=I,IMAX)
    WRITE (6,32) (I,II=I,IMAX)
    WRITE (6,31) (I,II=I,IMAX)
    WRITE (6,30) (I,II=I,IMAX)
    WRITE (6,29) (I,II=I,IMAX)
    WRITE (6,28) (I,II=I,IMAX)
    WRITE (6,27) (I,II=I,IMAX)
    WRITE (6,26) (I,II=I,IMAX)
    WRITE (6,25) (I,II=I,IMAX)
    WRITE (6,24) (I,II=I,IMAX)
    WRITE (6,23) (I,II=I,IMAX)
    WRITE (6,22) (I,II=I,IMAX)
    WRITE (6,21) (I,II=I,IMAX)
    WRITE (6,20) (I,II=I,IMAX)
    WRITE (6,19) (I,II=I,IMAX)
    WRITE (6,18) (I,II=I,IMAX)
    WRITE (6,17) (I,II=I,IMAX)
    WRITE (6,16) (I,II=I,IMAX)
    WRITE (6,15) (I,II=I,IMAX)
    WRITE (6,14) (I,II=I,IMAX)
    WRITE (6,13) (I,II=I,IMAX)
    WRITE (6,12) (I,II=I,IMAX)
    WRITE (6,11) (I,II=I,IMAX)
    WRITE (6,10) (I,II=I,IMAX)
    WRITE (6,9) (I,II=I,IMAX)
    WRITE (6,8) (I,II=I,IMAX)
    WRITE (6,7) (I,II=I,IMAX)
    WRITE (6,6) (I,II=I,IMAX)
    WRITE (6,5) (I,II=I,IMAX)
    WRITE (6,4) (I,II=I,IMAX)
    WRITE (6,3) (I,II=I,IMAX)
    WRITE (6,2) (I,II=I,IMAX)
    WRITE (6,1) (I,II=I,IMAX)

```

```

99  THE ARRAY OF INPUT DATA (G), OBTAINED BY GARRAY,
    Z=F7.3, CM=' '
    FOR I=1,IMAX
    DO 10 J=1,IMAX
    WRITE (6,90) (G(I,J),I=1,IMAX)
    WRITE (6,89) (G(I,J),I=1,IMAX)
    WRITE (6,88) (G(I,J),I=1,IMAX)
    WRITE (6,87) (G(I,J),I=1,IMAX)
    WRITE (6,86) (G(I,J),I=1,IMAX)
    WRITE (6,85) (G(I,J),I=1,IMAX)
    WRITE (6,84) (G(I,J),I=1,IMAX)
    WRITE (6,83) (G(I,J),I=1,IMAX)
    WRITE (6,82) (G(I,J),I=1,IMAX)
    WRITE (6,81) (G(I,J),I=1,IMAX)
    WRITE (6,80) (G(I,J),I=1,IMAX)
    WRITE (6,79) (G(I,J),I=1,IMAX)
    WRITE (6,78) (G(I,J),I=1,IMAX)
    WRITE (6,77) (G(I,J),I=1,IMAX)
    WRITE (6,76) (G(I,J),I=1,IMAX)
    WRITE (6,75) (G(I,J),I=1,IMAX)
    WRITE (6,74) (G(I,J),I=1,IMAX)
    WRITE (6,73) (G(I,J),I=1,IMAX)
    WRITE (6,72) (G(I,J),I=1,IMAX)
    WRITE (6,71) (G(I,J),I=1,IMAX)
    WRITE (6,70) (G(I,J),I=1,IMAX)
    WRITE (6,69) (G(I,J),I=1,IMAX)
    WRITE (6,68) (G(I,J),I=1,IMAX)
    WRITE (6,67) (G(I,J),I=1,IMAX)
    WRITE (6,66) (G(I,J),I=1,IMAX)
    WRITE (6,65) (G(I,J),I=1,IMAX)
    WRITE (6,64) (G(I,J),I=1,IMAX)
    WRITE (6,63) (G(I,J),I=1,IMAX)
    WRITE (6,62) (G(I,J),I=1,IMAX)
    WRITE (6,61) (G(I,J),I=1,IMAX)
    WRITE (6,60) (G(I,J),I=1,IMAX)
    WRITE (6,59) (G(I,J),I=1,IMAX)
    WRITE (6,58) (G(I,J),I=1,IMAX)
    WRITE (6,57) (G(I,J),I=1,IMAX)
    WRITE (6,56) (G(I,J),I=1,IMAX)
    WRITE (6,55) (G(I,J),I=1,IMAX)
    WRITE (6,54) (G(I,J),I=1,IMAX)
    WRITE (6,53) (G(I,J),I=1,IMAX)
    WRITE (6,52) (G(I,J),I=1,IMAX)
    WRITE (6,51) (G(I,J),I=1,IMAX)
    WRITE (6,50) (G(I,J),I=1,IMAX)
    WRITE (6,49) (G(I,J),I=1,IMAX)
    WRITE (6,48) (G(I,J),I=1,IMAX)
    WRITE (6,47) (G(I,J),I=1,IMAX)
    WRITE (6,46) (G(I,J),I=1,IMAX)
    WRITE (6,45) (G(I,J),I=1,IMAX)
    WRITE (6,44) (G(I,J),I=1,IMAX)
    WRITE (6,43) (G(I,J),I=1,IMAX)
    WRITE (6,42) (G(I,J),I=1,IMAX)
    WRITE (6,41) (G(I,J),I=1,IMAX)
    WRITE (6,40) (G(I,J),I=1,IMAX)
    WRITE (6,39) (G(I,J),I=1,IMAX)
    WRITE (6,38) (G(I,J),I=1,IMAX)
    WRITE (6,37) (G(I,J),I=1,IMAX)
    WRITE (6,36) (G(I,J),I=1,IMAX)
    WRITE (6,35) (G(I,J),I=1,IMAX)
    WRITE (6,34) (G(I,J),I=1,IMAX)
    WRITE (6,33) (G(I,J),I=1,IMAX)
    WRITE (6,32) (G(I,J),I=1,IMAX)
    WRITE (6,31) (G(I,J),I=1,IMAX)
    WRITE (6,30) (G(I,J),I=1,IMAX)
    WRITE (6,29) (G(I,J),I=1,IMAX)
    WRITE (6,28) (G(I,J),I=1,IMAX)
    WRITE (6,27) (G(I,J),I=1,IMAX)
    WRITE (6,26) (G(I,J),I=1,IMAX)
    WRITE (6,25) (G(I,J),I=1,IMAX)
    WRITE (6,24) (G(I,J),I=1,IMAX)
    WRITE (6,23) (G(I,J),I=1,IMAX)
    WRITE (6,22) (G(I,J),I=1,IMAX)
    WRITE (6,21) (G(I,J),I=1,IMAX)
    WRITE (6,20) (G(I,J),I=1,IMAX)
    WRITE (6,19) (G(I,J),I=1,IMAX)
    WRITE (6,18) (G(I,J),I=1,IMAX)
    WRITE (6,17) (G(I,J),I=1,IMAX)
    WRITE (6,16) (G(I,J),I=1,IMAX)
    WRITE (6,15) (G(I,J),I=1,IMAX)
    WRITE (6,14) (G(I,J),I=1,IMAX)
    WRITE (6,13) (G(I,J),I=1,IMAX)
    WRITE (6,12) (G(I,J),I=1,IMAX)
    WRITE (6,11) (G(I,J),I=1,IMAX)
    WRITE (6,10) (G(I,J),I=1,IMAX)
    WRITE (6,9) (G(I,J),I=1,IMAX)
    WRITE (6,8) (G(I,J),I=1,IMAX)
    WRITE (6,7) (G(I,J),I=1,IMAX)
    WRITE (6,6) (G(I,J),I=1,IMAX)
    WRITE (6,5) (G(I,J),I=1,IMAX)
    WRITE (6,4) (G(I,J),I=1,IMAX)
    WRITE (6,3) (G(I,J),I=1,IMAX)
    WRITE (6,2) (G(I,J),I=1,IMAX)
    WRITE (6,1) (G(I,J),I=1,IMAX)

```

```

SUBROUTINE GPUNCH (Z,XC,YO,PHS,NCF,IMX,JMX,G)
GPUNCH PUNCHES OUT THE FIRST NON-SYMMETRIC PORTION OF GARRAY
(OR WRITES IT ON FILE 7 IN CMS VERSION)
COMMON /SYM/ ISM,JSM,MSM,FCU,IMS,JMS,QSM
DIMENSION G(IMX,JMX)
WRITE (6,39) NCF,IMX,JMX,ISM,JSM,IMS,JMS
WRITE (6,38) ((G(I,J),I=1,IMS),J=1,JMS)
WRITE (6,37) ((G(I,J),I=1,IMS),J=1,JMS)
WRITE (6,36) ((G(I,J),I=1,IMS),J=1,JMS)
WRITE (6,35) ((G(I,J),I=1,IMS),J=1,JMS)
WRITE (6,34) ((G(I,J),I=1,IMS),J=1,JMS)
WRITE (6,33) ((G(I,J),I=1,IMS),J=1,JMS)
WRITE (6,32) ((G(I,J),I=1,IMS),J=1,JMS)
WRITE (6,31) ((G(I,J),I=1,IMS),J=1,JMS)
WRITE (6,30) ((G(I,J),I=1,IMS),J=1,JMS)
WRITE (6,29) ((G(I,J),I=1,IMS),J=1,JMS)
WRITE (6,28) ((G(I,J),I=1,IMS),J=1,JMS)
WRITE (6,27) ((G(I,J),I=1,IMS),J=1,JMS)
WRITE (6,26) ((G(I,J),I=1,IMS),J=1,JMS)
WRITE (6,25) ((G(I,J),I=1,IMS),J=1,JMS)
WRITE (6,24) ((G(I,J),I=1,IMS),J=1,JMS)
WRITE (6,23) ((G(I,J),I=1,IMS),J=1,JMS)
WRITE (6,22) ((G(I,J),I=1,IMS),J=1,JMS)
WRITE (6,21) ((G(I,J),I=1,IMS),J=1,JMS)
WRITE (6,20) ((G(I,J),I=1,IMS),J=1,JMS)
WRITE (6,19) ((G(I,J),I=1,IMS),J=1,JMS)
WRITE (6,18) ((G(I,J),I=1,IMS),J=1,JMS)
WRITE (6,17) ((G(I,J),I=1,IMS),J=1,JMS)
WRITE (6,16) ((G(I,J),I=1,IMS),J=1,JMS)
WRITE (6,15) ((G(I,J),I=1,IMS),J=1,JMS)
WRITE (6,14) ((G(I,J),I=1,IMS),J=1,JMS)
WRITE (6,13) ((G(I,J),I=1,IMS),J=1,JMS)
WRITE (6,12) ((G(I,J),I=1,IMS),J=1,JMS)
WRITE (6,11) ((G(I,J),I=1,IMS),J=1,JMS)
WRITE (6,10) ((G(I,J),I=1,IMS),J=1,JMS)
WRITE (6,9) ((G(I,J),I=1,IMS),J=1,JMS)
WRITE (6,8) ((G(I,J),I=1,IMS),J=1,JMS)
WRITE (6,7) ((G(I,J),I=1,IMS),J=1,JMS)
WRITE (6,6) ((G(I,J),I=1,IMS),J=1,JMS)
WRITE (6,5) ((G(I,J),I=1,IMS),J=1,JMS)
WRITE (6,4) ((G(I,J),I=1,IMS),J=1,JMS)
WRITE (6,3) ((G(I,J),I=1,IMS),J=1,JMS)
WRITE (6,2) ((G(I,J),I=1,IMS),J=1,JMS)
WRITE (6,1) ((G(I,J),I=1,IMS),J=1,JMS)

```





















A large grid of 100 small circular icons, each containing a different symbol or character, arranged in 10 rows and 10 columns.

DESCRIPTION OF PARAMETERS	INCREASING	ABSCISSA	ARRAY
X: MONOTONICALLY	CORRESPONDING	SUPPLIED	CORRESPONDING
Y: ORDER OF X	ABSCISSA	FOR WHICH	CORRESPONDING
M: NUMBER OF ABSCISSA	FOR WHICH	CORRESPONDING	CORRESPONDING
XINT: VALUE OF X	INTERPOLATED	(OR EXTRAPOLATED)	OR ORIGINATE VALUE
YINT: INTERPOLATED	(OR EXTRAPOLATED)	OR ORIGINATE	VALUE

REMARKS  
IF SPECIFIED X FALLS OUTSIDE OF RANGE, AN EXTRAPOLATED  
VALUE WILL BE SUPPLIED  
SUBROUTINES AND FUNCTION SUBPROGRAMS REQUIRED  
SUBROUTINE SPLICO IS INCLUDED IN SUBROUTINE SPLIN PACKAGE  
MATHEMATICAL METHOD  
UPON FIRST ENTRY TO SPLIN, A CALL TO SPLICO IS MADE TO  
DETERMINE THE COEFFICIENTS TO BE USED IN PERFORMING THE  
INTERPOLATIONS. SEARCH FOR PACKETING ARCS IN A VALUES IS  
ALWAYS MADE. THE SEARCH REFERENCE LAST USED IN INTERPOLATING.  
REFERENCE  
DENNING, RALPH H., "INTRODUCTORY COMPUTER METHODS AND  
NUMERICAL ANALYSIS", THE MACMILLAN COMPANY, NEW YORK, 1965

000  
 98765432109876543210987654321098765432109876543210  
 000  
 000  
 111  
 000  
 000

```

SUBROUTINE SPLINE(X,Y,M,XINT,YINT)
DIMENSION X(M),Y(M),C(4,300)
CALL SPLICC(X,Y,M,C)
K=1
DO 1 PY SPLINN(X,Y,M,XINT,YINT)
IF(XINT-X(1)) 7C,1,2
3C K=1
1C 7C
1 YINT=Y(1)
2 Y=TURN
2C IF(XINT-X(K+1)) 6,4,5
3 YINT=Y(K+1)
5 R=TURN
7C K=K+1
7C IF(M-K) 71,71,3
7C IF(M-1) 7
7C IF(XINT-X(K)) 13,12,11

```





```

12 YINT=Y(K)
13 RETURN
14 K=K-1
15 GO TO 6
16 I=1, XINT
17 PRINT(8PCXINT = E18.9, 32H, PUT OF RANGE FOR INTERPOLATION)
101 FORMAT(X(K+1)-XINT)*(C(1,K)*(X(K+1)-XINT)**2+C(3,K))
11 YINT=YINT+(XINT-X(K))*(C(2,K)*(XINT-X(K))**2+C(4,K))
12 RETURN
13 END

```

```

SUBROUTINE SPLICO(X,Y,M,C)
DIMENSION X(M),Y(M),C(4,300),D(300),P(300),E(300),A(300,3),B(300),
1(7,300)
MM=M-1
DO 2 K=1,MM
D(K)=X(K+1)-X(K)
D(K)=D(K)/6.
P(K)=(Y(K+1)-Y(K))/D(K)
3 DO 3 K=2,MM
B(K)=E(K)-E(K-1)
A(1,2)=-1.-D(1)/D(2)
A(1,3)=D(1)/D(2)
A(2,2)=D(2)-P(1)*A(1,3)
A(2,3)=2.*P(1)+P(2)-P(1)*A(1,2)
4 DO 4 K=3,MM
B(K)=B(K)/A(2,2)
A(K,2)=2.*P(K-1)+P(K)-P(K-1)*A(K-1,3)
E(K)=B(K)-P(K-1)*B(K-1)
A(K,3)=B(K)/A(K,2)
5 DO 5 M=2,MM-1
G=D(M-2)/D(M-1)
A(M,1)=1.+G+A(M-2,3)
A(M,2)=-G-A(M,1)*A(M-1,3)
A(M,3)=B(M)/A(M,2)
Z(M)=B(M)-A(M,1)*A(M,2)
MM=M-2
DO 6 I=1,MM
Z(K)=P(K)-A(K,3)*Z(K+1)
Z(1)=-A(1,2)*Z(2)-A(1,3)*Z(3)
6 DO 7 K=1,MM
C(1,K)=Z(K)
C(2,K)=Z(K)*Q
C(3,K)=Z(K+1)*Q
C(4,K)=Y(K)-Z(K)*P(K)

```



```

7 C(4,K)=Y(K+1)/D(K)-Z(K+1)*P(K)
  RETURN
END

```

```

SPLO11100
SPLO11110
SPLO11120

```

```

CCCCC2C

```

```

** ** ** ** ** ** ** ** ** ** ** ** ** ** ** ** ** ** ** ** ** ** ** ** ** ** ** ** ** ** ** ** 
SUBROUTINE MTMPII
PURPOSE
    MTMPII WILL PRODUCE, ON THE PRINTER, A CONTOUR MAP
    OF ANY SINGLE PRECISION TWO DIMENSIONAL ARRAY.

USAGE
    CALL MTMPII(Y,N,M,T,RND,AZ,BZ,AMIN,IJT,ICCN)

DESCRIPTION OF PARAMETERS
    Y - THE ARRAY TO BE CONTOURED. DIMENSIONED Y(N,M)
    N - NUMBER OF ROWS IN Y.
    M - NUMBER OF COLUMNS IN Y.
    T - ARRAY FOR PLOT TITLE. REAL*4 T(24).
    RND - A BANDWIDTH WILL BE CALCULATED AS FOLLOWS
        BND=(MAX(Y)-MIN(Y))/15. MAYBE PERFORMED ON
        A LINEAR TRANSFORMATION FOLLOWING FORM AZ*Y+BZ.
        IF AZ=0 THEN AZ WILL BE COMPUTED SUCH THAT
        MAX(1 MAX(Y),1,1 MIN(Y)) WILL BE LESS THAN 1,
        AND BZ WILL BE LEFT AS INPUT.
    AZ - SEE UNDER AZ
    BZ - SEE UNDER AZ
    AMIN - THE LEVEL AT WHICH COUTOURING WILL BEGIN. IF
        AMIN > MIN(Y) THEN AMIN WILL BE CALCULATED.
        TCNTR=MIN(Y) REFERENCE AT ZERO, THE NEXT LOWER
        CONTOUR LEVEL
    RND,IJT=0 AMIN WILL BE CALCULATED AS DESCRIBED
        ABOVE.
    ICCN - IF ICCN=0 NO COUTOURING WILL BE DONE BUT THE
        ARRAY Y WILL BE PRINTED IN THE PLOT FORMAT.

REMARKS
    MTMPII REQUIRES A PRINTER WITH 132 PRINT POSITIONS.
    IF NECESSARY THE MAP WILL BE SEGMENTED COLUMNWISE.
    THE NECESSARY AND COLUMNS ARE NUMBERED ALONG THE EDGES.
    THAT A SEGMENTED MAP MAY BE EASILY JOINED TOGETHER.

```

```

MET000010
MET000020
MET000030
MET000040
MET000050
MET000060
MET000070
MET000080
MET000090
MET000100
MET000110
MET000120
MET000130
MET000140
MET000150
MET000160
MET000170
MET000180
MET000190
MET000200
MET000210
MET000220
MET000230
MET000240
MET000250
MET000260
MET000270
MET000280
MET000290
MET000300
MET000310
MET000320
MET000330
MET000340
MET000350
MET000360
MET000370
MET000380
MET000390
MET000400
MET000410
MET000420

```













```

NCP=NCP+1
73 IF(NCP-M) 8C,8C,75
78 CCONTINUE
80 J=-2
85 C
C SET
95 C
95 C
100 CCONTINUE
110 J=J+1
120 IF(KI-100) 13C,12C,12C
135 A(J)=K(L+1)
140 J=J+1
150 IF(KI/10) 15C,14C,14C
155 A(J)=K(LL+1)
160 CCONTINUE
165 CCONTINUE
170 CCONTINUE
180 CCONTINUE
185 CCONTINUE
190 CCONTINUE
195 CCONTINUE
200 CCONTINUE
205 CCONTINUE
210 CCONTINUE
215 CCONTINUE
220 CCONTINUE
225 CCONTINUE
230 CCONTINUE
235 CCONTINUE
240 CCONTINUE
245 CCONTINUE
250 CCONTINUE
255 CCONTINUE
260 CCONTINUE
265 CCONTINUE
270 CCONTINUE
275 CCONTINUE
280 CCONTINUE
285 CCONTINUE
290 CCONTINUE
295 CCONTINUE
300 CCONTINUE
305 CCONTINUE
310 CCONTINUE
315 CCONTINUE
320 CCONTINUE
325 CCONTINUE
330 CCONTINUE
335 CCONTINUE
340 CCONTINUE
345 CCONTINUE
350 CCONTINUE
355 CCONTINUE
360 CCONTINUE
365 CCONTINUE
370 CCONTINUE
375 CCONTINUE
380 CCONTINUE
385 CCONTINUE
390 CCONTINUE
395 CCONTINUE
400 CCONTINUE
405 CCONTINUE
410 CCONTINUE
415 CCONTINUE
420 CCONTINUE
425 CCONTINUE
430 CCONTINUE
435 CCONTINUE
440 CCONTINUE
445 CCONTINUE
450 CCONTINUE
455 CCONTINUE
460 CCONTINUE
465 CCONTINUE
470 CCONTINUE
475 CCONTINUE
480 CCONTINUE
485 CCONTINUE
490 CCONTINUE
495 CCONTINUE
500 CCONTINUE
505 CCONTINUE
510 CCONTINUE
515 CCONTINUE
520 CCONTINUE
525 CCONTINUE
530 CCONTINUE
535 CCONTINUE
540 CCONTINUE
545 CCONTINUE
550 CCONTINUE
555 CCONTINUE
560 CCONTINUE
565 CCONTINUE
570 CCONTINUE
575 CCONTINUE
580 CCONTINUE
585 CCONTINUE
590 CCONTINUE
595 CCONTINUE
600 CCONTINUE
605 CCONTINUE
610 CCONTINUE
615 CCONTINUE
620 CCONTINUE
625 CCONTINUE
630 CCONTINUE
635 CCONTINUE
640 CCONTINUE
645 CCONTINUE
650 CCONTINUE
655 CCONTINUE
660 CCONTINUE
665 CCONTINUE
670 CCONTINUE
675 CCONTINUE
680 CCONTINUE
685 CCONTINUE
690 CCONTINUE
695 CCONTINUE
700 CCONTINUE
705 CCONTINUE
710 CCONTINUE
715 CCONTINUE
720 CCONTINUE
725 CCONTINUE
730 CCONTINUE
735 CCONTINUE
740 CCONTINUE
745 CCONTINUE
750 CCONTINUE
755 CCONTINUE
760 CCONTINUE
765 CCONTINUE
770 CCONTINUE
775 CCONTINUE
780 CCONTINUE
785 CCONTINUE
790 CCONTINUE
795 CCONTINUE
800 CCONTINUE
805 CCONTINUE
810 CCONTINUE
815 CCONTINUE
820 CCONTINUE
825 CCONTINUE
830 CCONTINUE
835 CCONTINUE
840 CCONTINUE
845 CCONTINUE
850 CCONTINUE
855 CCONTINUE
860 CCONTINUE
865 CCONTINUE
870 CCONTINUE
875 CCONTINUE
880 CCONTINUE
885 CCONTINUE
890 CCONTINUE
895 CCONTINUE
900 CCONTINUE
905 CCONTINUE
910 CCONTINUE
915 CCONTINUE
920 CCONTINUE
925 CCONTINUE
930 CCONTINUE
935 CCONTINUE
940 CCONTINUE
945 CCONTINUE
950 CCONTINUE
955 CCONTINUE
960 CCONTINUE
965 CCONTINUE
970 CCONTINUE
975 CCONTINUE
980 CCONTINUE
985 CCONTINUE
990 CCONTINUE
995 CCONTINUE
1000 CCONTINUE

```



```

190 F(I) = BLK
191 FCNT=INUB
195 IF (ICCP-I) 195,260,195
J=4
195 IF (ICCP-I) 195,260,195
200 J=5
210 IF (ICCP-I) 195,260,195
220 J=6
230 IF (ICCP-I) 195,260,195
240 J=7
250 IF (ICCP-I) 195,260,195
260 J=8
270 IF (ICCP-I) 195,260,195
280 J=9
290 IF (ICCP-I) 195,260,195
300 J=10
310 IF (ICCP-I) 195,260,195
320 J=11
330 IF (ICCP-I) 195,260,195
340 J=12
350 IF (ICCP-I) 195,260,195
360 J=13
370 IF (ICCP-I) 195,260,195
380 J=14
390 IF (ICCP-I) 195,260,195
400 J=15
410 IF (ICCP-I) 195,260,195
420 J=16
430 IF (ICCP-I) 195,260,195
440 J=17
450 IF (ICCP-I) 195,260,195
460 J=18
470 IF (ICCP-I) 195,260,195
480 J=19
490 IF (ICCP-I) 195,260,195
500 J=20
510 IF (ICCP-I) 195,260,195
520 J=21
530 IF (ICCP-I) 195,260,195
540 J=22
550 IF (ICCP-I) 195,260,195
560 J=23
570 IF (ICCP-I) 195,260,195
580 J=24
590 IF (ICCP-I) 195,260,195
600 J=25
610 IF (ICCP-I) 195,260,195
620 J=26
630 IF (ICCP-I) 195,260,195
640 J=27
650 IF (ICCP-I) 195,260,195
660 J=28
670 IF (ICCP-I) 195,260,195
680 J=29
690 IF (ICCP-I) 195,260,195
700 J=30
710 IF (ICCP-I) 195,260,195
720 J=31
730 IF (ICCP-I) 195,260,195
740 J=32
750 IF (ICCP-I) 195,260,195
760 J=33
770 IF (ICCP-I) 195,260,195
780 J=34
790 IF (ICCP-I) 195,260,195
800 J=35
810 IF (ICCP-I) 195,260,195
820 J=36
830 IF (ICCP-I) 195,260,195
840 J=37
850 IF (ICCP-I) 195,260,195
860 J=38
870 IF (ICCP-I) 195,260,195
880 J=39
890 IF (ICCP-I) 195,260,195
900 J=40
910 IF (ICCP-I) 195,260,195
920 J=41
930 IF (ICCP-I) 195,260,195
940 J=42
950 IF (ICCP-I) 195,260,195
960 J=43
970 IF (ICCP-I) 195,260,195
980 J=44
990 IF (ICCP-I) 195,260,195
1000 J=45

```



[illegible]



```

345 IF(KI-IC) 35C,345,345
    LL=KI/IC
    F(J)=KG(LL+1)
    KI=KI-IC*LL
35C GO TO 35E
35E F(J)=KG(I)
    J=J+1
    F(J)=KG(KI+1)
    J=J-1
    IF(NCY-1) 27C,27C,35C
36C IF(NLINT-1)362,362,368
362 PRINT,7C,(A(I),I=1,132),(R(IP1),IP1=1,132),(H(IP2),IP2=1,132),
    GO TO 37C
368 PRINT,7C,(A(I),I=1,132),(R(IP1),IP1=1,132),(C(IP2),IP2=1,132),
    GO INTP3),IP3=1,132),(E(IP4),IP4=1,132),(F(IP5),IP5=1,132),
    GO INTP7),IP6=1,132),(H(IP7),IP7=1,132)
37C FOR TO 17C
    GO TO 39C IF=1,135
38C 4(I)=BLK
    F(I)=BLK
    C(I)=BLK
    C(I)=BLK
    CONTINUE
39C J=-2
    IF(NCCP-1) 395,395,40C
39C J=-1 3C L=NCCP,NCP
40C J=J+3
    J=L
    IF(KI-IC) 410,405,405
40C LL=KI/IC
    C(J)=KG(LL+1)
    KI=KI-IC*LL
41C GO TO 412
412 C(J)=KG(I)
    J=J+1
    IF(KI-IC) 420,415,415
41C LL=KI/IC
    C(J)=KG(LL+1)
    KI=KI-IC*LL
42C GO TO 422
422 J=J+1
    IF(NC-M)4C,50C,50C
43C CONTINUE, (R(IP1),IP1=1,132),(C(IP2),IP2=1,132)
    PRINT,7C,(A(I),I=1,132),(H(IP2),IP2=1,132),
    GO INTP3),IP3=1,132),(E(IP4),IP4=1,132),(F(IP5),IP5=1,132),
    GO INTP7),IP6=1,132),(H(IP7),IP7=1,132)

```





22  
23  
24  
25  
26  
27  
28

CO  
S  
CAUS

000  
1-7

S S S  
J J J  
A A A  
C C C

COALS  
COALS

100

00  
U  
-  
S  
J  
A  
C

[illegible]

CALLS 220

CO  
NE  
NO

SS  
DU  
TA  
CC

20  
15  
10  
5  
0

00  
7  
0  
5  
2  
1  
0







```

SEEDS SHOULD BE CHOSEN IN ACCORDANCE WITH THE DISCUSSION THAT
GIVEN IN THE POINT RANDOM NUMBERS ARE DESIRED, AS ARE THE
IF AVAILABLE POINT RANDOM NUMBERS ARE CHANGED AND A TRAILING LOW
EVENING ZERO BIT IN THEIR PROBABILITY PART.
ORDER ZERO BIT IN THEIR PROBABILITY PART.

SUBROUTINES AND FUNCTION SUBPROGRAMS REQUIRED
NONE

METHOD
POWER RESIDUE METHOD DISCUSSED IN IBM MANUAL C20-8011,
RANDOM NUMBER GENERATION AND TESTING
.....

```

```

SUBROUTINE FANDU(IY, YFL)
  IY=IX*65536
  IF(IY) 5,6,7
  IY=IY+2147483647+1
  YFL=YFL*46566135-9
  RETURN
END

```



5. The Input Data Files Used in the Experiment:

p garray hi45,0a Axisymmetric, 60 psia, z= .05 cm.

450	100	1	2	100	50	1			
0.00	0.00	0.00	0.00	0.00	0.00	0.00	0.00	0.00	0.06
1.08	2.28	3.28	4.26	5.10	6.04	6.88	7.76	8.42	9.14
09.50	09.80	10.15	10.60	10.95	11.30	11.60	11.94	12.15	12.42
12.70	12.90	13.10	13.30	13.40	13.55	13.65	13.80	13.87	13.92
14.05	14.15	14.20	14.22	14.28	14.32	14.38	14.40	14.42	14.42

R; T=0.03/0.10 17.28.59

p garray ay hi45,2.5 Axisymmetric, 60 psia, z= .25 cm.

452	100	1	2	100	50	1			
0.00	0.00	0.00	0.00	0.03	0.24	0.62	1.26	1.64	1.90
2.10	2.32	2.62	2.91	3.40	3.90	4.43	5.03	5.50	6.00
6.51	6.98	7.35	7.70	8.02	8.44	8.90	9.32	9.63	9.91
10.18	10.40	10.60	10.84	11.04	11.20	11.35	11.50	11.65	11.70
12.00	12.09	12.15	12.21	12.25	12.29	12.32	12.36	12.38	12.39

R; T=0.03/0.10 17.30.09

p garray hi45,5a Axisymmetric, 60 psia, z= .5 cm.

542	100	1	2	100	50	1			
5.0									
0.00	0.00	0.03	0.32	0.82	1.33	1.93	2.19	2.30	2.44
2.53	2.63	2.72	2.79	2.88	3.00	3.15	3.36	3.60	3.80
4.00	4.28	4.64	4.94	5.20	5.53	5.90	6.18	6.44	6.70
6.95	7.19	7.40	7.61	7.80	7.97	8.12	8.22	8.48	8.62
8.75	8.88	8.98	9.10	9.19	9.28	9.37	9.42	9.44	9.45

R; T=0.03/0.10 17.31.06





p garray hi45,7.5 Axisymmetric, 60 psia, z= .75 cm

455	120	1	2	100	60	1			
0.00	0.00	0.00	0.00	0.00	0.00	0.00	0.00	0.00	0.18
0.68	0.98	1.45	1.75	2.28	2.55	2.73	2.84	2.95	3.02
3.08	3.10	3.11	3.12	3.13	3.11	3.09	3.06	3.06	3.12
3.25	3.40	3.59	3.75	3.93	4.10	4.30	4.50	4.66	4.83
5.00	5.13	5.35	5.50	5.65	5.85	6.03	6.17	6.28	6.38
6.50	6.58	6.64	6.72	6.78	6.84	6.88	6.90	6.94	6.96

R; T=0.03/0.10 17.32.03

p garray hi45,10. Axisymmetric, 60 psia, z= 1.0 cm.

4510	120	1	2	100	60	1			
1.0	0.00	0.00	0.00	0.00	0.00	0.00	0.15	0.38	0.65
0.00	1.30	1.60	2.10	2.37	2.62	2.78	2.91	3.03	3.15
1.04	3.30	3.34	3.36	3.34	3.28	3.20	3.12	3.05	2.98
3.22	2.90	2.90	2.90	2.92	2.97	3.00	3.06	3.12	3.18
2.92	3.35	3.42	3.52	3.63	3.74	3.81	3.90	3.99	4.05
3.28	4.27	4.22	4.27	4.32	4.37	4.40	4.42	4.48	4.50

R; T=0.03/0.10 17.33.11

p garray hi45,12. Axisymmetric, 60 psia, z= 1.25 cm.

4512	120	1	2	100	60	1			
1.25	0.00	0.00	0.00	0.00	0.04	0.20	0.44	0.70	1.10
0.00	1.88	2.18	2.36	2.52	2.62	2.77	2.87	2.94	3.02
1.55	3.16	3.20	3.24	3.20	3.16	3.11	3.01	2.88	2.70
3.03	2.47	2.38	2.28	2.21	2.14	2.10	2.05	2.05	2.06
2.56	2.16	2.20	2.25	2.31	2.37	2.43	2.50	2.55	2.60
2.10	2.71	2.78	2.85	2.90	2.95	2.99	3.02	3.05	3.07

R; T=0.03/0.10 17.34.27



p garray hi45,15. Axisymmetric, 60 psia, z=1.5 cm.

4515	120	1	2	100	60	1			
01.5									
0.01	0.02	0.03	0.05	0.08	0.12	0.31	0.59	0.89	1.20
1.68	2.09	2.31	2.50	2.61	2.72	2.90	2.86	2.90	2.95
2.98	3.00	2.99	2.98	2.94	2.86	2.79	2.68	2.58	2.44
2.28	2.15	2.00	1.85	1.76	1.70	1.63	1.59	1.55	1.52
1.51	1.49	1.48	1.47	1.45	1.46	1.47	1.48	1.49	1.50
1.51	1.52	1.53	1.55	1.57	1.58	1.59	1.60	1.61	1.61

R; T=0.03/0.10 17.35.38

p garray hi45,20. Axisymmetric, 60 psia, z=2.0 cm.

4520	120	1	2	100	60	1			
2.0									
0.00	0.03	0.10	0.20	0.35	0.58	0.79	0.90	1.07	1.30
1.55	1.75	2.00	2.28	2.45	2.60	2.72	2.85	2.95	3.02
3.09	3.11	3.15	3.17	3.18	3.17	3.16	3.10	3.04	2.97
2.89	2.79	2.68	2.54	2.38	2.14	1.87	1.69	1.50	1.35
1.18	1.03	0.92	0.79	0.65	0.58	0.48	0.39	0.34	0.30
0.25	0.21	0.20	0.20	0.19	0.19	0.18	0.18	0.18	0.17

R; T=0.03/0.10 17.36.38







9.72	9.70	9.65	9.50	9.22	8.90	8.52	8.15	7.73	7.32
6.88	6.32	5.80	5.13	4.50	3.77	3.30	2.89	2.50	2.10
1.65	1.12	0.28	0.00	0.00	0.00	0.00	0.00	0.00	0.00
0.00	0.00	0.00	0.00	0.15	0.90	1.77	2.16	2.57	2.71
2.72	2.70	2.88	3.14	3.61	4.14	4.70	5.24	4.77	6.28
6.75	7.20	7.60	8.00	8.33	8.63	8.90	9.13	9.34	9.51
9.64	9.62	9.57	9.45	9.30	9.09	8.81	8.48	8.07	7.55
7.11	6.52	5.98	5.32	4.70	4.16	3.60	3.05	2.76	2.55
2.21	1.47	0.67	0.05	0.00	0.00	0.00	0.00	0.00	0.00
0.00	0.00	0.00	0.00	0.32	1.00	1.83	2.31	2.59	2.58
2.55	2.59	2.73	3.05	3.45	3.97	4.52	5.05	5.56	6.11
6.62	7.10	7.55	7.95	8.32	8.62	9.00	9.28	9.50	9.62
9.69	9.69	9.65	9.53	9.34	9.00	8.00	6.70	5.33	3.00
7.53	7.17	6.59	5.99	5.17	4.54	3.90	3.37	2.84	2.53
2.12	1.50	0.84	0.10	0.00	0.00	0.00	0.00	0.00	0.00
0.00	0.00	0.00	0.00	0.50	1.20	1.84	2.28	2.40	2.30
2.30	2.42	2.67	2.97	3.38	3.82	4.32	4.78	5.30	5.82
6.29	6.78	7.00	7.33	7.70	8.02	8.35	8.62	8.90	9.09
9.21	9.19	9.10	9.00	8.86	8.65	8.42	8.10	7.75	7.38
6.92	6.45	5.96	5.42	4.78	4.17	3.40	2.87	2.53	2.18
1.69	1.06	0.38	0.00	0.00	0.00	0.00	0.00	0.00	0.00
0.00	0.00	0.03	0.36	0.80	1.25	1.61	1.92	2.22	2.38
2.38	2.30	2.38	2.70	3.02	3.50	3.93	4.42	5.01	5.56
5.95	6.35	6.72	7.03	7.45	7.77	8.08	8.32	8.50	8.62
8.70	8.68	8.60	8.50	8.35	8.20	7.98	7.70	7.38	7.00
6.64	6.20	5.70	5.12	4.52	3.89	3.25	2.62	2.25	2.00
1.70	1.17	0.47	0.09	0.00	0.00	0.00	0.00	0.00	0.00

R: T=0.09/0.60 17.44.25





## BIBLIOGRAPHY

- Bennet, F. D. , Carter, W. C. , and Bergdolt, V. E. , "Interferometric Analysis of Airflow About Projectiles in Free Flight," Journal of Applied Physics, Vol. 23, No. 4, pp. 453-469, April 1952.
- Born, M. , and Wolf, E. , Principles of Optics, Pergamon Press, Ltd. , London, 1959.
- Bhatia, A. B. , and Wolf, E. , Proceedings of the Cambridge Philosophical Society, 50, 40, 1954.
- Brandt, G. B. , "Techniques and Applications of Holography," Electro-Technology , pp. 53-72, April 1968.
- Brooks, R. E. , Heflinger, L. O. , Wuerker, R. F. , and Briones, R. A. , "Holographic Photography of High Speed Phenomena with Conventional and Q-Switched Ruby Lasers," Applied Physics Letters, Vol. 7, No. 4, pp. 92-94, 15 August 1965.
- Brooks, R. E. , "New Dimension for Interferometry," Electronics, pp. 88-93, 15 May 1967.
- Brooks, R. E. , Heflinger, L. O. , and Wuerker, R. F. , "9A9-Pulsed Laser Holograms," IEEE Journal of Quantum Electronics, Vol. QE-2, No. 8, pp. 275-299, August 1966.
- Cavanaugh, L. , Cain, D. , and Hauer, A. , Third Quarterly Technical Report on Optical Methods for the Visualization and Measurement of Flow in Turbomachinery, Pratt and Whitney Aircraft Report PWA-3870, January 1970. (Third of a series of three quarterly reports).
- Chambers, R. P. , and Courtney-Pratt, J. S. , "Bibliography on Holograms, I, II, and III," Journal of the SMPTE: Vol. 75, pp. 373-435, April 1966; Vol. 75, pp. 759-809, August 1966; Vol. 76, pp. 392-395, April 1967.
- Erdelyi, A. , Magnus, F. , Oberhettinger, F. , and Tricomi, F. G. , Tables of Integral Transforms, Vols. I, II, McGraw Hill, New York, 1963; Higher Transcendental Functions, Vols. I, II, III, McGraw Hill, New York, 1963.



- Gabor, D. , "A New Microscopic Principle," Nature, Vol. 161, pp. 777-778, May, 1948.
- Gabor, D. , "Microscopy by Reconstructed Wavefronts," Proceedings of the Royal Society, Vol. A197, pp. 454-487, 1949.
- Gabor, D. , "Microscopy by Reconstructed Wavefronts: II," Proceedings of the Physical Society, Vol. 64, pt. 6, pp. 449-470, 1 June 1951.
- Heflinger, L. O. , Wuerker, R. F. , and Brooks, R. E. , "Holographic Interferometry," Journal of Applied Physics, Vol. 37, No. 2. , pp. 642-649, February 1966.
- Herlitz, S. I. , "A Method for Computing the Emission Distribution in Cylindrical Light Sources," Arkiv för Fysik, Band 23, No. 49, pp. 571-574, 1 March 1963.
- Hildebrand, F. B. , Introduction to Numerical Analysis, McGraw-Hill, New York, 1956.
- Holds, J. H. , Aeronautical Applications of Holographic Interferometry, Masters Thesis, Naval Postgraduate School, 1967.
- Holds, J. H. , and Fuhs, A. E. , "A Refined Analysis of a Holographic Interferogram," Journal of Applied Physics, Vol. 38, No. 13, pp. 5408-5409, December 1967.
- Ladenberg, R. , Van Voorhis, C. C. , and Winckler, J. , "Interferometric Studies of Faster than Sound Phenomena. , Part II. Analysis of Supersonic Air Jets," Physical Review, Vol. 76, No. 5, pp. 662-677, 1 September, 1949.
- Ladenberg, R. W. , et. al. , ed. , Physical Measurements in Gas Dynamics and Combustion, Princeton University Press, 1954.
- Latta, J. N. , "A Classified Bibliography on Holography and Related Fields," Journal of the SMPTE , Vol. , 77, pp. 422-458, April 1968.
- Liepmann, H. W. , and Roshko, A. , Elements of Gas Dynamics, p. 165, John Wiley and Sons, Inc. , 1957.
- Madelung, E. , "Die Mathematischen Hilfsmittel des Physikers," 5th. ed. , Springer-Verlag, Berlin, 1953.



- Maldonado, C. D. , Caron, A. P. , and Olsen, H. N. , "New Method for Obtaining Emission Coefficients from Emitted Spectral Intensities. Part I-Circularly Symmetric Light Sources," Journal of the Optical Society of America, Vol. 55, No. 10, pp. 1247-1254, October 1965.
- Maldonado, C. D. , "Note on Orthogonal Polynomials which are 'Invariant in Form' to Rotations of Axes," Journal of Mathematical Physics, Vol. 6, No. 12, pp. 1935-1938, December 1965.
- Maldonado, C. D. , and Olsen, H. N. , "New Method for Obtaining Emission Coefficients from Emitted Spectral Intensities. Part II-Asymmetrical Sources," Journal of the Optical Society of America, Vol. 56, No. 10, pp. 1305-1313, October 1966.
- Mathews, B. J. , and Wuerker, R. F. , The Investigation of Liquid Rocket Combustion Using Pulsed Laser Holography, Paper prepared for the AIAA 5th Propulsion Joint Specialist Conference, U.S. Air Force Academy, Colorado Springs, Colorado, 9-13 June 1969.
- Matulka, R. D. , Holds, J. H. , Sullivan, J. G. , and Fuhs, A. E. , Aeronautical Application of Holographic Interferometry, Naval Postgraduate School Report NPS-57FU8101A, 1968.
- Olsen, H. N. , Maldonado, C. D. , Duckworth, G. D. , and Caron, A. P. , Investigation of the Interaction of an External Magnetic Field with an Electric Arc, Aerospace Research Laboratories Report ARL66-0016, January 1966.
- Olsen, H. N. , Maldonado, C. D. , and Duckworth, G. D. , "A Numerical Method for Obtaining Internal Emission Coefficients from Externally Measured Spectral Intensities of Asymmetrical Plasmas," J. Quant. Spectrosc. Radiat. Transfer, Vol. 8, pp. 1419-1430, 1968.
- Rowley, P. D. , "Quantitative Interpretation of Three-Dimensional Weakly Refractive Phase Objects Using Holographic Interferometry," Journal of the Optical Society of America, Vol. 59, pp. 1496-1498, November 1969.
- Sangster, D. K. , and Shaw, G. A. , Analysis of Errors in the Reduction of Interferometric Data, A. C. Electronics-Defense Research Laboratory Report TR68-59, October 1968.



Sansone, G. , Orthogonal Functions, Chapt. IV, Interscience Publishers , Inc. , New York 1959.

Sullivan, J. G. , An Investigation of Three-Dimensionality in Holographic Interferometry, Masters Thesis, Naval Postgraduate School, 1968.

Whittaker, E. T. , and Watson, G. N. , A Course In Modern Analysis , 4th. ed. , Cambridge University Press, Cambridge, 1927.

Winckler, J. , "The Mach Interferometer Applied to Studying an Axially Symmetric Supersonic Airjet," The Review of Scientific Instruments, Vol. 19, No. 5, pp. 307-322, May 1948.

Witte, A. B. , and Wuerker, R. F. , Laser Holographic Interferometry Study of High Speed Flow Fields, project report, Advanced Research Projects Agency, DOD Contract No. DAHC 60-69-C-0006, 1968.





# INITIAL DISTRIBUTION LIST

	No. Copies
1. Defense Documentation Center Cameron Station Alexandria, Virginia 22314	2
2. Library, Code 0212 Naval Postgraduate School Monterey, California 93940	2
3. Chairman, Department of Aeronautics Naval Postgraduate School Monterey, California 93940	1
4. Professor D. J. Collins, Code 57Co (thesis advisor) Department of Aeronautics Naval Postgraduate School Monterey, California 93940	46
5. LCDR Robert D. Matulka, USN Office of Naval Research Arlington, Virginia 22217	3
6. Professor T. H. Gawain Department of Aeronautics Naval Postgraduate School Monterey, California 93940	1
7. Professor R. L. Kelly Department of Physics Naval Postgraduate School Monterey, California 93940	1
8. Associate Professor L. V. Schmidt Department of Aeronautics Naval Postgraduate School Monterey, California 93940	1
9. Associate Professor G. D. Sackman Department of Electrical Engineering Naval Postgraduate School Monterey, California 93940	1



INITIAL DISTRIBUTION LIST (Cont'd)

	No. Copies
10. Professor Allen E. Fuhs Department of Aeronautics Monterey, California 93940	1
11. Arvel B. Witte, R4/2050 TRW Systems Group One Space Park Redondo Beach, California 90278	1



## DOCUMENT CONTROL DATA - R &amp; D

(Security classification of title, body of abstract and indexing annotation must be entered when the overall report is classified)

1. ORIGINATING ACTIVITY (Corporate author)		2a. REPORT SECURITY CLASSIFICATION	
Naval Postgraduate School Monterey, California 93940		Unclassified	
		2b. GROUP	
3. REPORT TITLE			
The Application of Holographic Interferometry to the Determination of Asymmetric Three-Dimensional Density Fields in Free Jet Flow			
4. DESCRIPTIVE NOTES (Type of report and, inclusive dates)			
Ph. D. Thesis (June 1970)			
5. AUTHOR(S) (First name, middle initial, last name)			
Robert Dale Matulka			
6. REPORT DATE		7a. TOTAL NO. OF PAGES	7b. NO. OF REFS
June 1970		156	37
8a. CONTRACT OR GRANT NO.		9a. ORIGINATOR'S REPORT NUMBER(S)	
NAVAIR A33-330-551-69			
b. PROJECT NO.			
c.		9b. OTHER REPORT NO(S) (Any other numbers that may be assigned this report)	
d.			
10. DISTRIBUTION STATEMENT			
This document has been approved for public release and sale; its distribution is unlimited.			
11. SUPPLEMENTARY NOTES		12. SPONSORING MILITARY ACTIVITY	
		Naval Postgraduate School Monterey, California 93940	
13. ABSTRACT			
<p>The successful application of holographic interferometry, and an associated mathematical reduction process, to the determination of an asymmetric three-dimensional density field of an aerodynamic phenomenon is reported.</p> <p>An integral inversion method from the field of plasma physics has been computerized, extensively evaluated and applied to the determination of functions, both axisymmetric and asymmetric, which simulate aerodynamic density fields.</p> <p>The application of holographic interferometry has been extended to provide multiple holograms about a test region, with sufficient coverage to provide interferometric data for the successful solution of the density field.</p> <p>The analytical and experimental methods developed were applied to an experimental axisymmetric test field, the supersonic flow from a free jet, and shown to be comparable to a previous solution obtained by the Abel inversion method. Further, the free jet was tilted to provide a test field which was asymmetric in the plane of solution. Comparison of the resulting asymmetric solution was shown to be self-consistent with the previously obtained axisymmetric solution.</p>			



KEY WORDS	LINK A		LINK B		LINK C	
	ROLE	WT	ROLE	WT	ROLE	WT
1. Holography						
2. Interferometry						
3. Three-Dimensional						
4. Asymmetric						
5. Three-Dimensional Density Measurement						
6. Asymmetric Field Solution						





26 OCT 73  
26 OCT 73

19435  
19369  
19369  
2057

Thesis  
M3835  
c.1

Matulka

122517

The application of  
holographic inter-  
ferometry to the  
determination of  
asymmetric three-  
dimensional density  
fields in free jet  
flow.

26 OCT 73

19435  
19369

Thesis  
M3835  
c.1

Matulka

122517

The application of  
holographic inter-  
ferometry to the  
determination of  
asymmetric three-  
dimensional density  
fields in free jet  
flow.

thesM3835

The application of holographic interfero



3 2768 002 12535 3

DUDLEY KNOX LIBRARY